

Geometry of Neuroscience

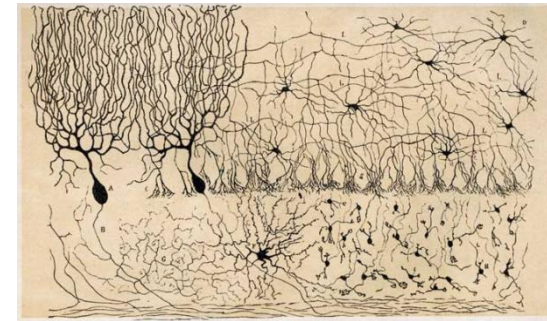
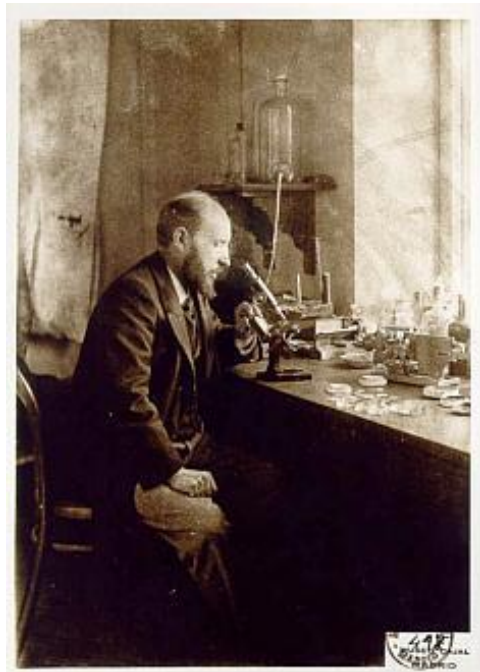
Matilde Marcolli & Doris Tsao

Jan 16: The Visual System

References for this lecture

- 1977 Hubel, D. H., Wiesel, T. N., Ferrier lecture
- 2010 Freiwald, W., Tsao, DY. „Functional compartmentalization and viewpoint generalization in the macaque face patch system“
- 2013 Nature Mante, Susillo, Shenoy, Newsome, „Context-dependent computation by recurrent dynamics in prefrontal cortex.“

Santiago Ramon y Cajal (1 May 1852 – 18 October 1934)

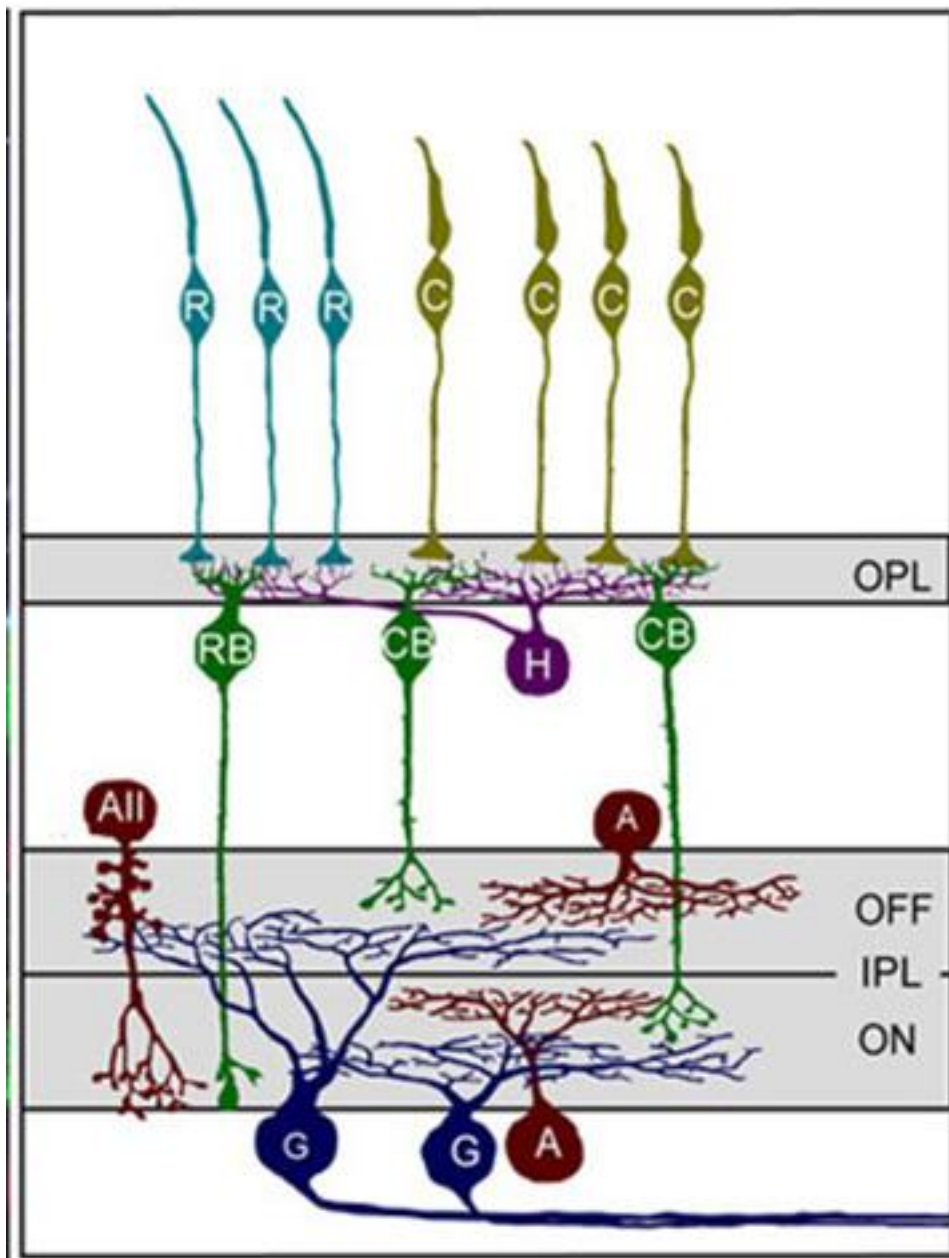


Neuron doctrine: The brain is made up of discrete individual cells.

Vision is explicable in terms of the firing patterns that emerge from the interactions among many individual neurons.

- Characterizing functional transformations along anatomically-connected pathways
- Characterizing population dynamics among large groups of neurons

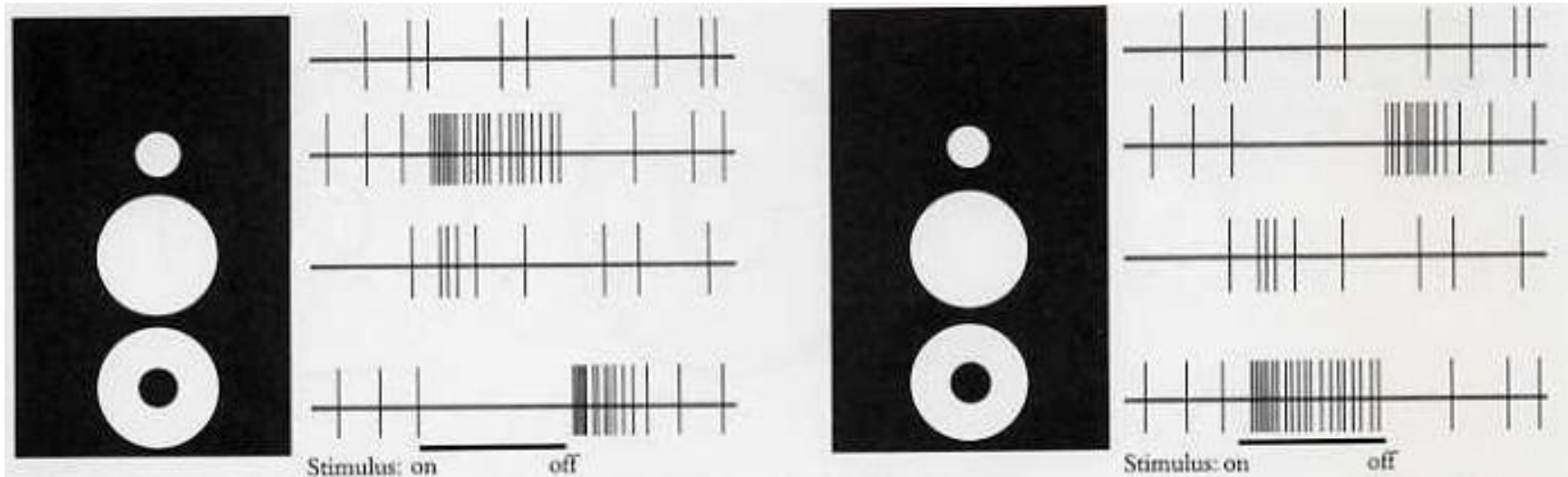
Retina



Visual processing in the retina

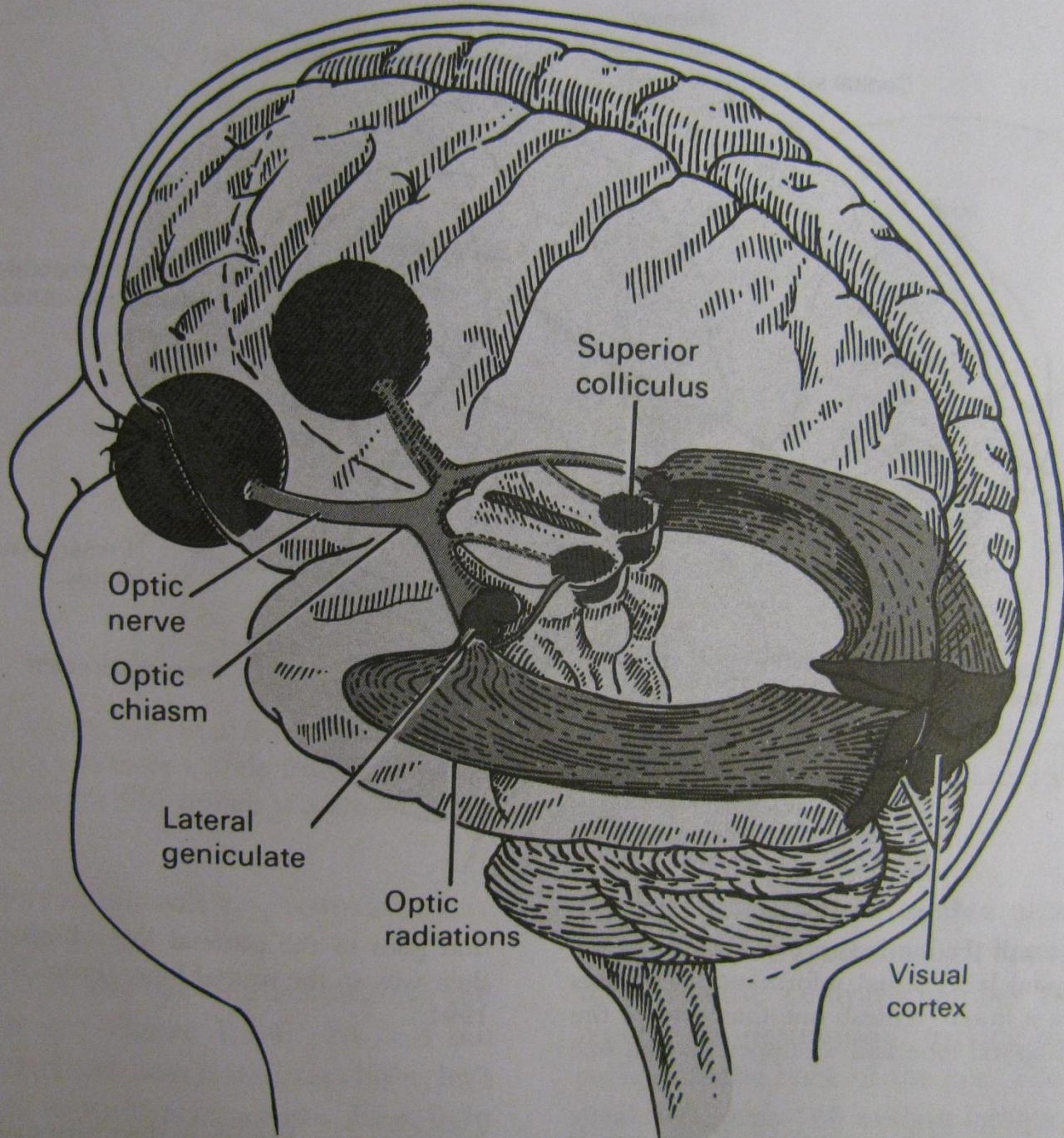


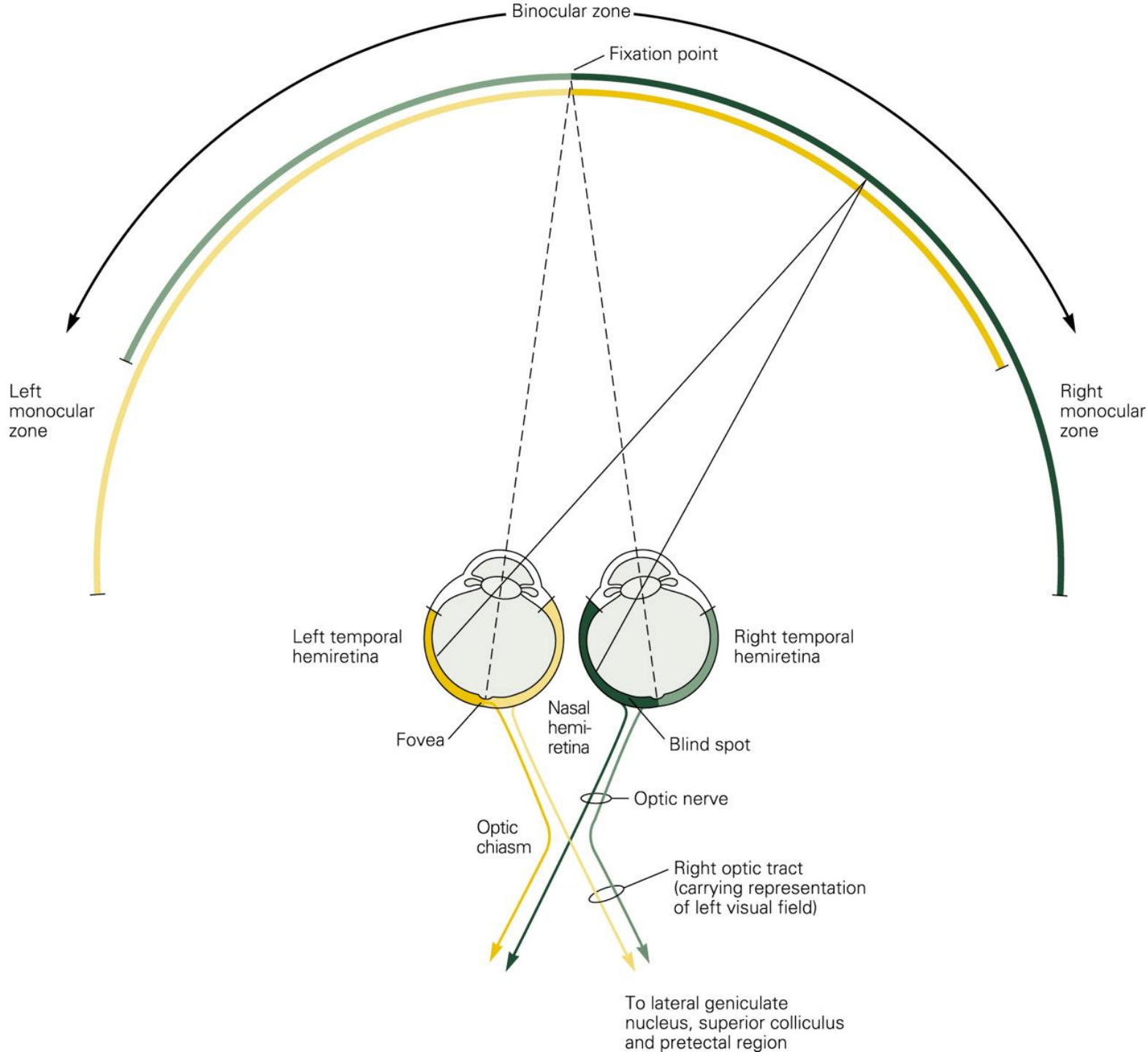
Stephen Kuffler

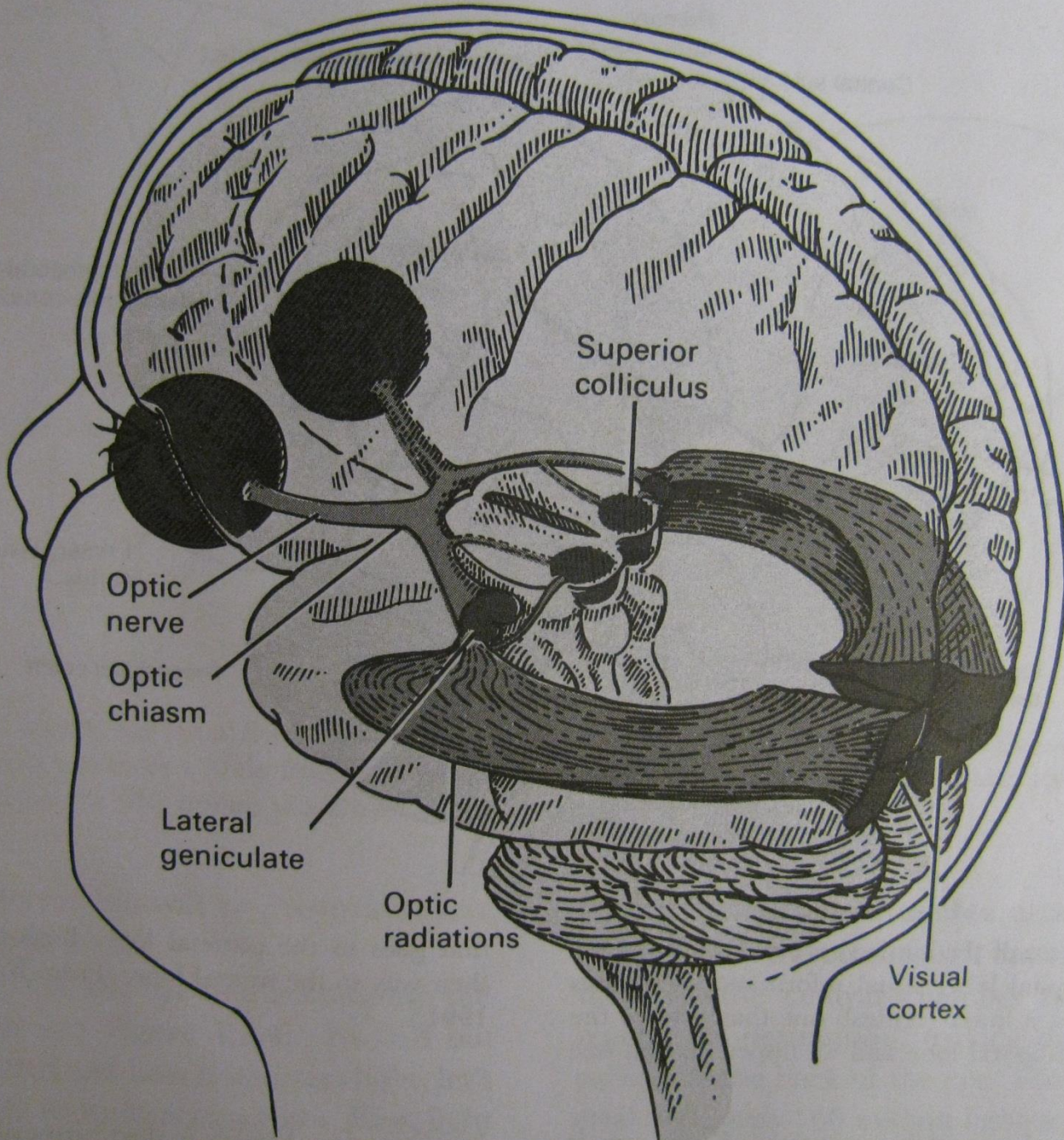


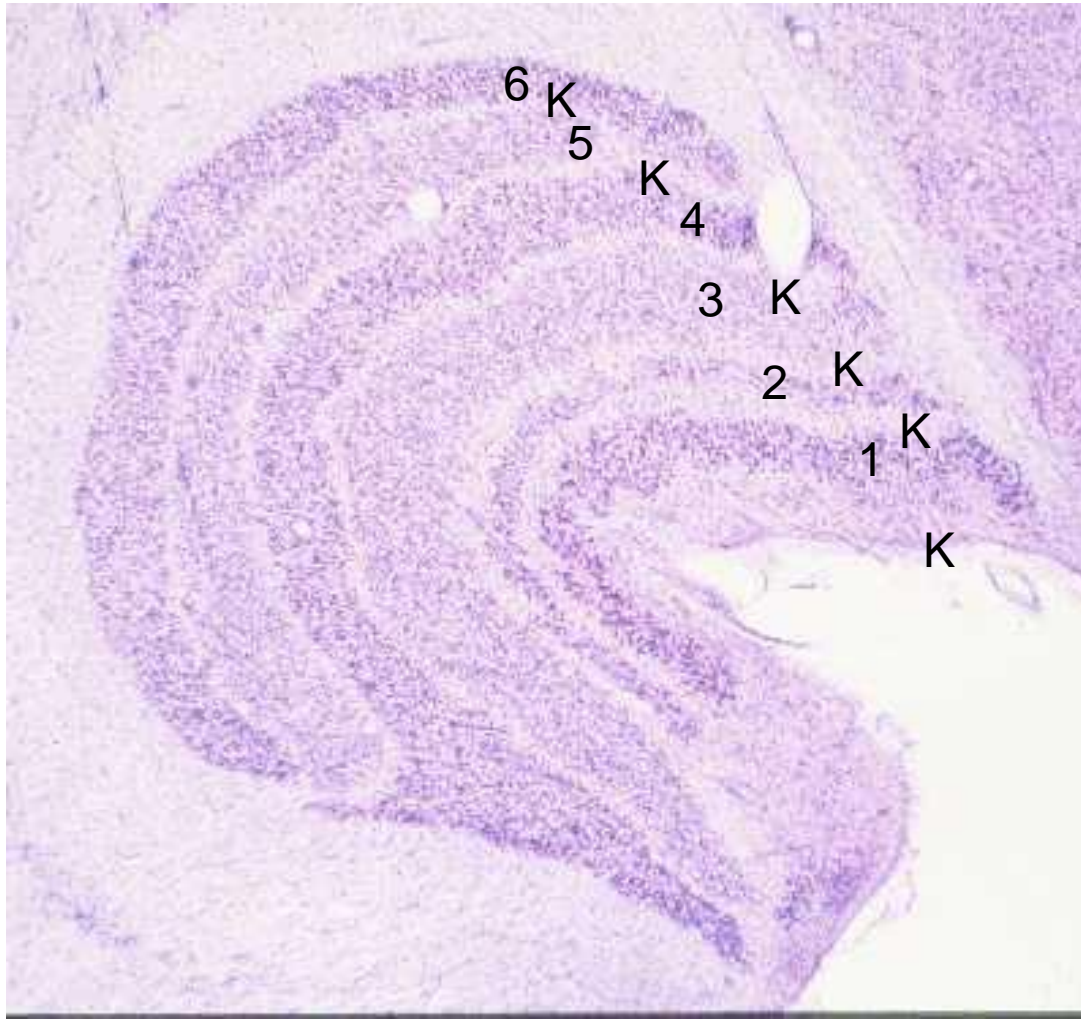
David Hubel, "Eye, Brain, Vision"

LGN









1-2: “Magno” fast and transient, large RF

2-6: “Parvo” slow and sustained, small RF

K: innervate extrastriate cortex

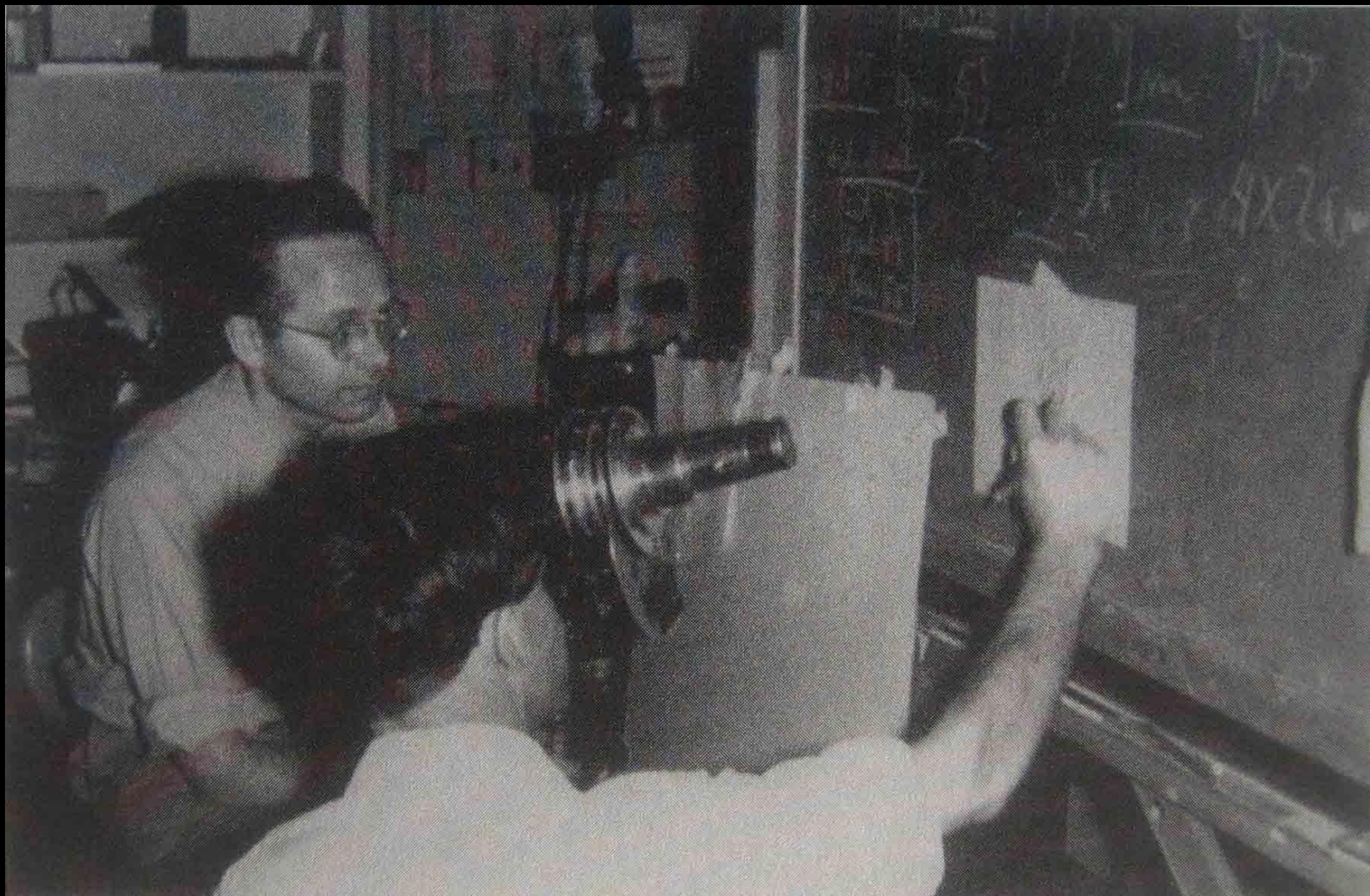
V1

“Primary Visual cortex”

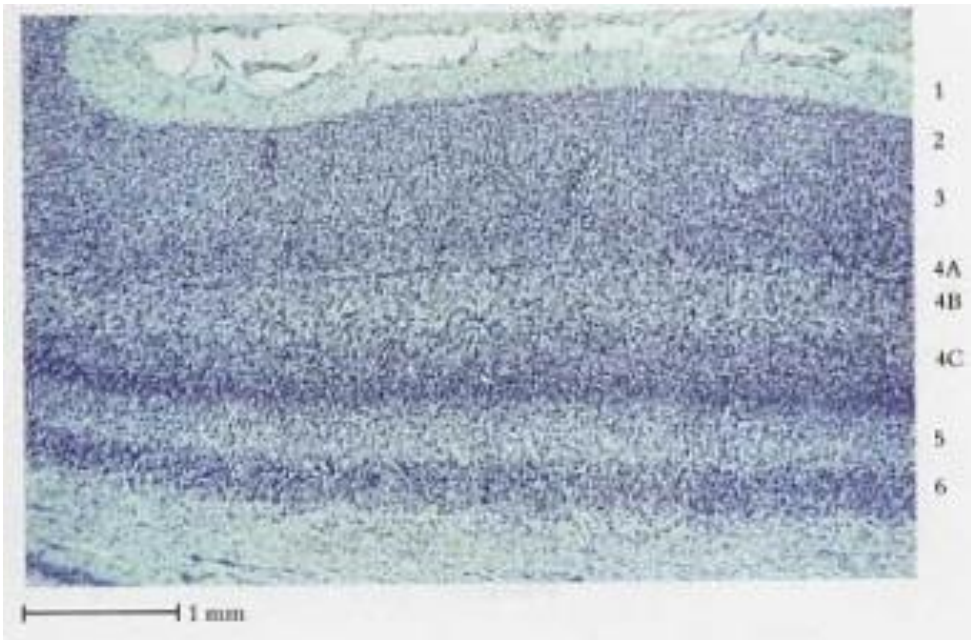
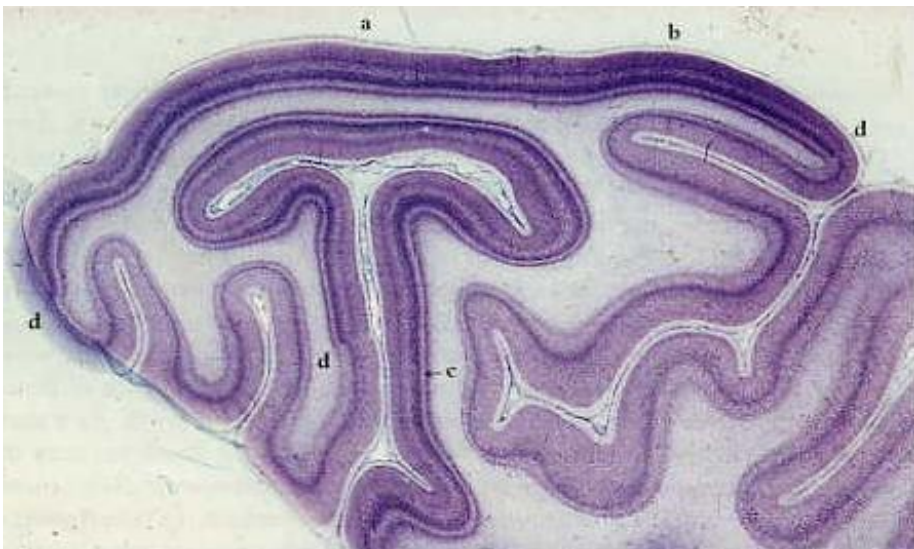
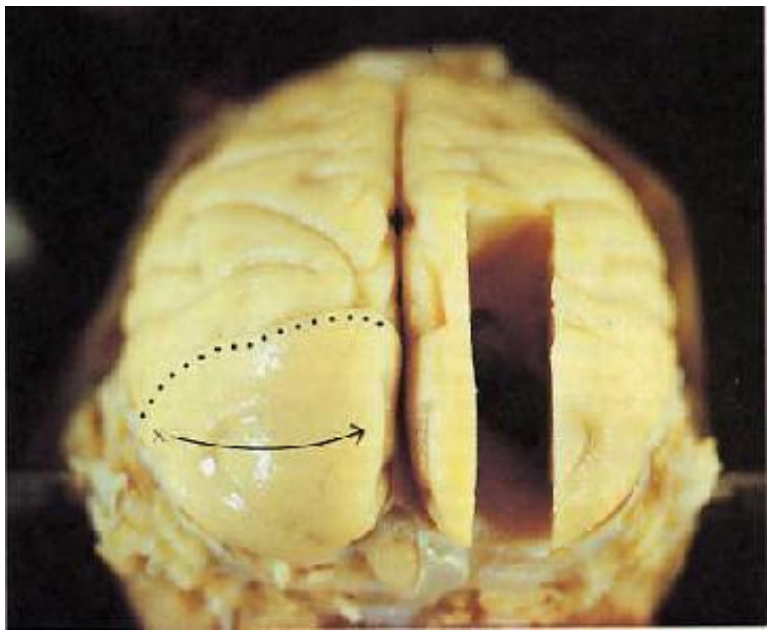
“Striate cortex”

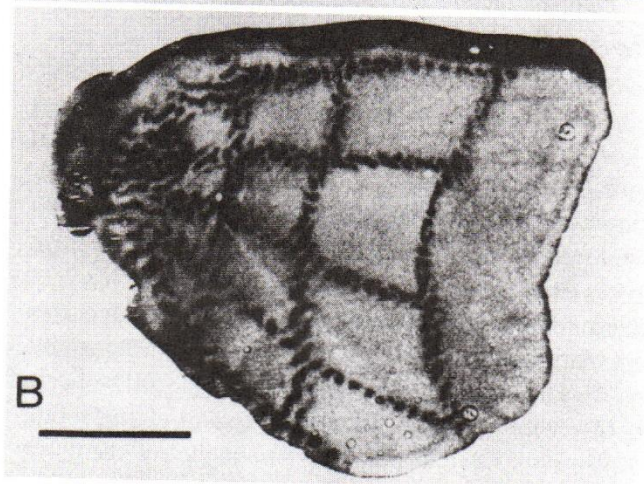
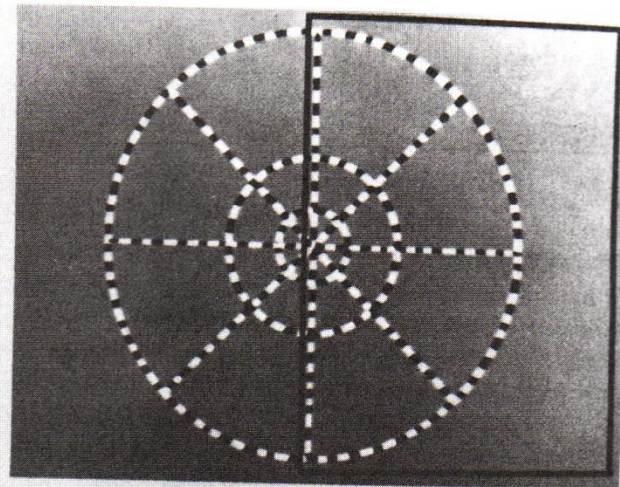
“Area 17”

Hubel & Wiesel, 1959 (HMS)

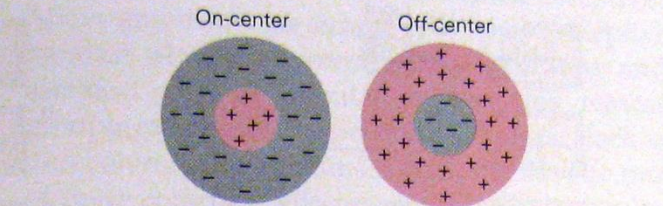




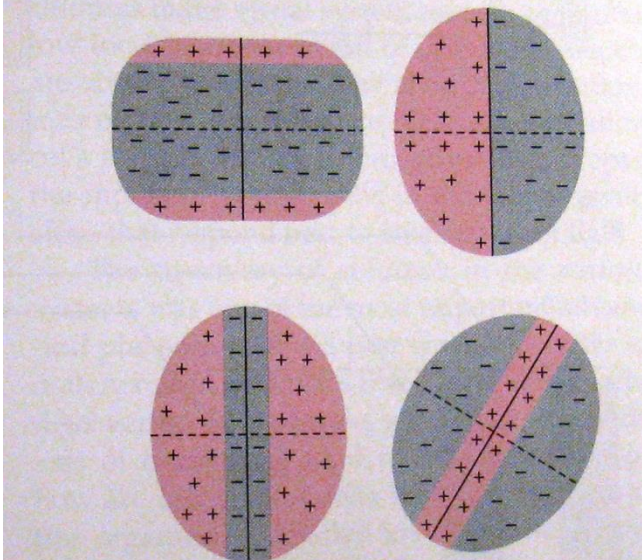




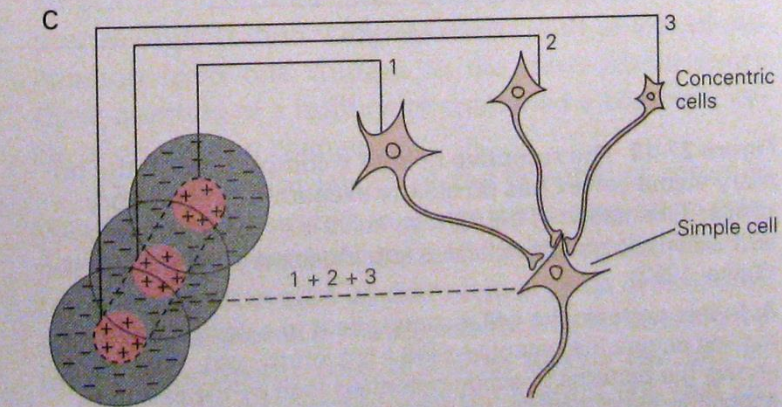
A Receptive fields of concentric cells of retina and lateral geniculate nucleus



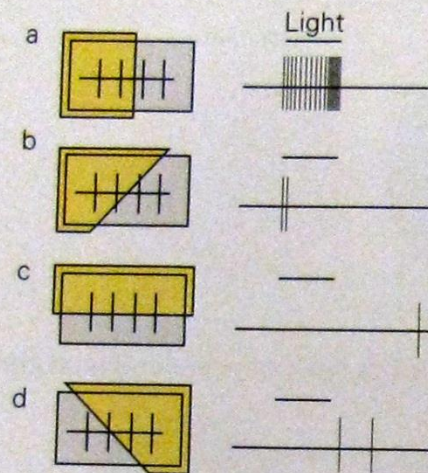
B Receptive fields of simple cells of primary visual cortex



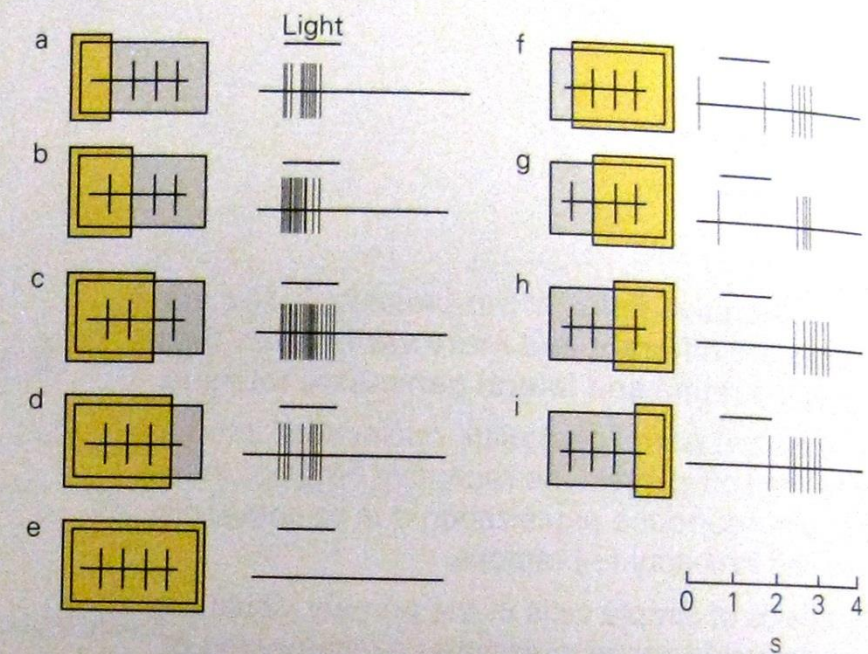
C



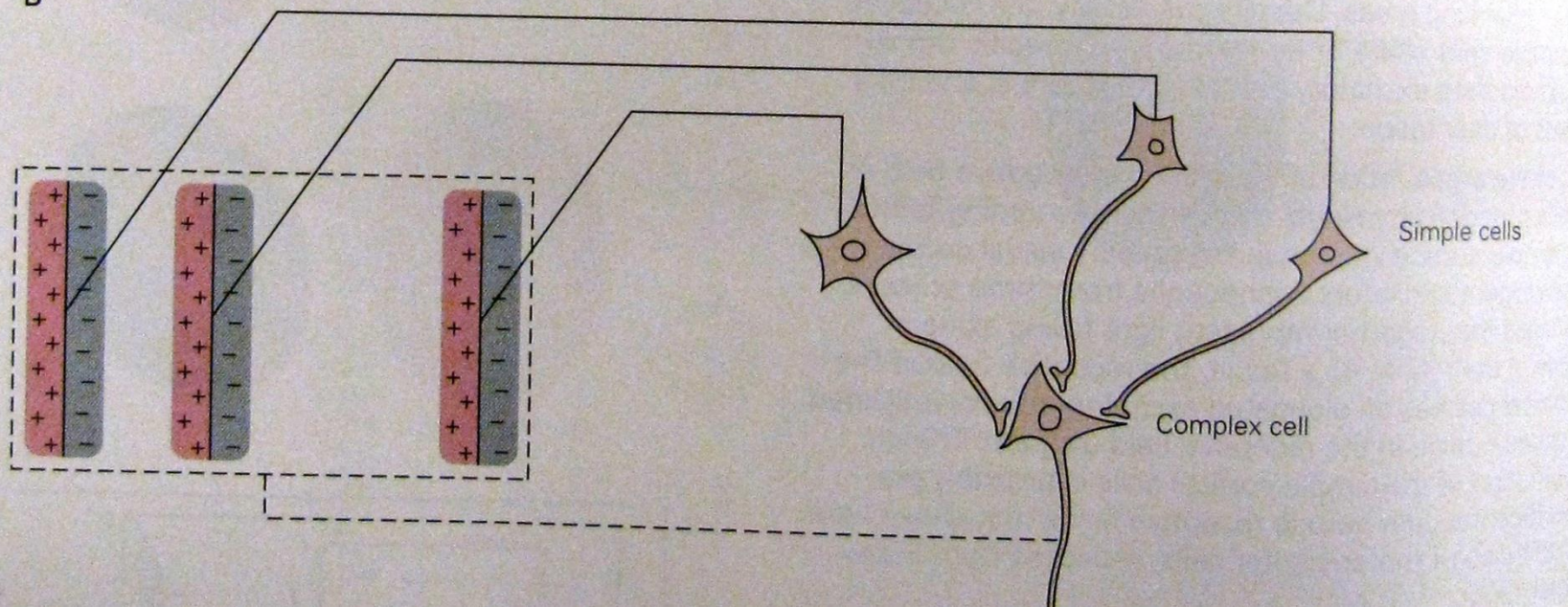
A₁ Response to orientation of stimulus



A₂ Response to position of stimulus



B



Unit 3003 CAT CONTRAlateral

Oct 2/58

Frontal 0, no H&C

Pen: 3004, 3005

Depth less than 2 mm.

Tungsten, fine.

Anes. nembutal, succ.chl., surital.

Near centralis: just on edge, contralateral field

Some spont. act., not very brisk. Responses good.

Pictures taken of mvt. back & forth 3-9 & 6-12;

4 hours, had died when lesion made also spot vs donut, 2 resp?

Cell very probably-- typical notch

Lesion: 5uAmps x 5 secs., made while recording

unit 3004 which accompanied this unit for many

hours but outlasted it. Cylinder yanked off by mist

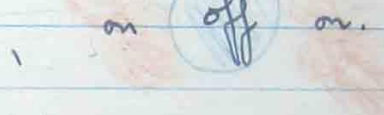
ake before retracting elect., which however was not

badly hooked. Perfusion OK, brain out stat.

(cent.
twis)

3004 cental
OK

off



2 resp?

1 resp.

158 rot
24.5 az.

1 resp.

Comments: Field asymm. circularly, fairly symm about a horizontal axis with an off centre & on areas to either side. 1° spot effective. 2 resp. to mvt. to right (as seen thro ophthslmoscope) one to left. To up & down one or no resp--hard to compare the 2 but up seemed better. Whole area took in 10° or so. 2-12 donut ineffective but 4-12 gave a nice on resp, if a little late.

Unit 3004 CAT Contralateral

Oct 2/58

Frontal 0 (no H-C)

Pen: 3003, 3005

Depth less than 2 mm.

Tungsten, fine

(Inc of surital gave no

Anes nemb, succ chl, surital : (change in act or resps.

Near Centralis: contralat edge of it

Spont act more than companion 3003

Pictures: Nice ones of 11, 2:30, 5:30, 8:30

4 hours: killed by lesion.

Cell very probably: typical notch

Lesion: see 3003

contralat

only
mvt

the
further
one.

→
2 resp?

contral
3003.

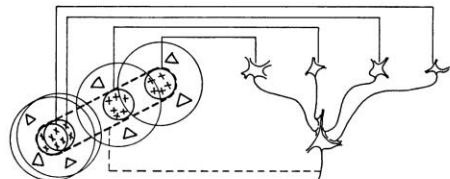
Comments: Receptive field v. sim. to 3003-- all little nearer to centralis, likewise an off centre. Perhaps a bit smaller. Centre was clearly elongated in a vertical axis roughly, while peripheral regions were concentrated to either side, with nothing apparently above or below. Again, 2 resps to mvt away from the centralis, only one for 'leftward' mvt. Up & down sim hard to assess: at most one response. 1° stat spot was good; $\frac{1}{2}$ ° worked. Donuts not so hot, as one would expect.

Hubel & Wiesel, 1962

142

D. H. HUBEL AND T. N. WIESEL

field such as that of Text-fig. 2F) are of the same order of magnitude as the diameters of geniculate receptive-field centres, at least for fields in or near the area centralis. Hence the fineness of discrimination implied by the small size of geniculate receptive-field centres is not necessarily lost at the cortical level, despite the relatively large total size of many cortical fields; rather, it is incorporated into the detailed substructure of the cortical fields.



Text-fig. 19. Possible scheme for explaining the organization of simple receptive fields. A large number of lateral geniculate cells, of which four are illustrated in the upper right in the figure, have receptive fields with 'on' centres arranged along a straight line on the retina. All of these project upon a single cortical cell, and the synapses are supposed to be excitatory. The receptive field of the cortical cell will then have an elongated 'on' centre indicated by the interrupted lines in the receptive-field diagram to the left of the figure.

In a similar way, the simple fields of Text-fig. 2D-G may be constructed by supposing that the afferent 'on'- or 'off'-centre geniculate cells have their field centres appropriately placed. For example, field-type G could be formed by having geniculate afferents with 'off' centres situated in the region below and to the right of the boundary, and 'on' centres above and to the left. An asymmetry of flanking regions, as in field E, would be produced if the two flanks were unequally reinforced by 'on'-centre afferents.

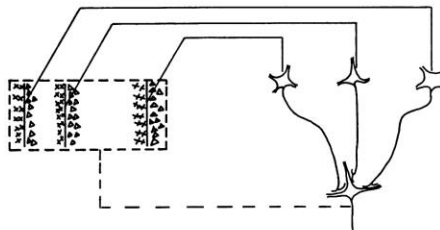
The model of Text-fig. 19 is based on excitatory synapses. Here the suppression of firing on illuminating an inhibitory part of the receptive field is presumed to be the result of withdrawal of tonic excitation, i.e. the inhibition takes place at a lower level. That such mechanisms occur in the visual system is clear from studies of the lateral geniculate body, where an 'off'-centre cell is suppressed on illuminating its field centre because of suppression of firing in its main excitatory afferent (Hubel & Wiesel, 1961). In the proposed scheme one should, however, consider the possibility of direct inhibitory connexions. In Text-fig. 19 we may replace any of the excitatory endings by inhibitory ones, provided we replace the corresponding geniculate cells by ones of opposite type ('on'-centre instead of 'off'-centre, and conversely). Up to the present the two mechanisms have

CAT VISUAL CORTEX

143

not been distinguished, but there is no reason to think that both do not occur.

The properties of complex fields are not easily accounted for by supposing that these cells receive afferents directly from the lateral geniculate body. Rather, the correspondence between simple and complex fields noted in Part I suggests that cells with complex fields are of higher order, having cells with simple fields as their afferents. These simple fields would all have identical axis orientation, but would differ from one another in their exact retinal positions. An example of such a scheme is given in Text-fig. 20. The hypothetical cell illustrated has a complex field like that



Text-fig. 20. Possible scheme for explaining the organization of complex receptive fields. A number of cells with simple fields, of which three are shown schematically, are imagined to project to a single cortical cell of higher order. Each projecting neurone has a receptive field arranged as shown to the left: an excitatory region to the left and an inhibitory region to the right of a vertical straight-line boundary. The boundaries of the fields are staggered within an area outlined by the interrupted lines. Any vertical-edge stimulus falling across this rectangle, regardless of its position, will excite some simple-field cells, leading to excitation of the higher-order cell.

of Text-figs. 5 and 6. One may imagine that it receives afferents from a set of simple cortical cells with fields of type G, Text-fig. 2, all with vertical axis orientation, and staggered along a horizontal line. An edge of light would activate one or more of these simple cells wherever it fell within the complex field, and this would tend to excite the higher-order cell.

Similar schemes may be proposed to explain the behaviour of other complex units. One need only use the corresponding simple fields as building blocks, staggering them over an appropriately wide region. A cell with the properties shown in Text-fig. 3 would require two types of horizontally oriented simple fields, having 'off' centres above the horizontal line, and 'on' centres below it. A slit of the same width as these centre regions would strongly activate only those cells whose long narrow

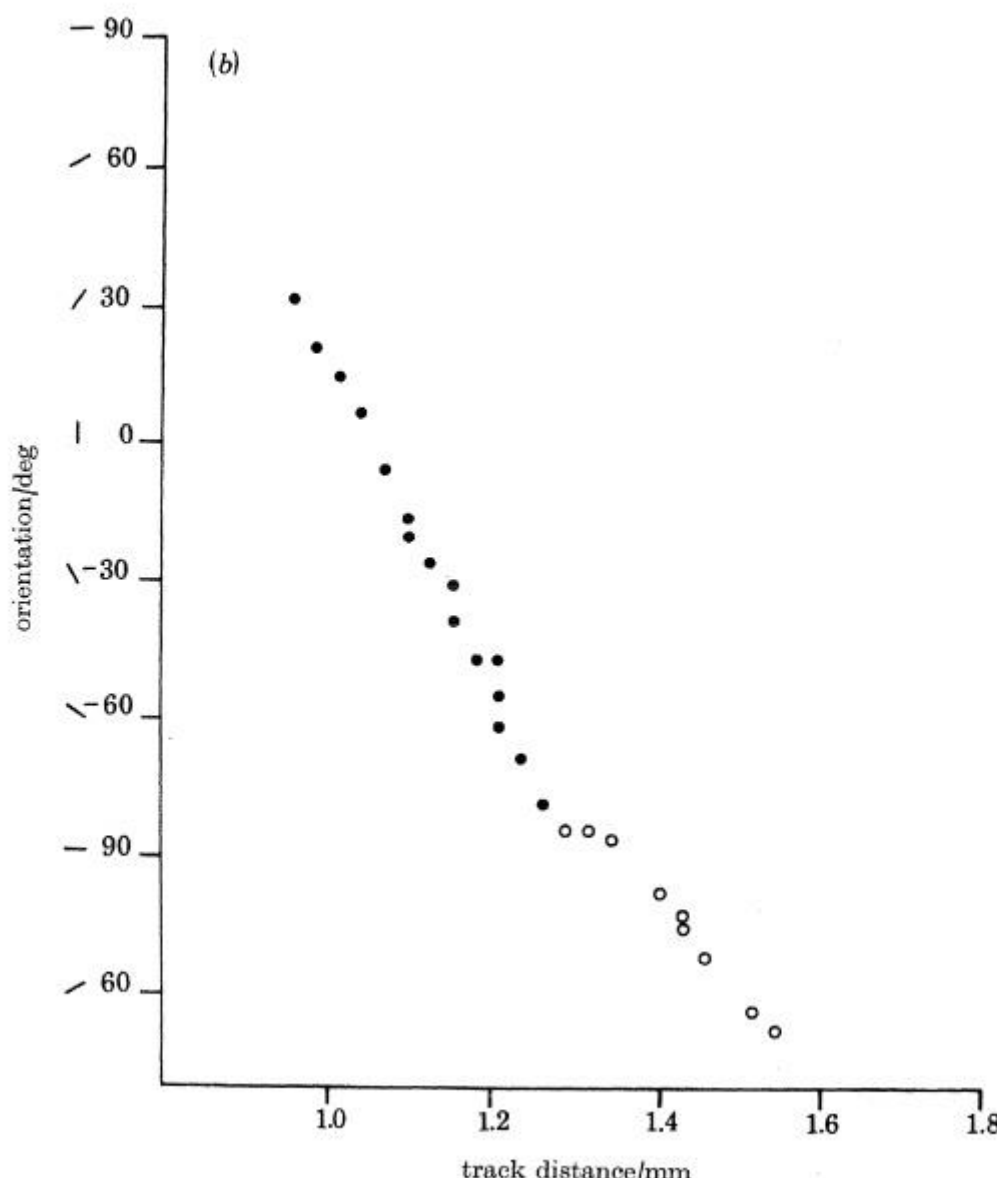


FIGURE 15(b). Graph of orientation in degrees plotted against electrode track distance in millimetres, for the sequence illustrated in 15a. ●, cells dominated by right eye; ○, left eye.

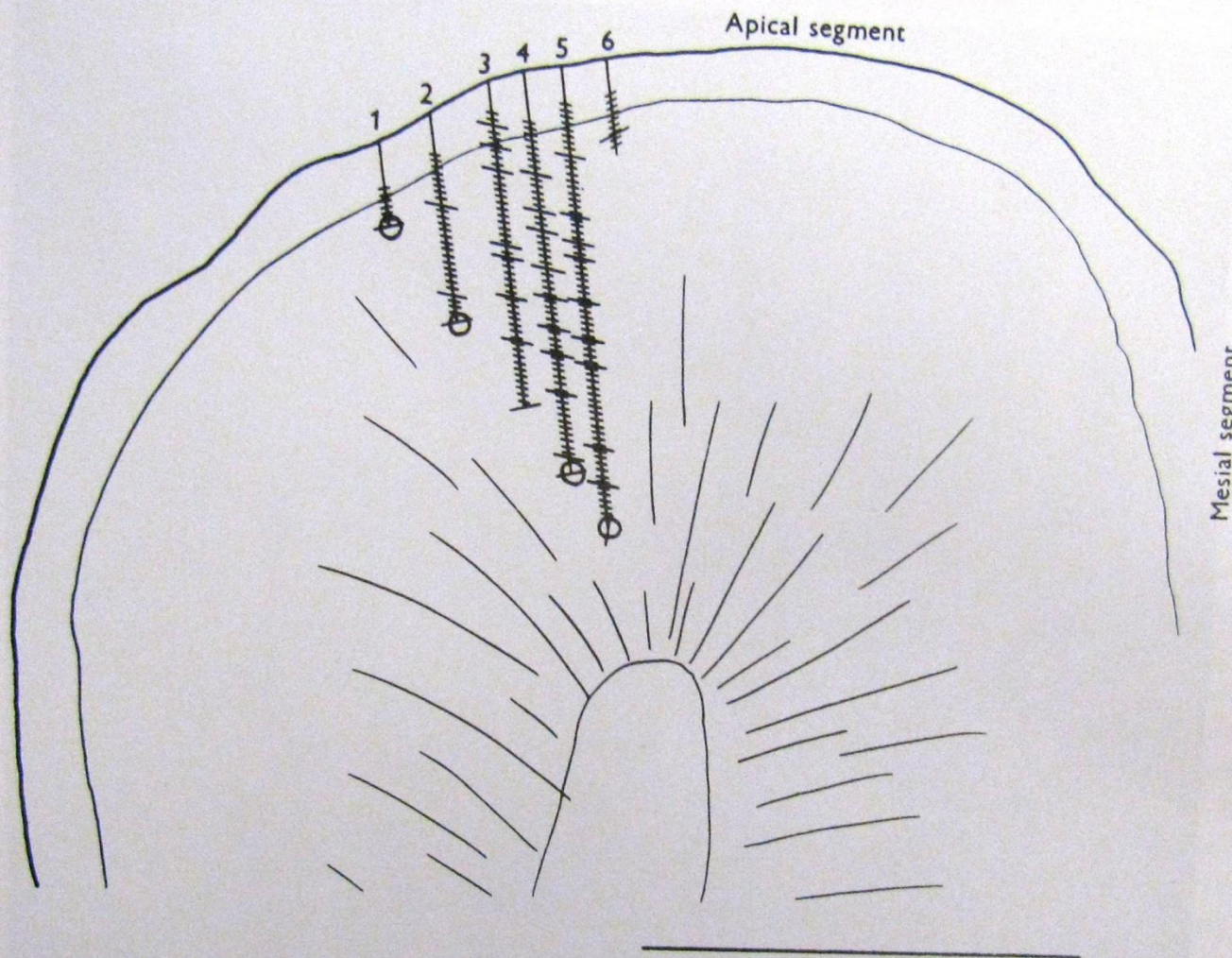


Fig. 8. Coronal section through cat visual cortex showing reconstructions of 6 parallel microelectrode penetrations. (Nos. 1, 2, 4 and 5 end with lesions shown as circles.) Short lines perpendicular to tracks indicate receptive-field orientation; lines perpendicular to tracks represent horizontal orientation. (The longer of these lines represent single cells, the shorter ones, multiple unit recordings). Most of the territory traversed by penetrations 2–5 is in one orientation column, whose left hand border lies at the ends of tracks 2–4. Scale 1 mm. (Figure 2 (18)).

Functional Architecture

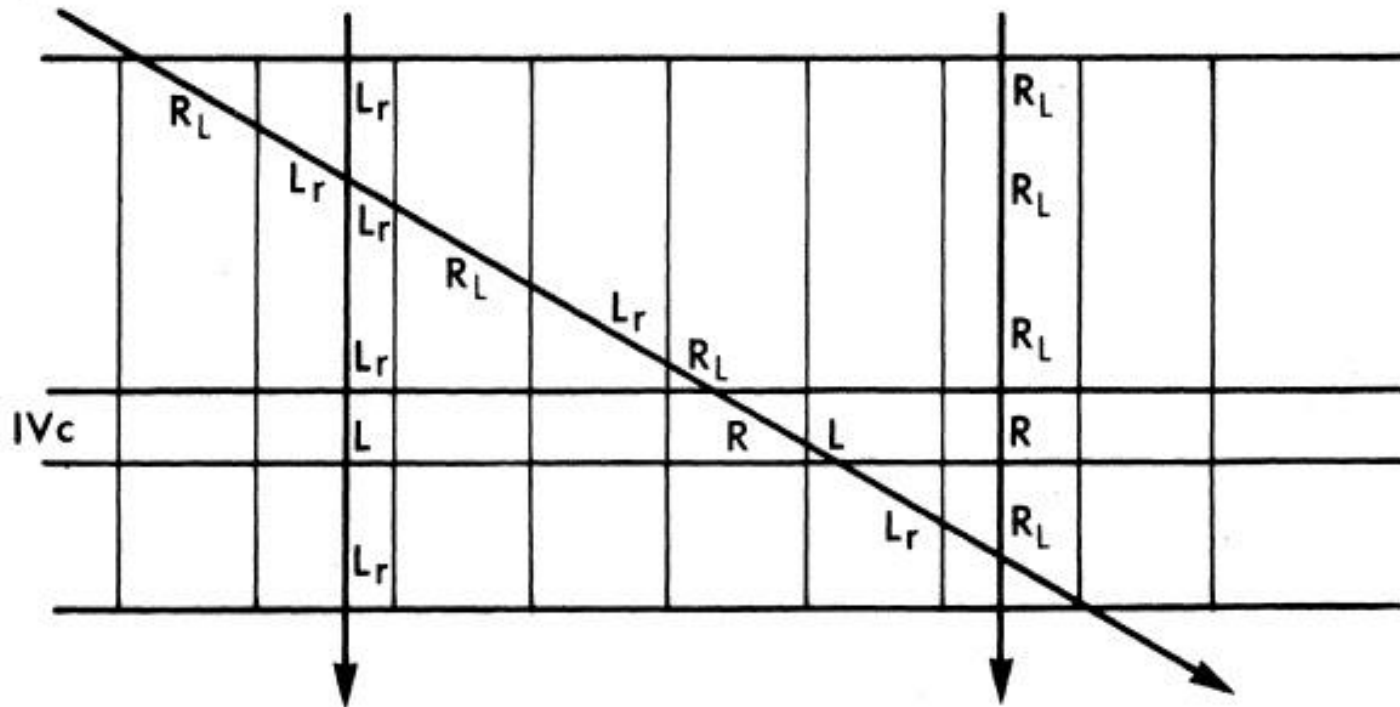
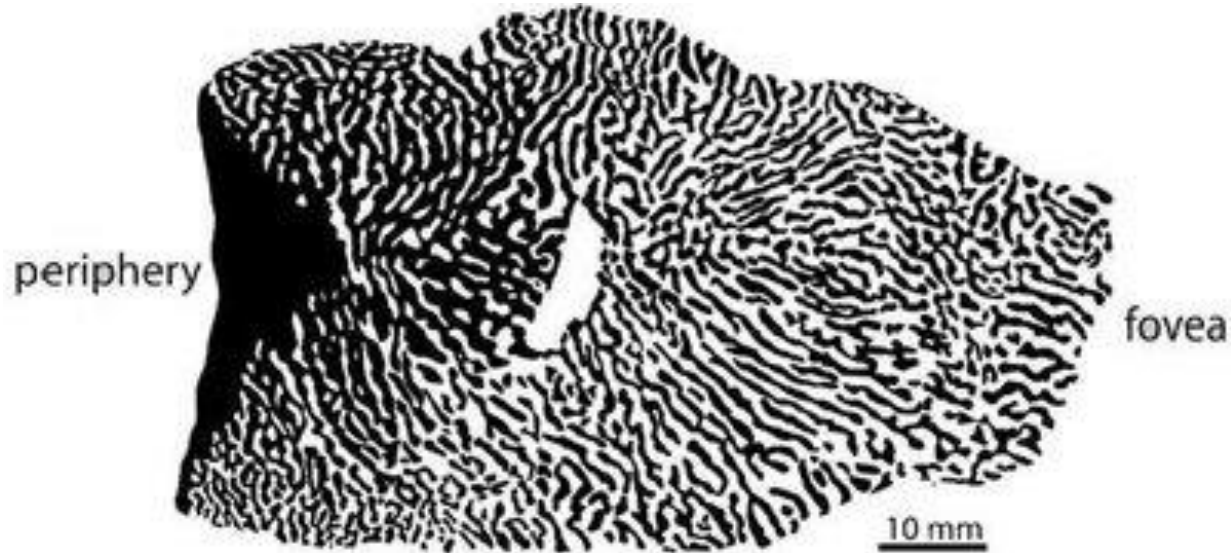
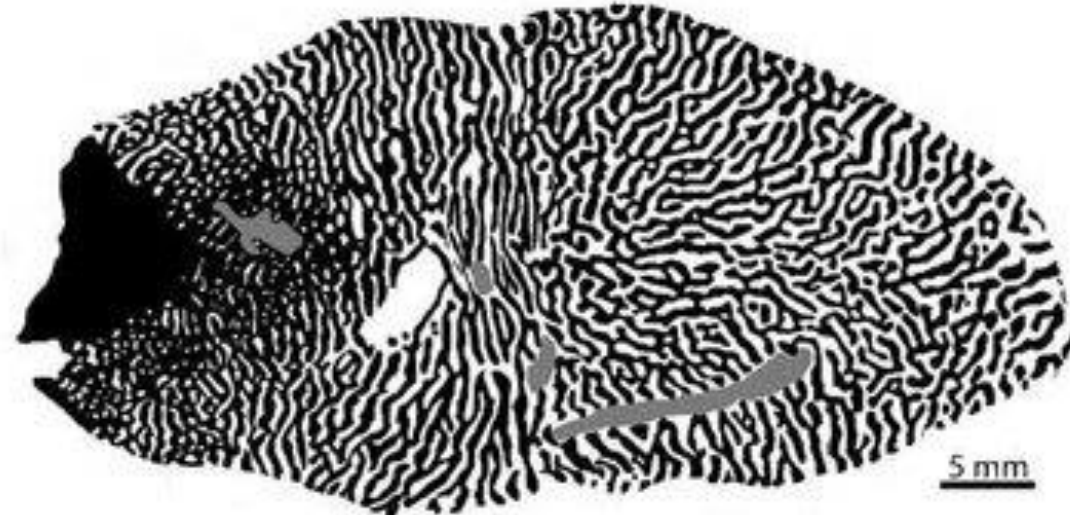


FIGURE 11. Illustration of ocular dominance columns in macaque monkey. The diagram represents a cross section through striate cortex, with surface at top and border between layer VI and white matter below. Two vertical penetrations and one oblique are illustrated. Letters refer to expected eye dominance at various stages in each penetration. R_L stands for a region in which there is a mixture of binocular cells preferring the right eye, and monocular cells responding to the right eye. R stands for a region containing only cells driven exclusively from the right eye. Layer IVc contains only monocular cells, grouped separately in patches according to eye affiliation. Layers above and below IVc contain binocular cells, grouped in columns according to eye preference. When a vertical penetration reaches IVc the eye that has been preferred all along comes to monopolize. In an oblique or horizontal penetration there is a regular alternation of eye preference as the electrode goes from column to column.

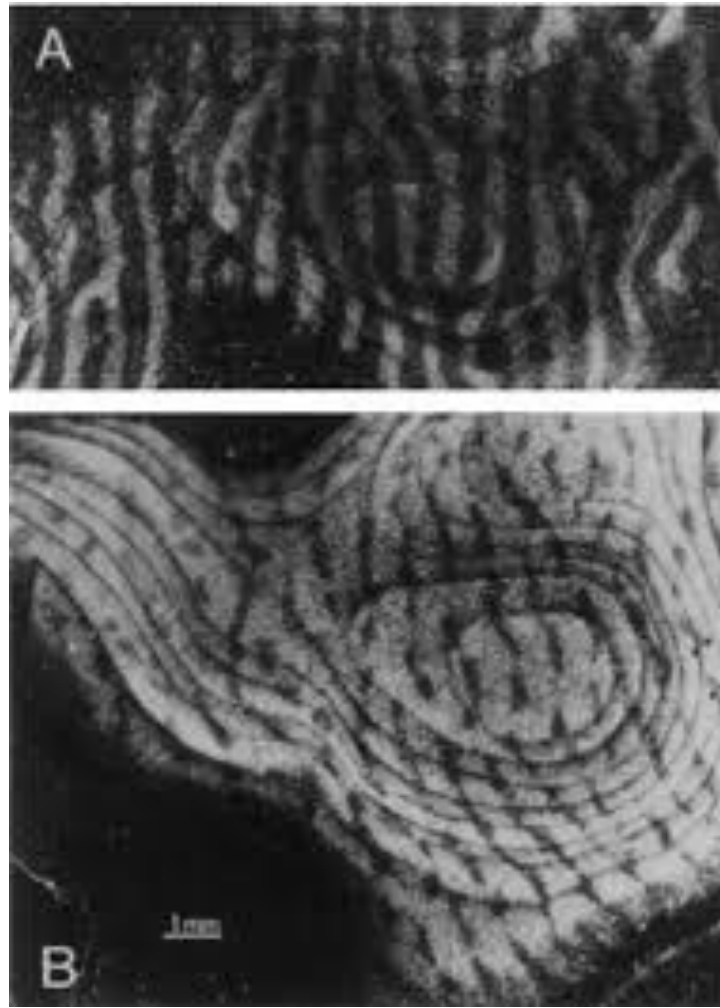


Monkey



Human

Critical Period



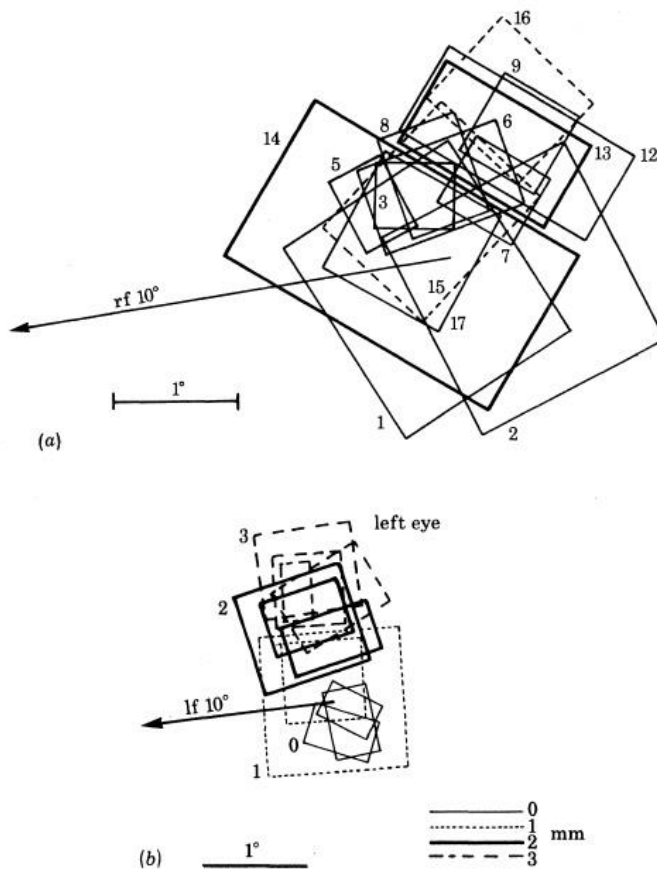


FIGURE 8. (a) Receptive-field scatter: Receptive-field boundaries of 17 cells recorded in a penetration through monkey striate cortex, in a direction perpendicular to the surface. Note the variation in size, and the more or less random scatter in the precise positions of the fields. The penetration was made in a part of the cortex corresponding to a visual field location 10° from the centre of gaze, just above the horizontal meridian. Fields are shown for one eye only. Numbers indicate the order in which the cells were recorded. (From Hubel & Wiesel 1974b.) (b) Receptive-field drift: Receptive fields mapped during an oblique, almost tangential penetration through striate cortex, in roughly the same region as in a. A few fields were mapped along each of four $100\ \mu\text{m}$ segments, spaced at $1\ \text{mm}$ intervals. These four groups of fields were labelled 0, 1, 2 and 3. Each new set of fields was slightly above the other, as predicted from the direction of movement of the electrode. Roughly a $2\ \text{mm}$ movement through cortex was required to displace the fields from one region to an entirely new region. (From Hubel & Wiesel 1974b.)

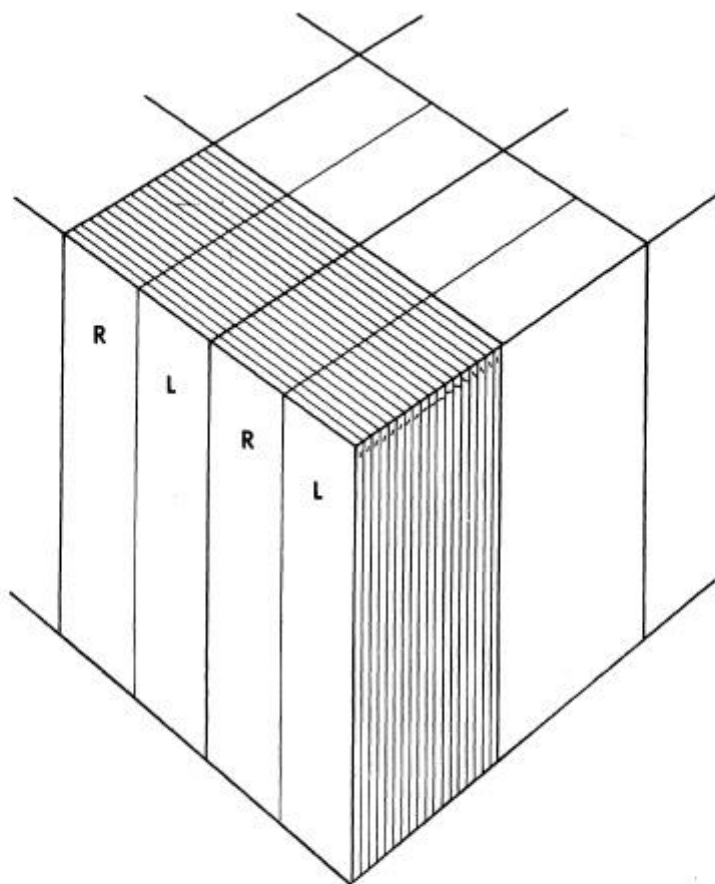
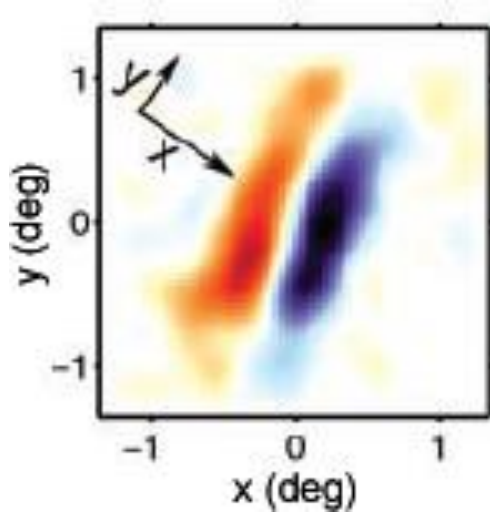
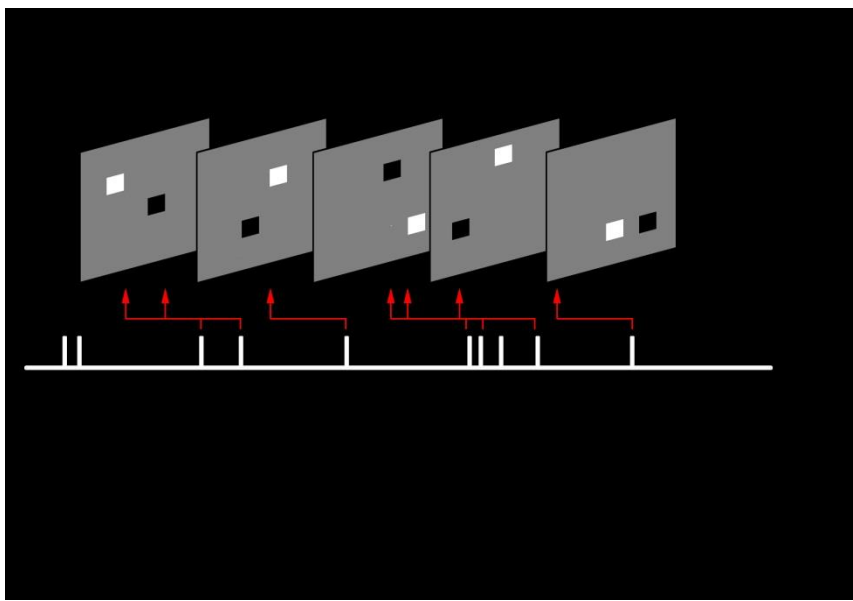
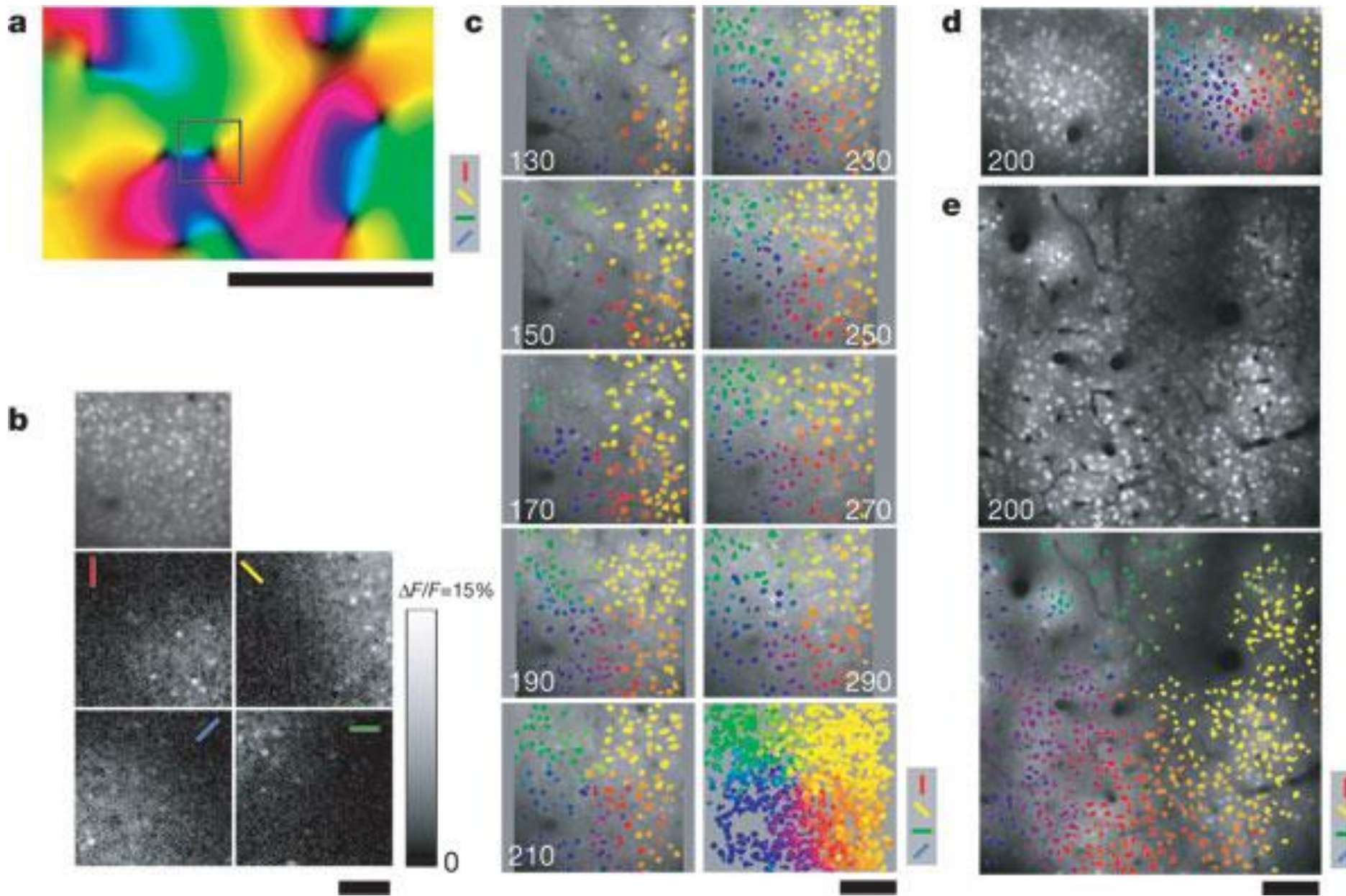


FIGURE 27. Model of the striate cortex, to show roughly the dimensions of the ocular dominance slabs (L, R) in relation to the orientation slabs and the cortical thickness. Thinner lines separate individual columns; thicker lines demarcate hypercolumns, two pairs of ocular dominance columns and two sets of orientation columns. The placing of these hypercolumn boundaries is of course arbitrary; one could as well begin at horizontal or any of the obliques. The decision to show the two sets of columns as intersecting at right angles is also arbitrary, since there is at present no evidence as to the relationship between the two sets. Finally, for convenience the slabs are shown as plane surfaces, but whereas the dominance columns are indeed more or less flat, the orientation columns are not known to be so, and may when viewed from above have the form of swirls.





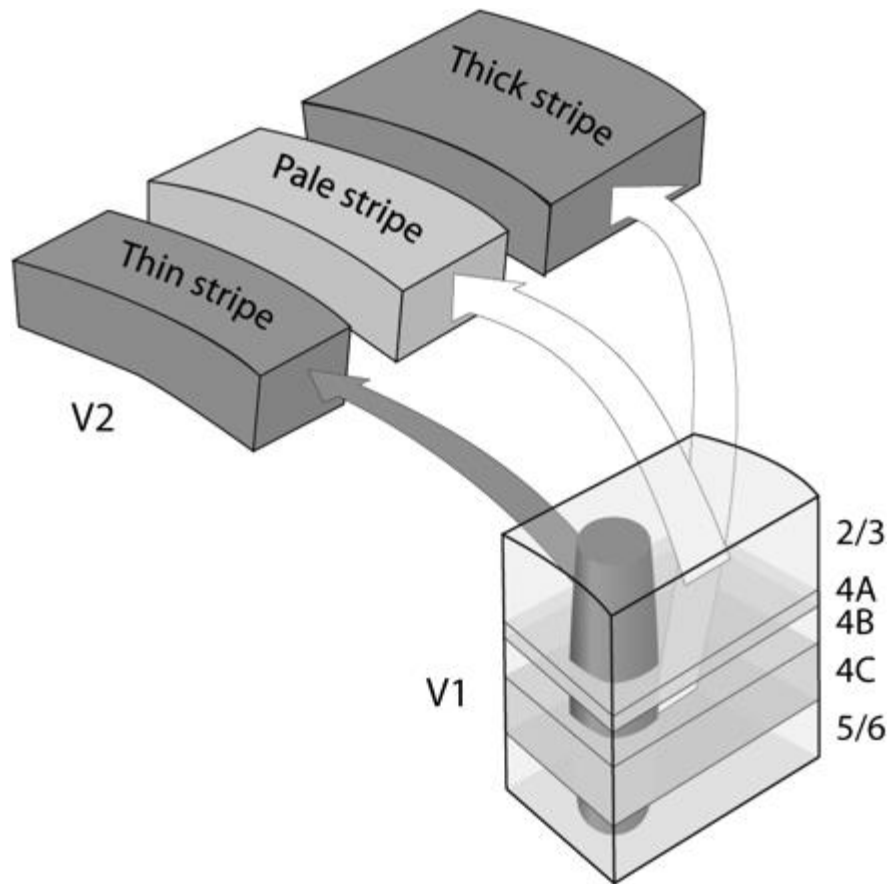
Features computed by V1

- Orientation
- Color
- Motion
- Binocular Disparity

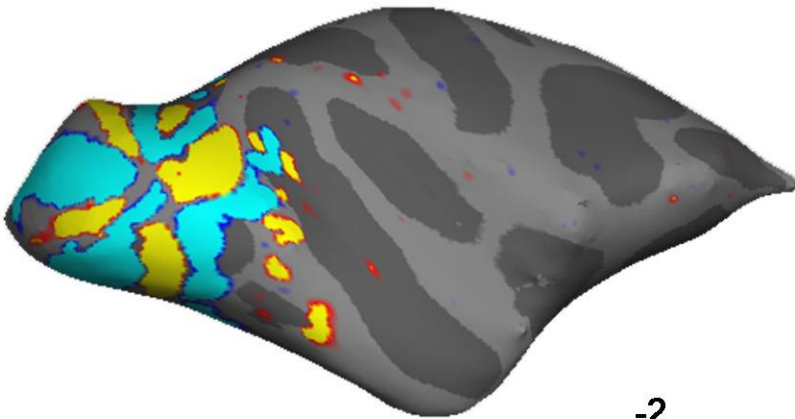
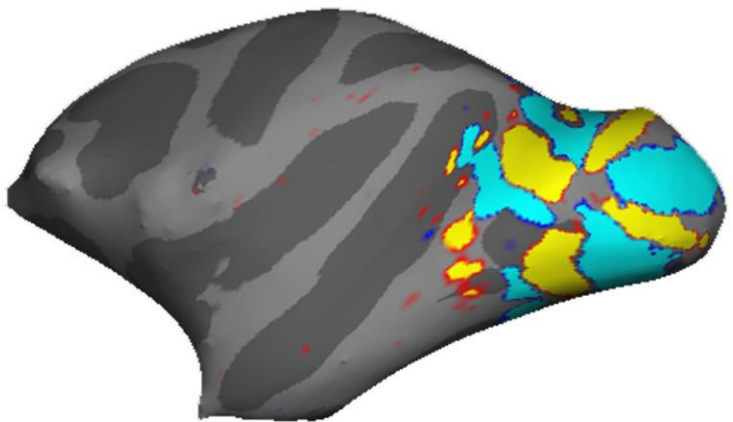
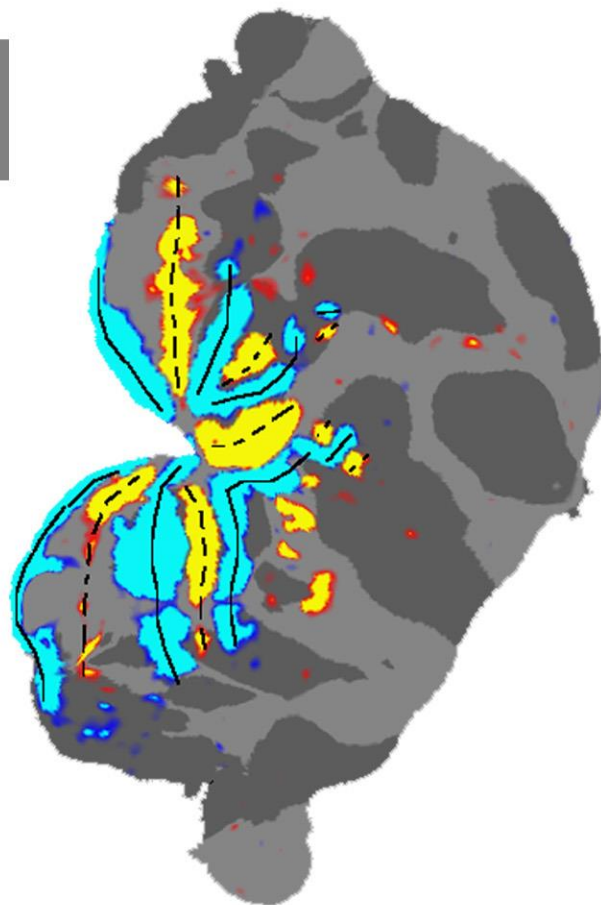
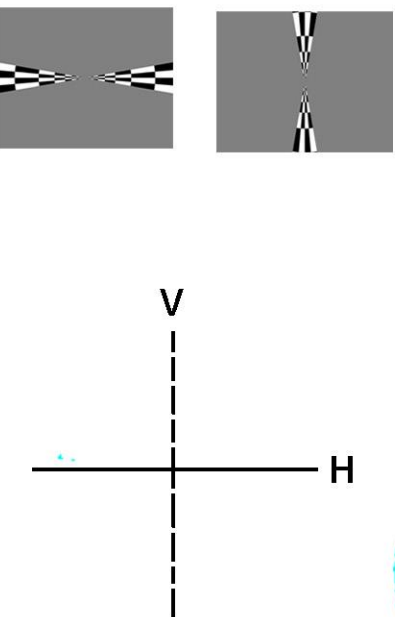
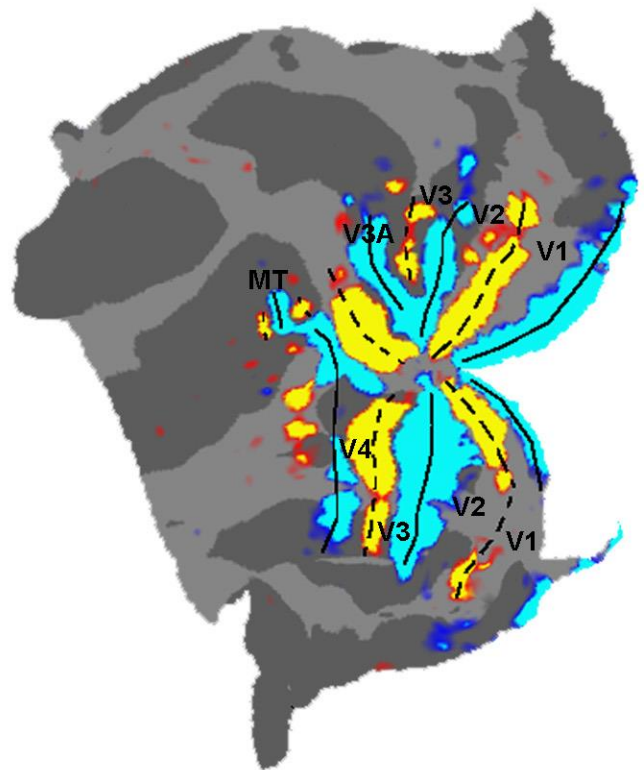
What happens to visual information after V1?



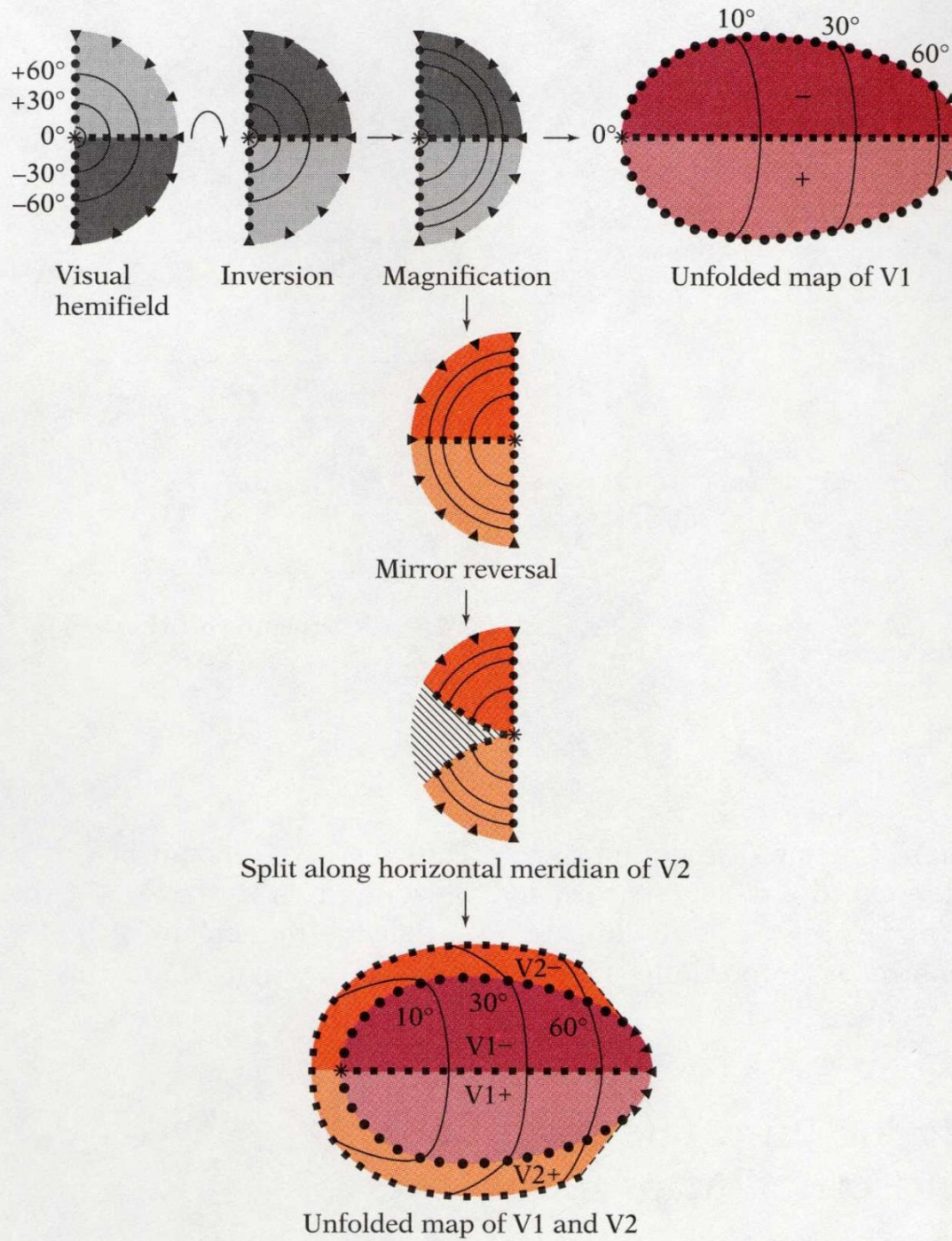
Sincich, LC and Horton, JC. 2005
Annu. Rev. Neurosci. 28: 303–26



What happens to visual information after V2?

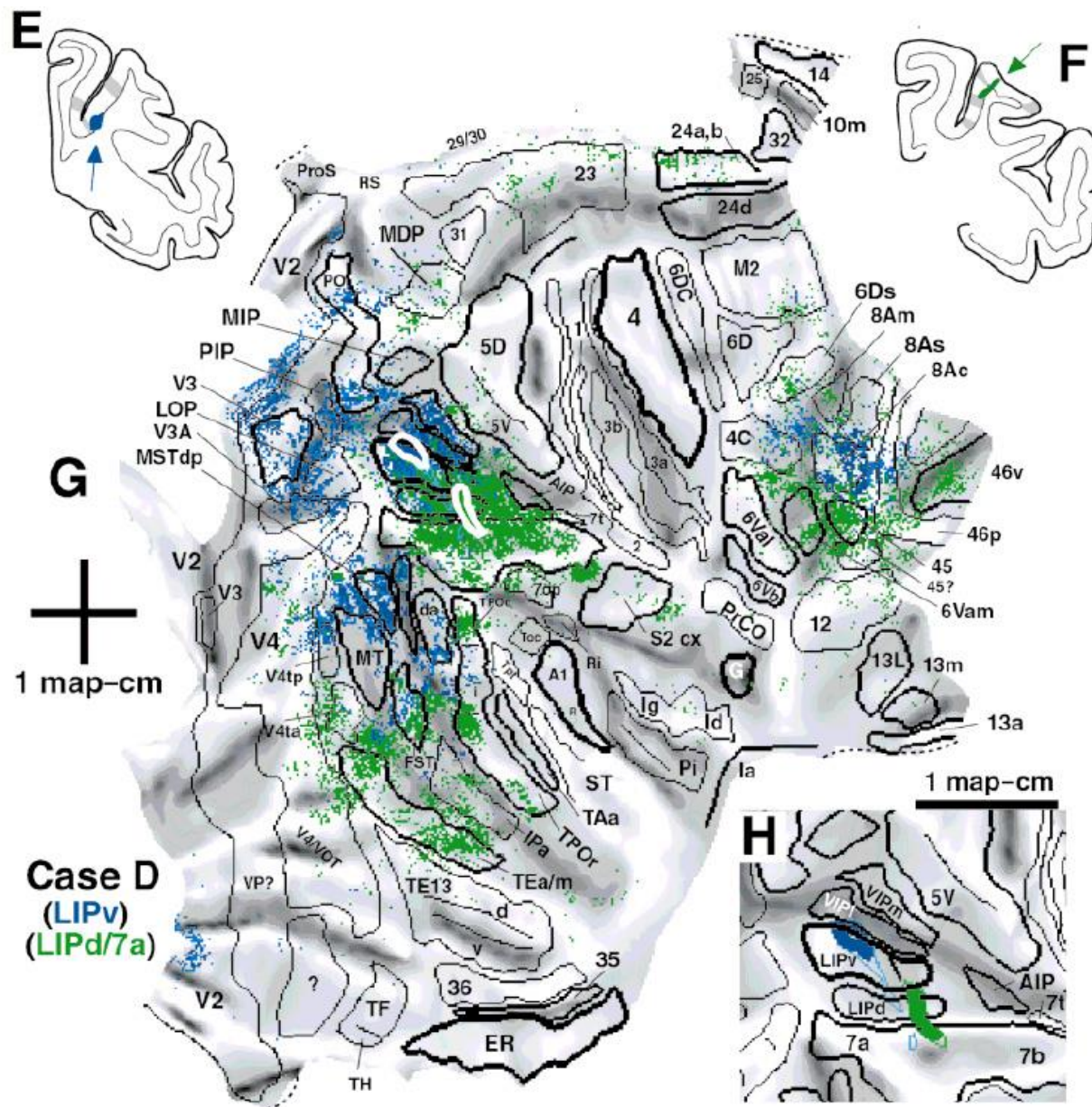


$p < 10^{-2}$

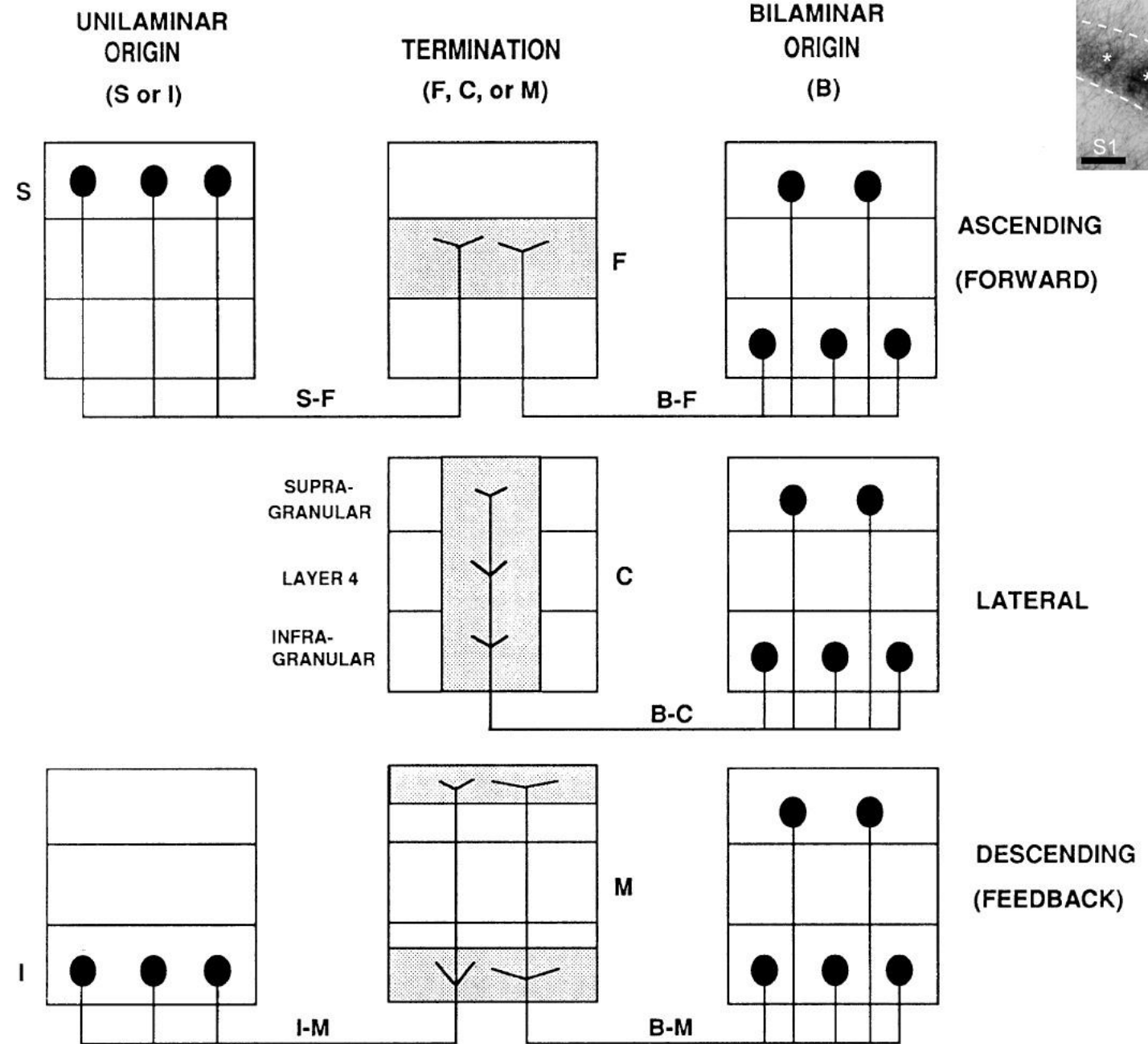


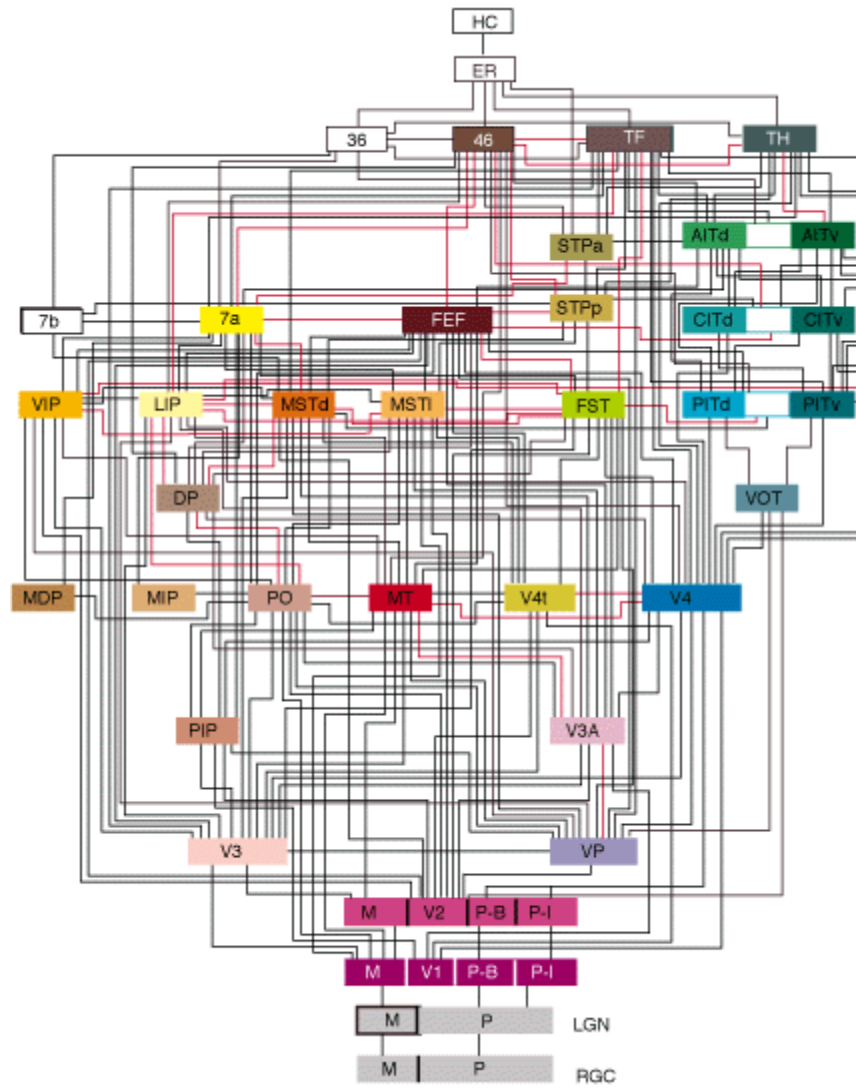
Criteria for Cortical Area

- Topographic map
- Unique connections
- Unique cytoarchitecture
- Unique function



Lewis and Van Essen 2000





Felleman and Van Essen 1991

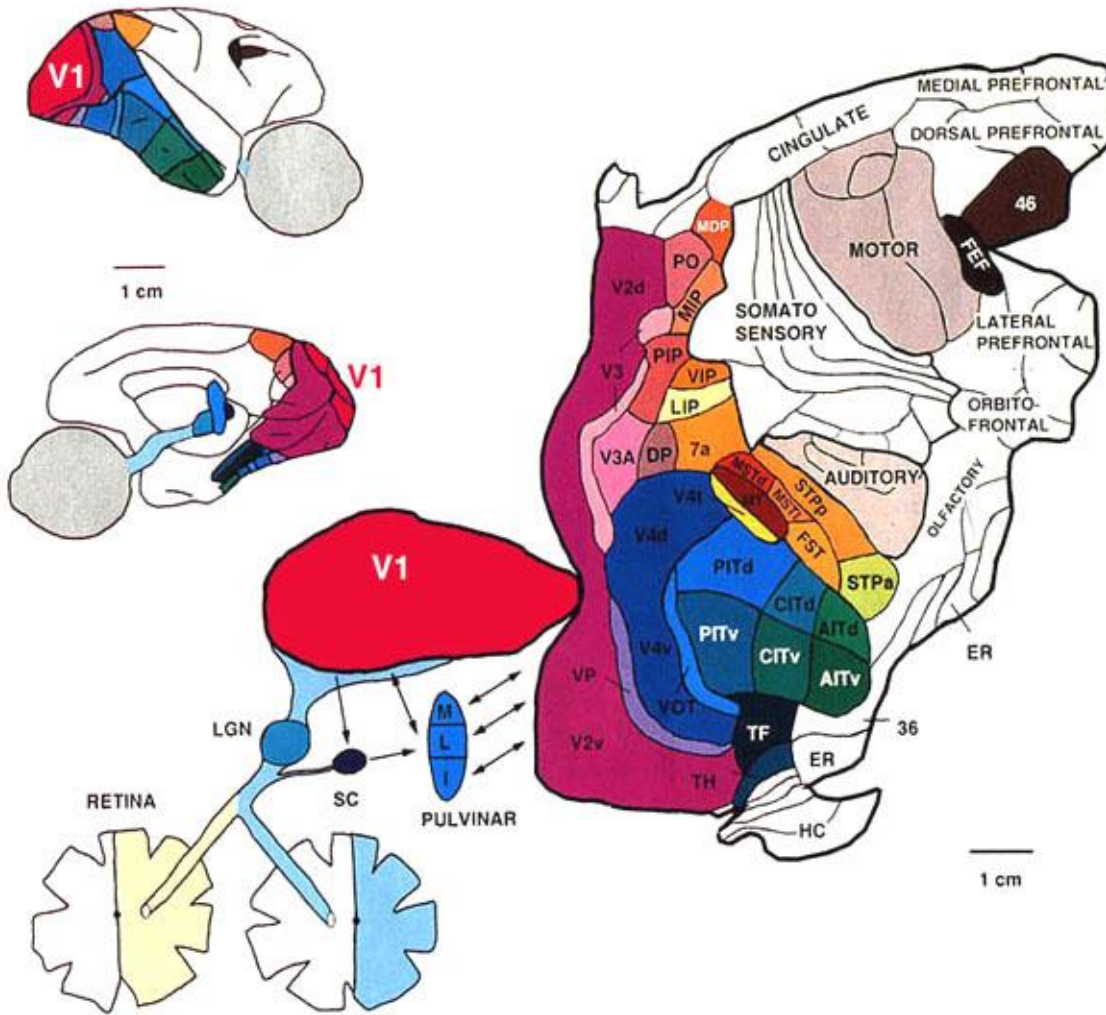
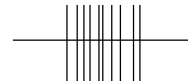


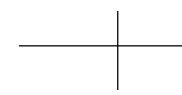
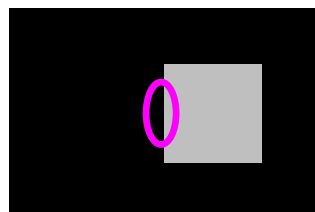
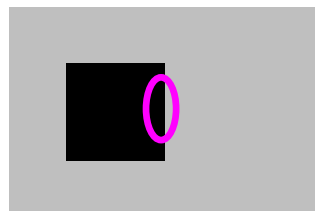
Figure 19. Much of V1 is located in the calcarine sulci and its relationship to other brain areas is best shown by unfolding the brain and showing it flattened open. The visually responsive areas of the macaque monkey are shown in color.
From Van Essen et al. (1992).

Border ownership cell

V1 Simple cell
(Hubel & Wiesel)



**V2 Border-ownership
cell**
(von der Heydt)



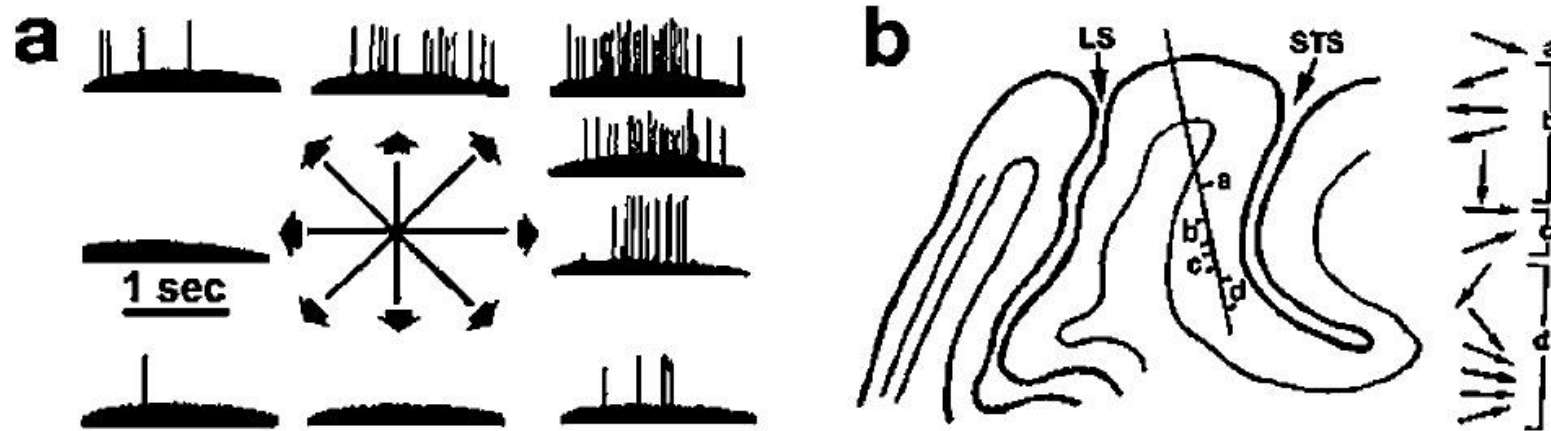
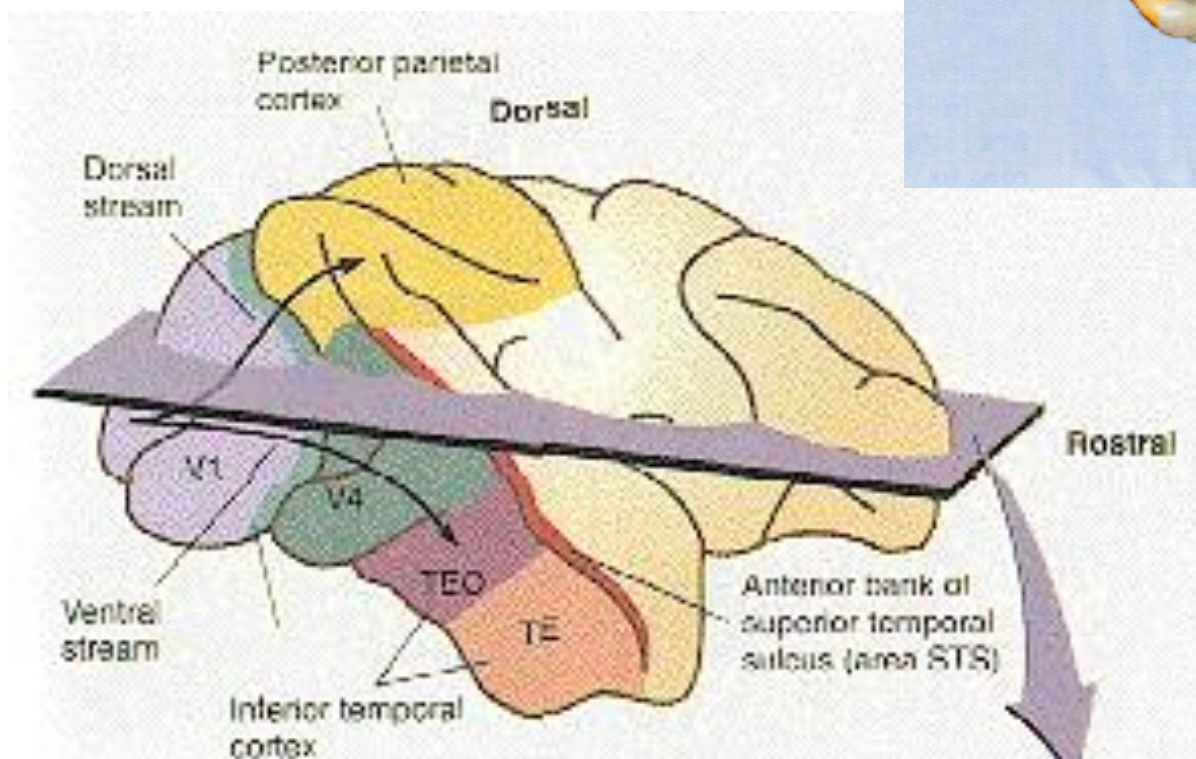
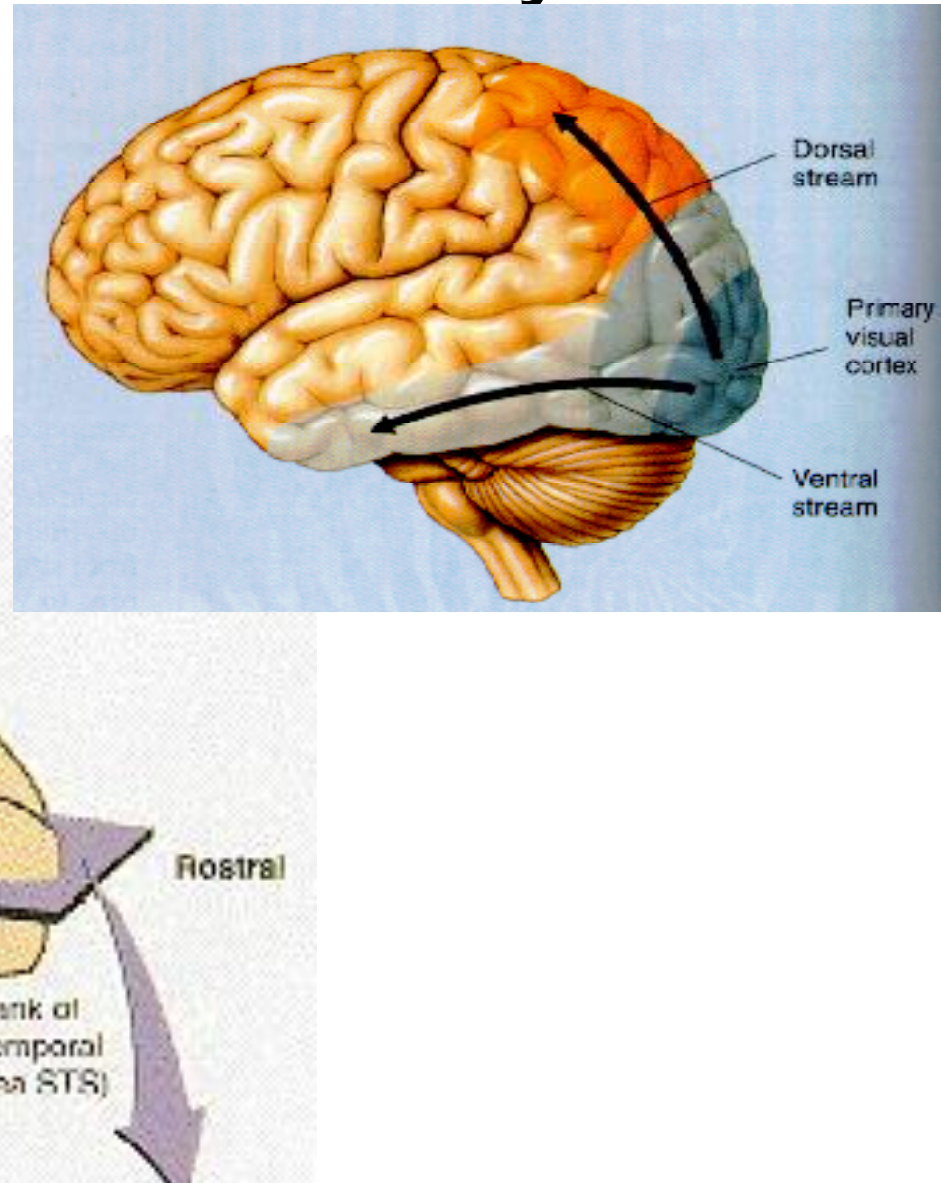


Figure 1

First demonstration of direction selectivity in macaque MT/V5 by Dubner & Zeki (1971). (a) Neuronal responses to a bar of light swept across the receptive field in different directions (modified from figure 1 of Dubner & Zeki 1971). Each trace shows the spiking activity of the neuron as the bar was swept in the direction indicated by the arrow. The neuron's preferred direction was up and to the right. (b) Oblique penetration through MT (modified from figure 3 of Dubner & Zeki 1971) showing the shifts in preferred direction indicative of the direction columns subsequently demonstrated by Albright et al. (1984). See also **Figure 4**.

What & Where Pathways

“Vision is knowing what is where by looking” –David Marr

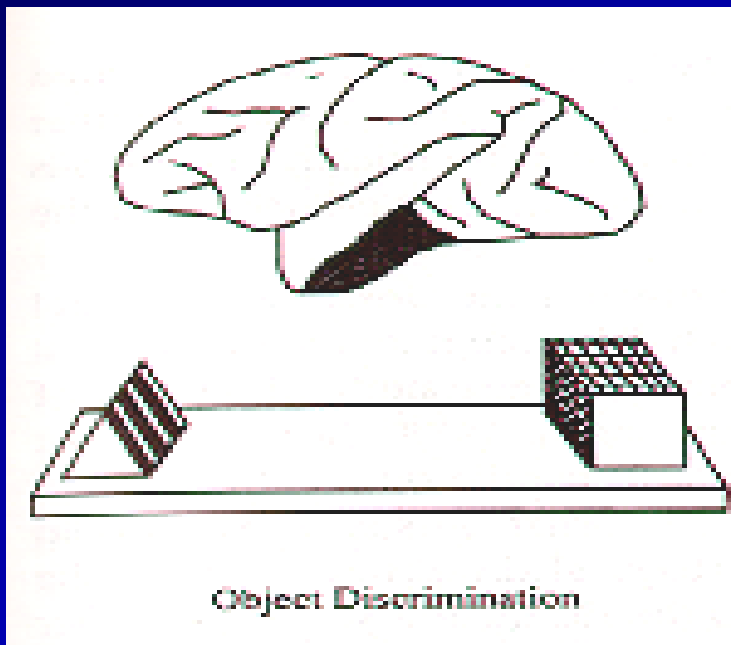


The Ungerleider & Mishkin (1982) Experiment

Task 1:

Object discrimination

- study an object
- select the familiar object
(reward)

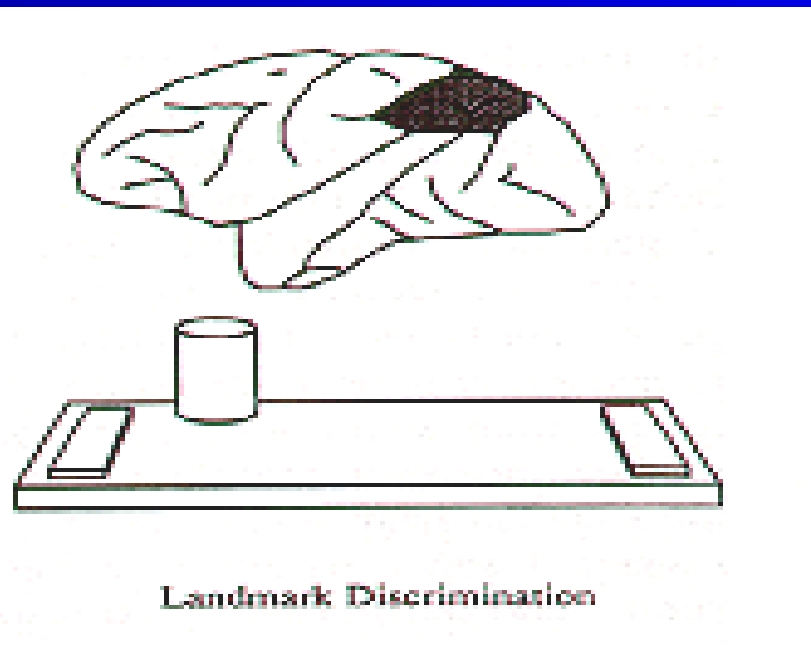


temporal lesions
impair OBJECT TASK

Task 2:

Landmark discrimination

- select foodwell closest to the TOWER



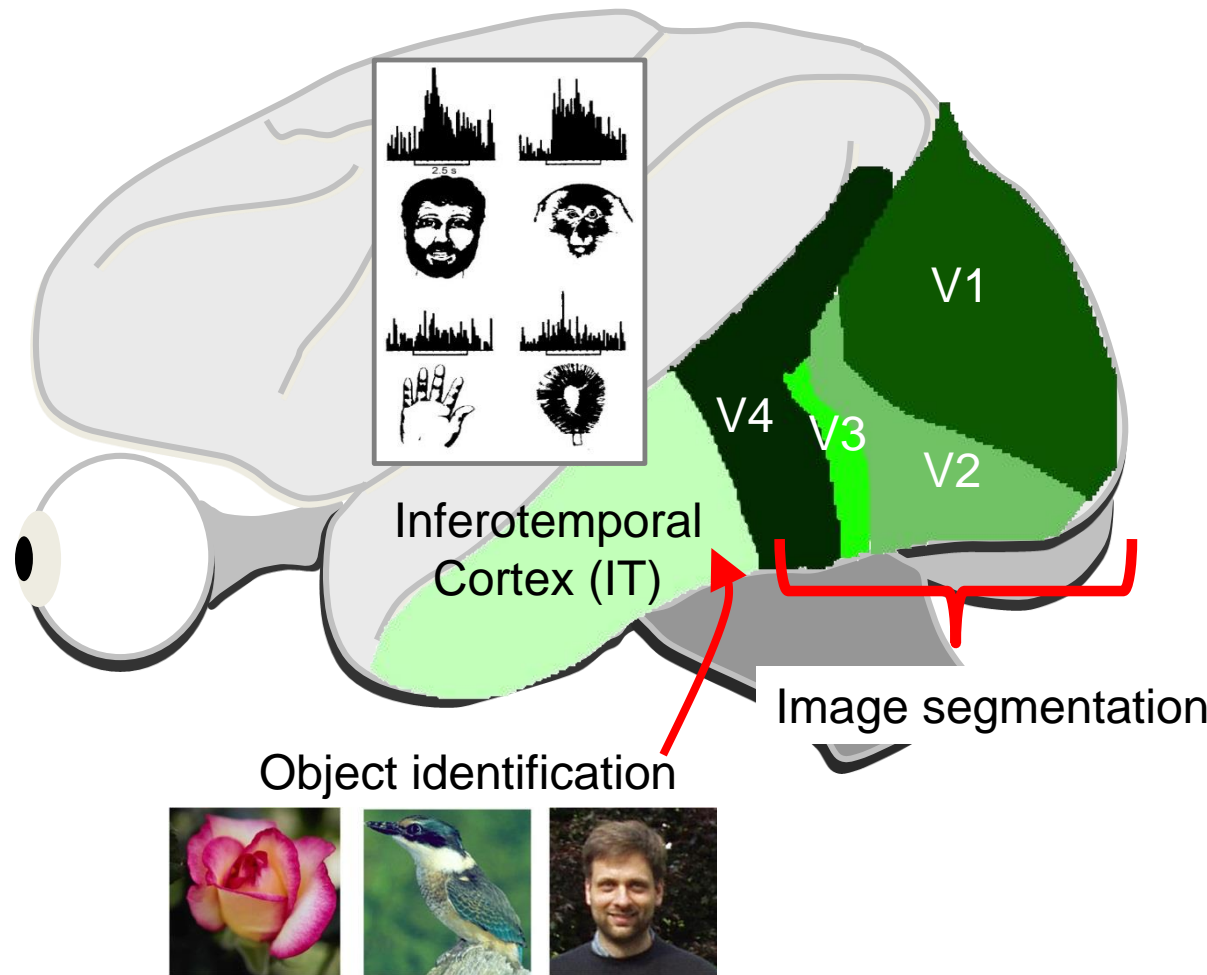
parietal lesions
impair LANDMARK TASK

The macaque face patch system

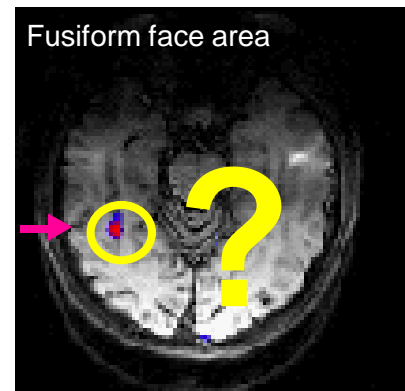
Pathway for object representation



Charles Gross



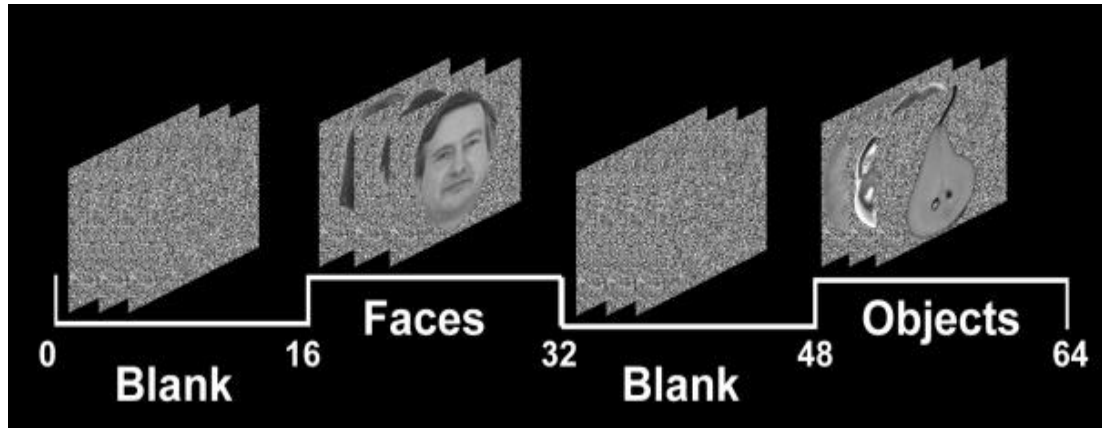
"Discouraged by my inability to understand the frontal lobe...I decided to turn my attention to the cortex on the inferior convexity of the temporal lobe" –Charles Gross, *History of Neuroscience autobiography*



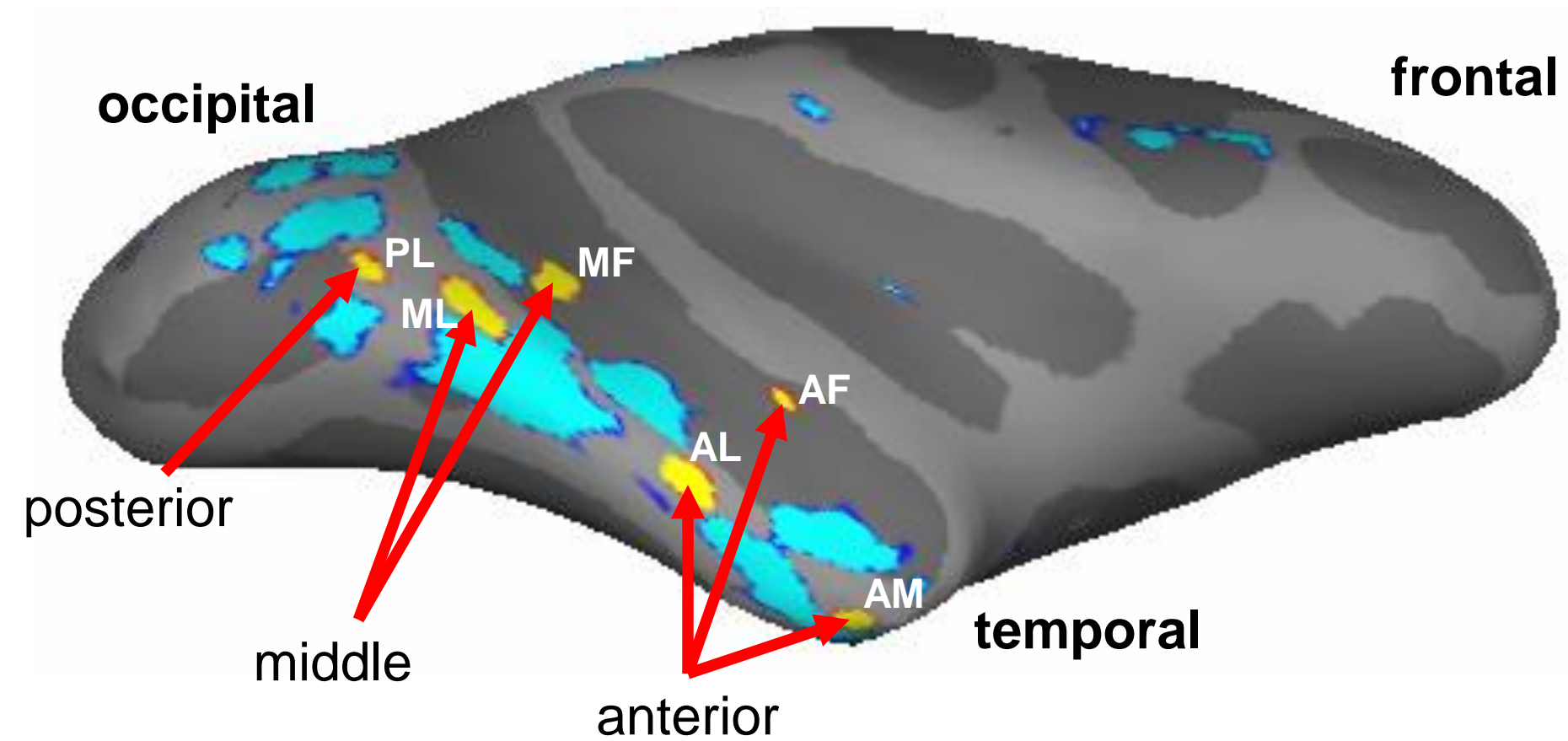
Kanwisher, McDermott, & Chun, J. Neurosci, 1997

Face-selective regions exist in monkeys



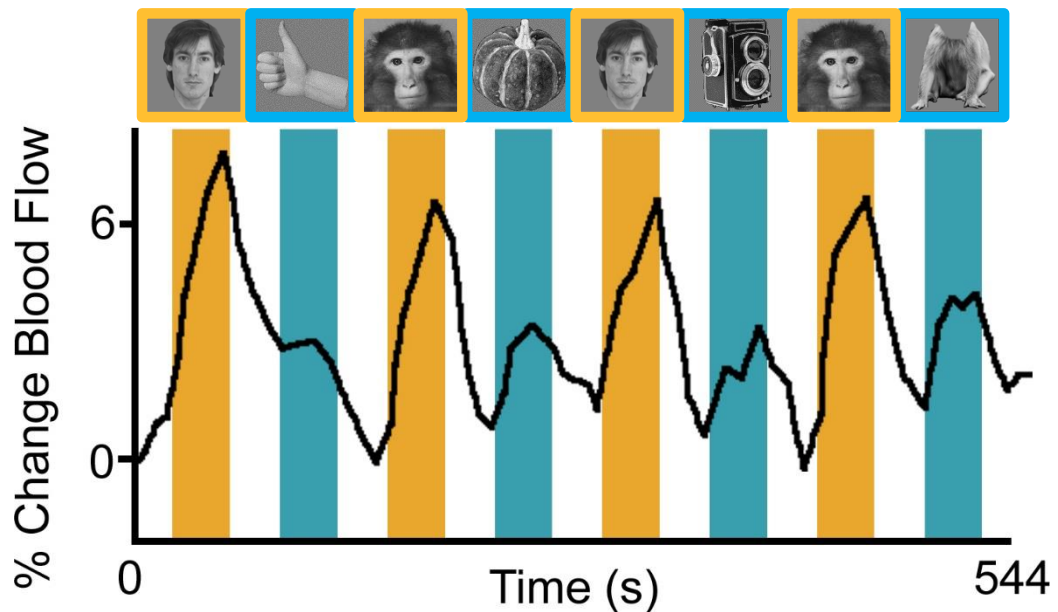


Localization of face patches

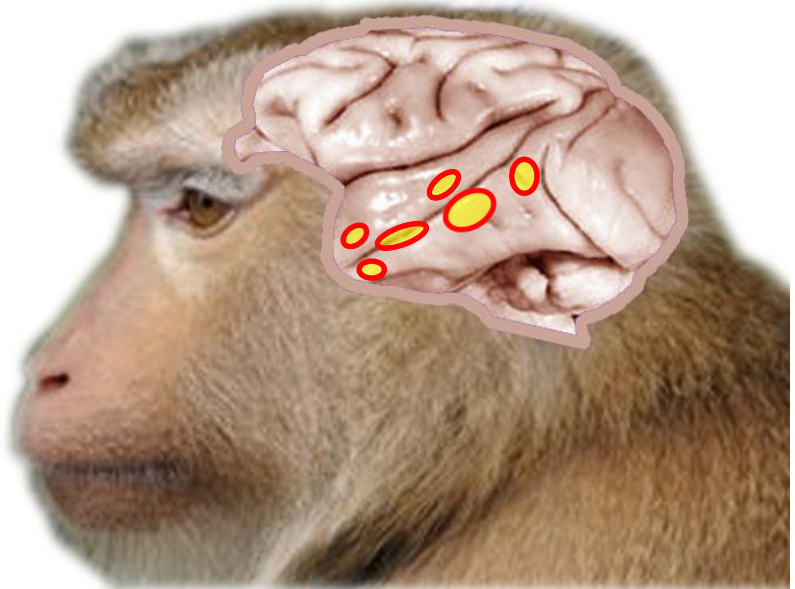


Faces vs. objects

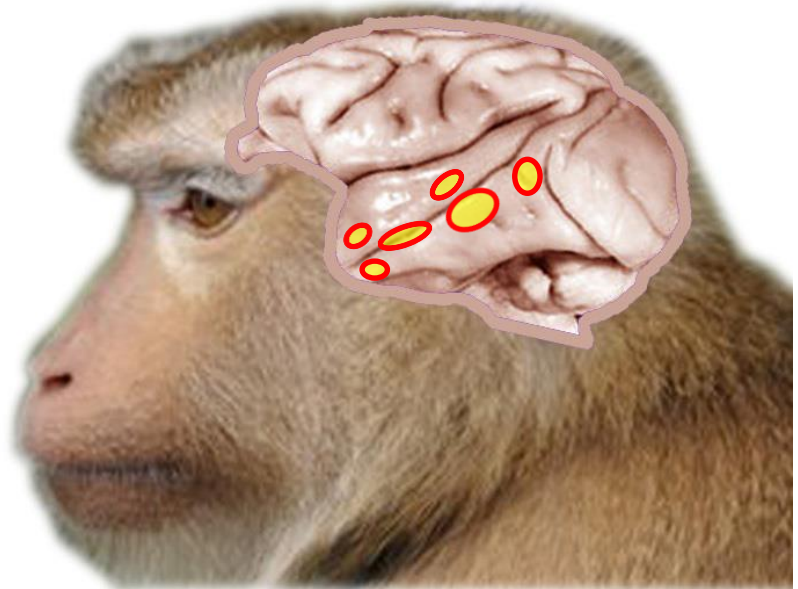
FMRI response time course from middle face patch ML



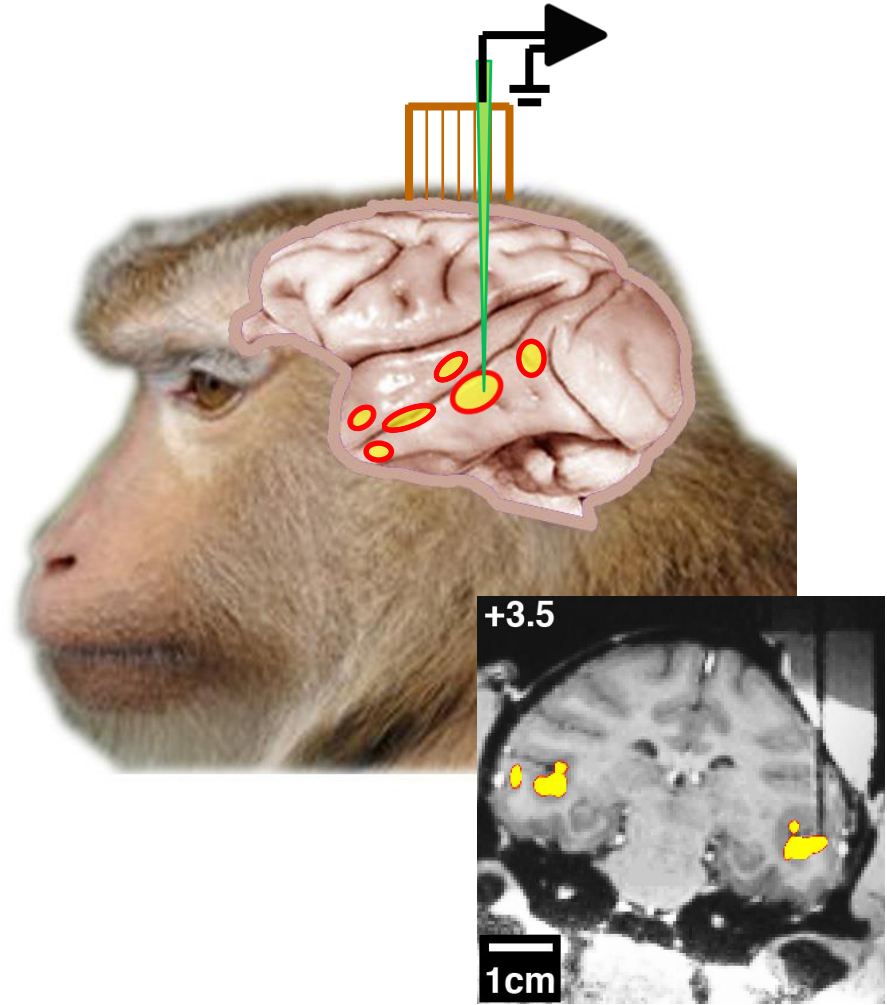
What is the selectivity of single neurons in each patch?



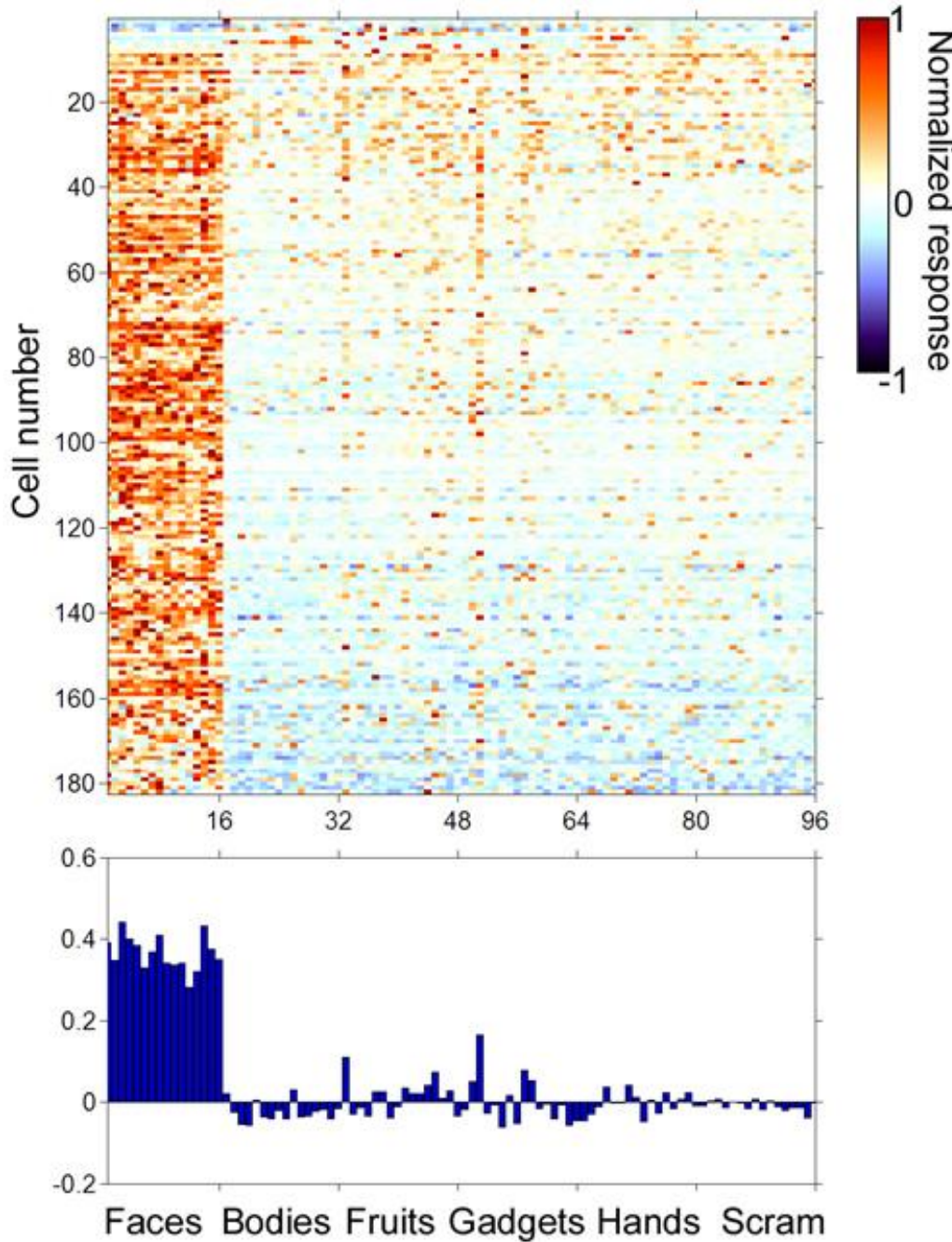
What is the selectivity of single neurons in each patch?



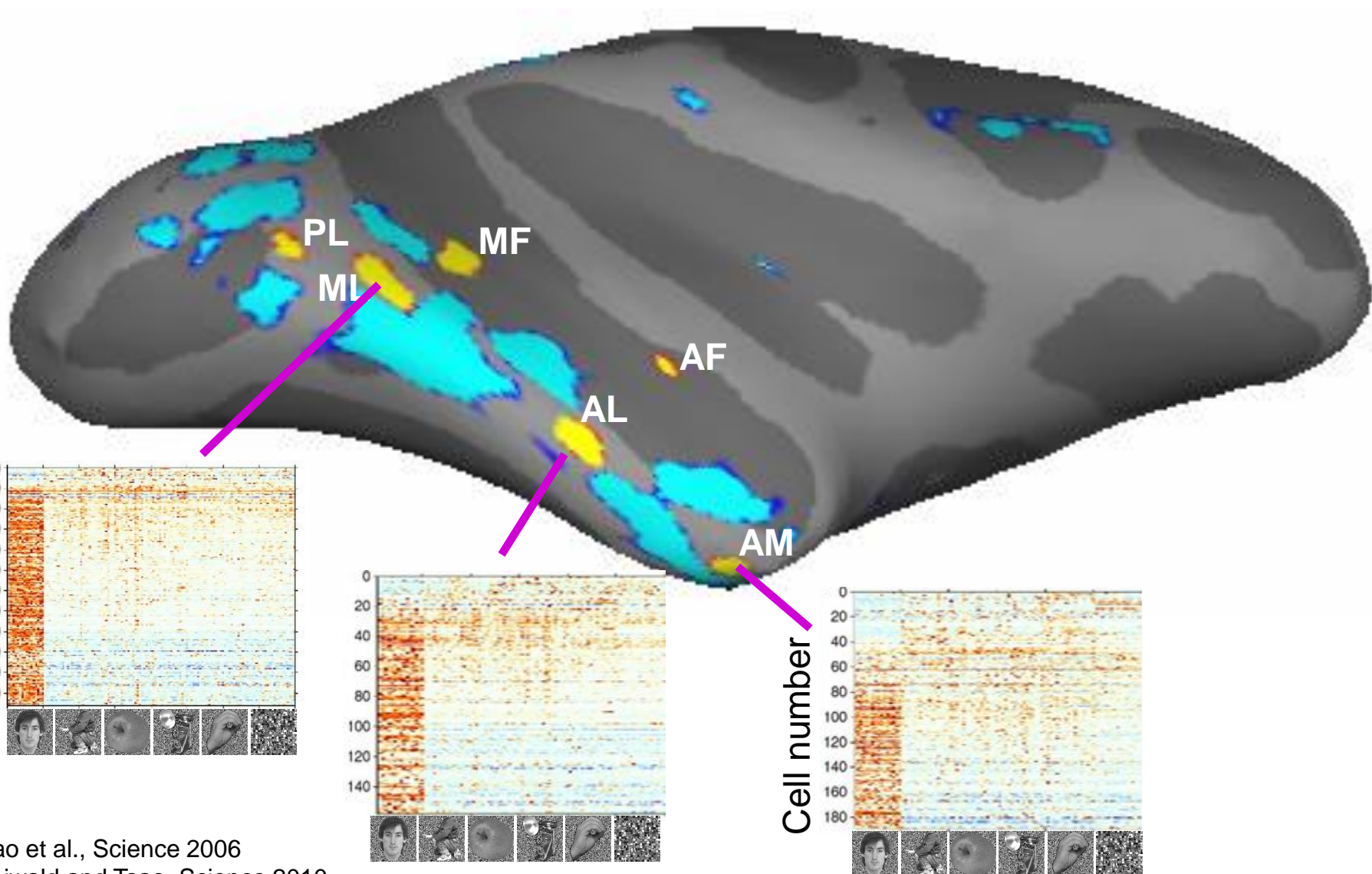
What is the selectivity of single neurons in each patch?



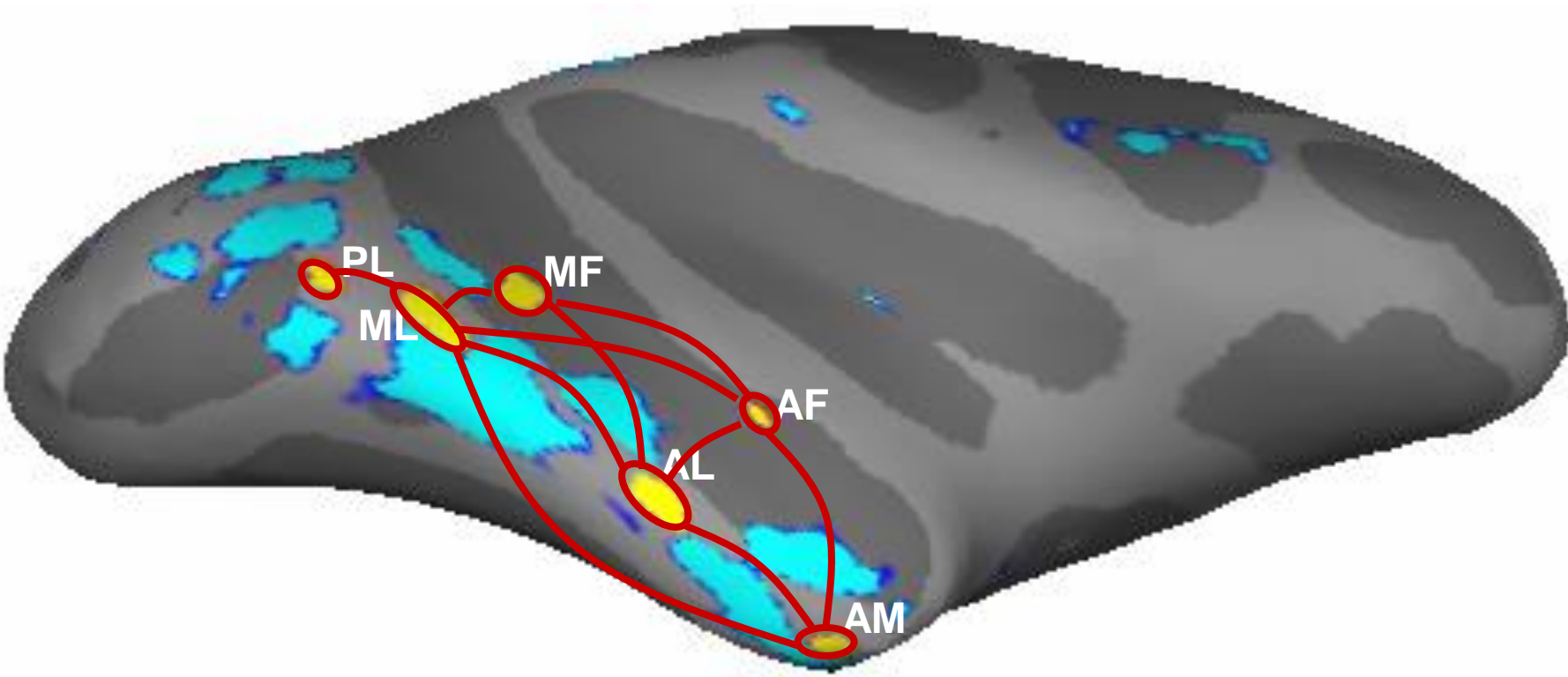
Single cell from middle face patch



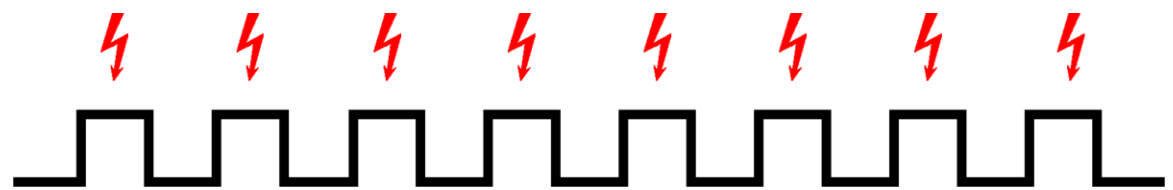
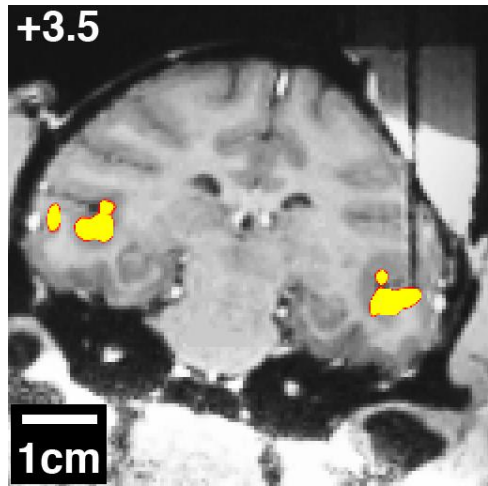
Face cells are clustered in face patches



Face patches are strongly and specifically connected to each other

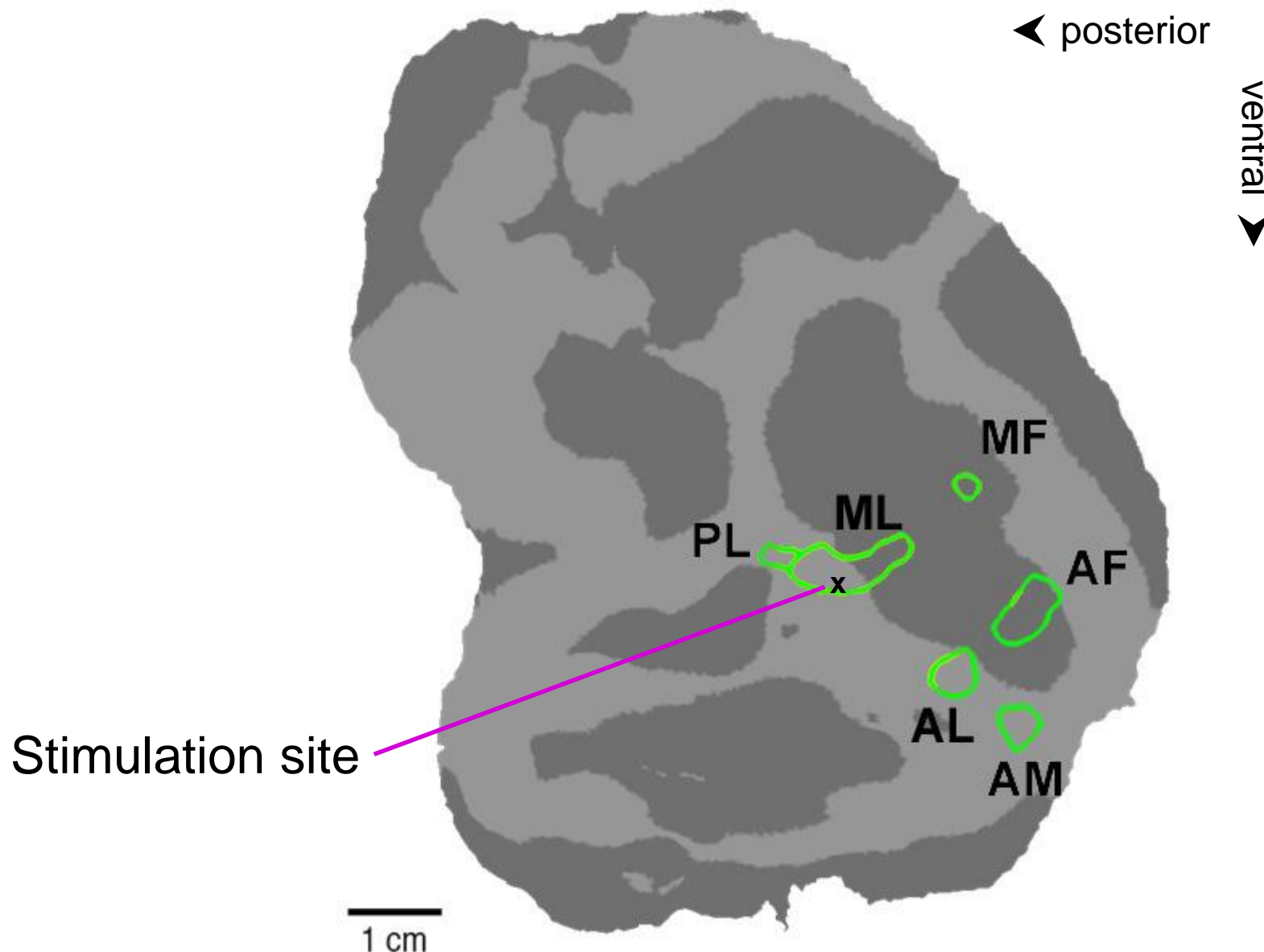


Probing connectivity of face patches: Microstimulation combined with fMRI

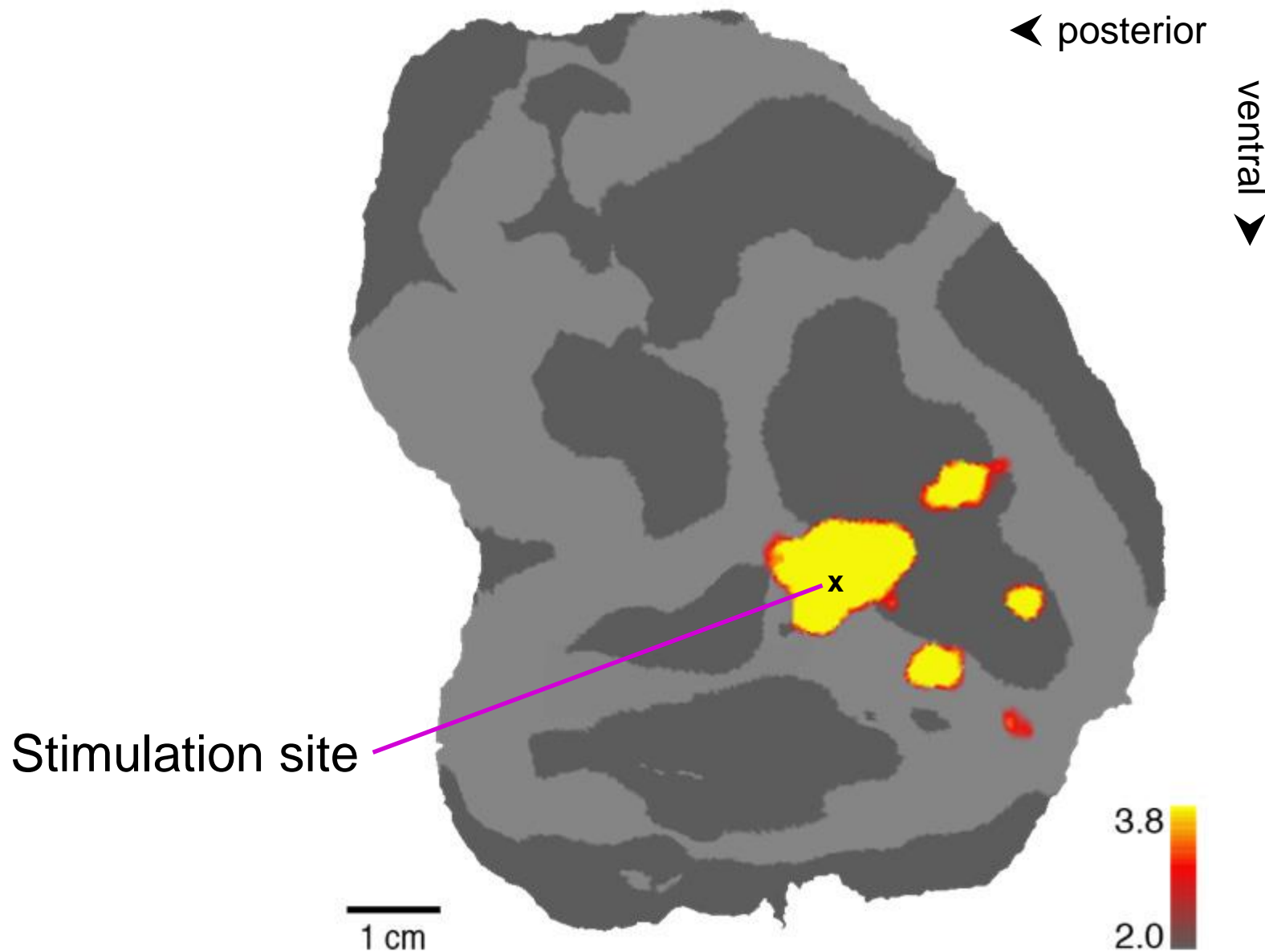


Sebastian Möller

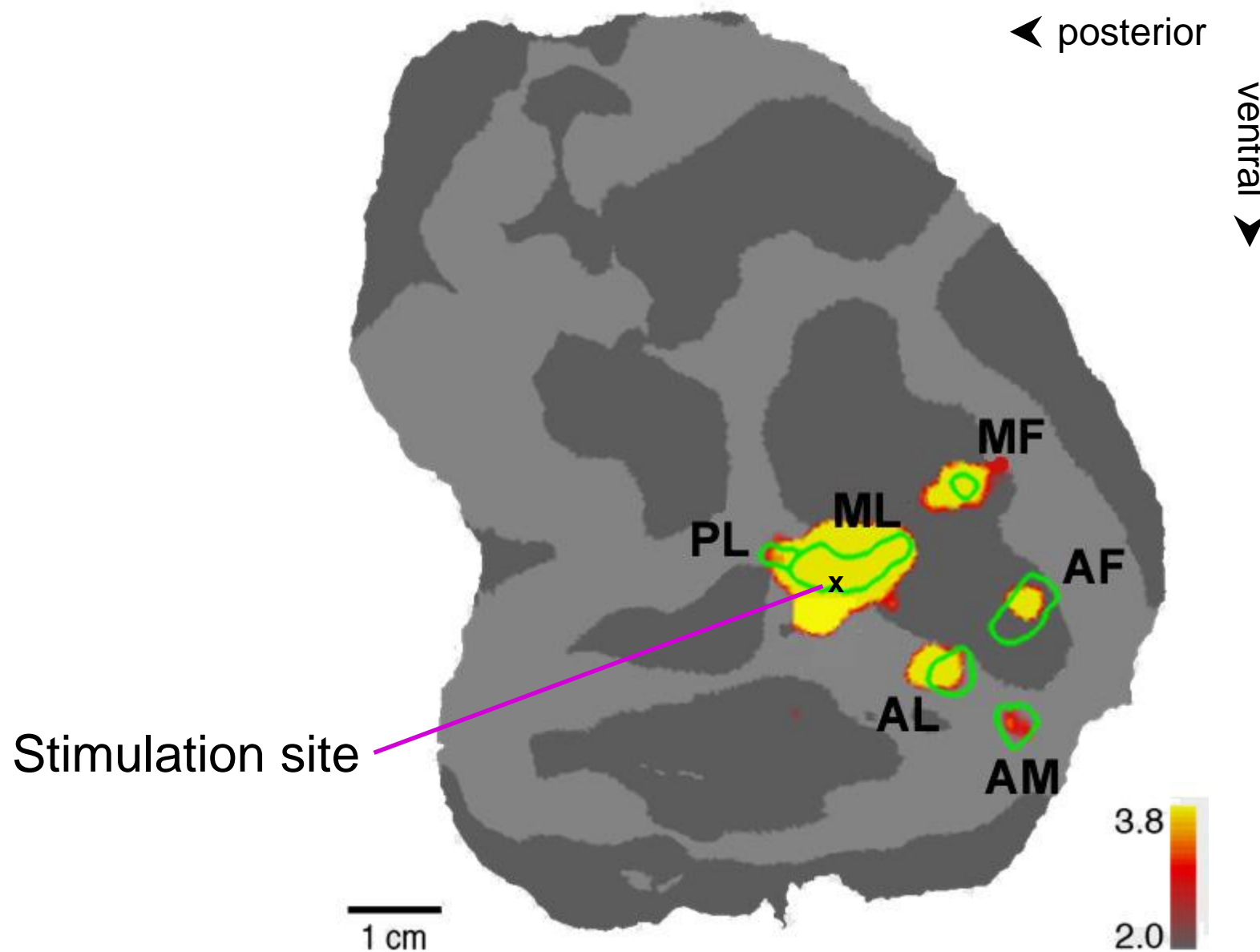
Stimulation site on the flatmap



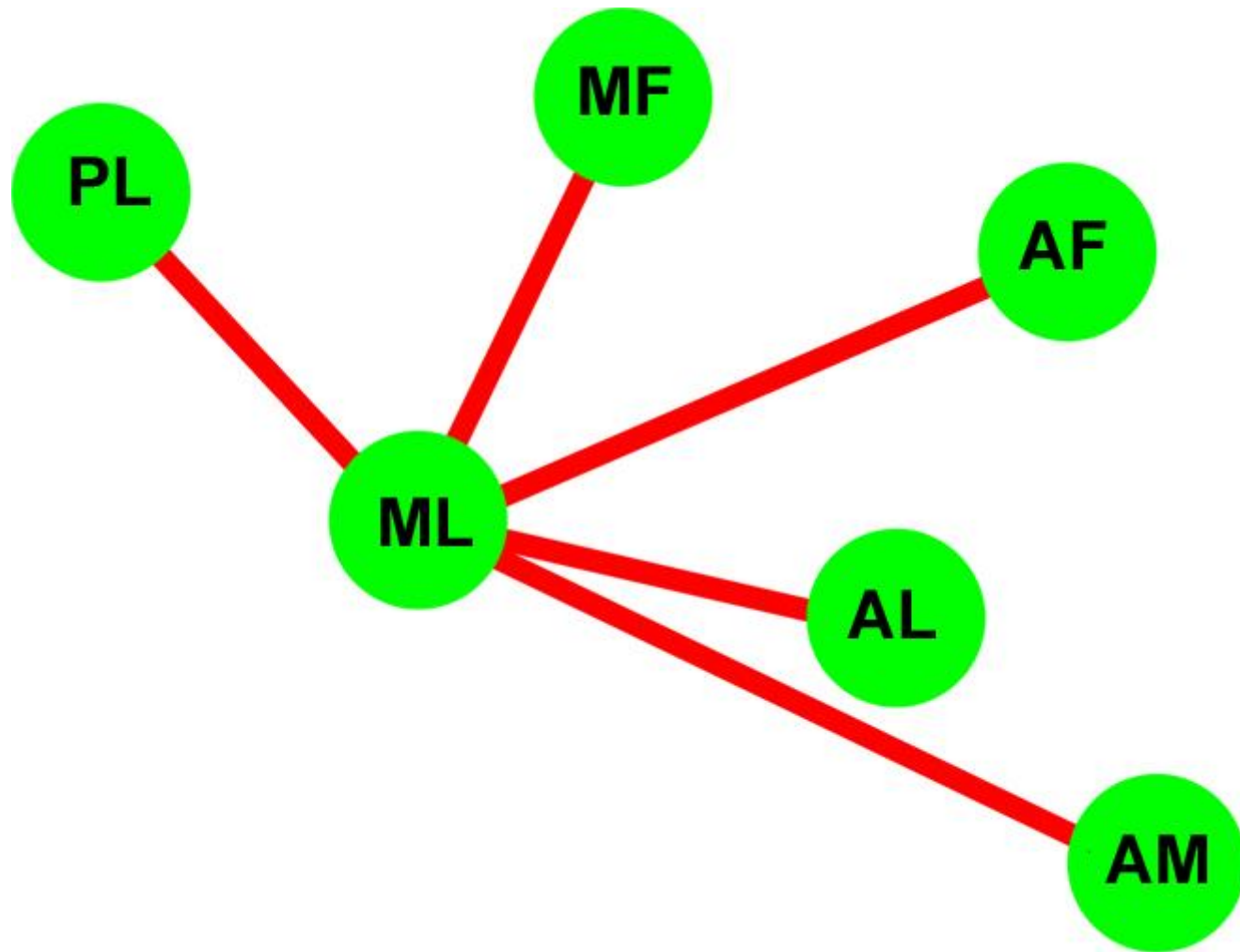
Microstimulation >> Blank



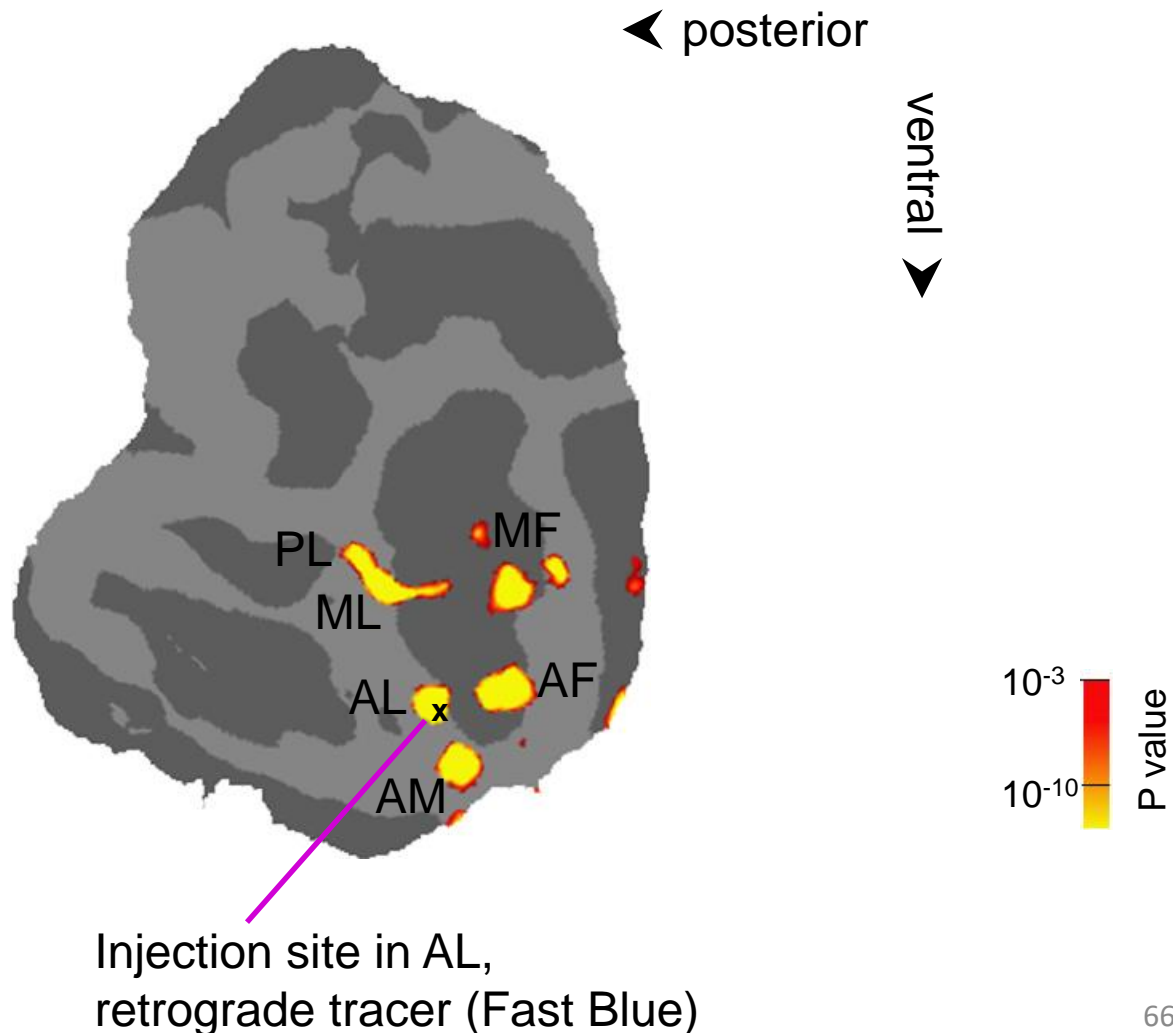
ML projection map overlaps with other face patches



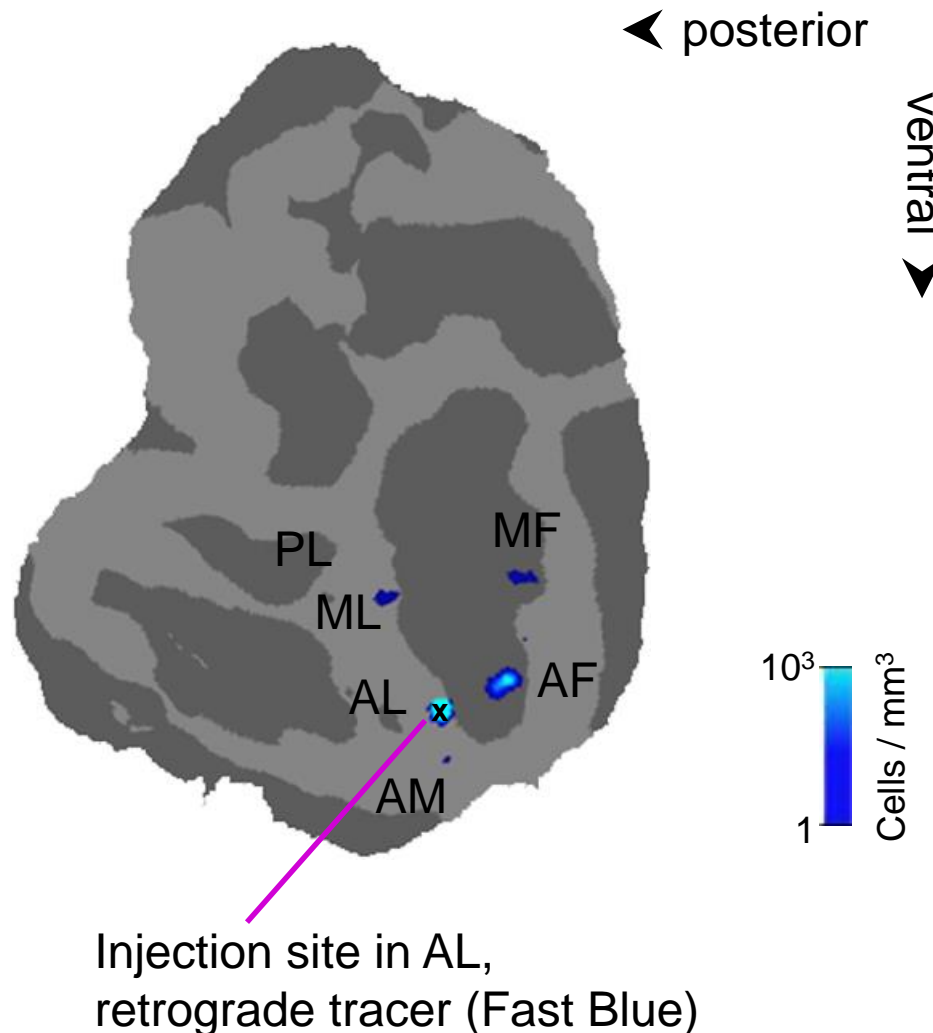
Connections of ML



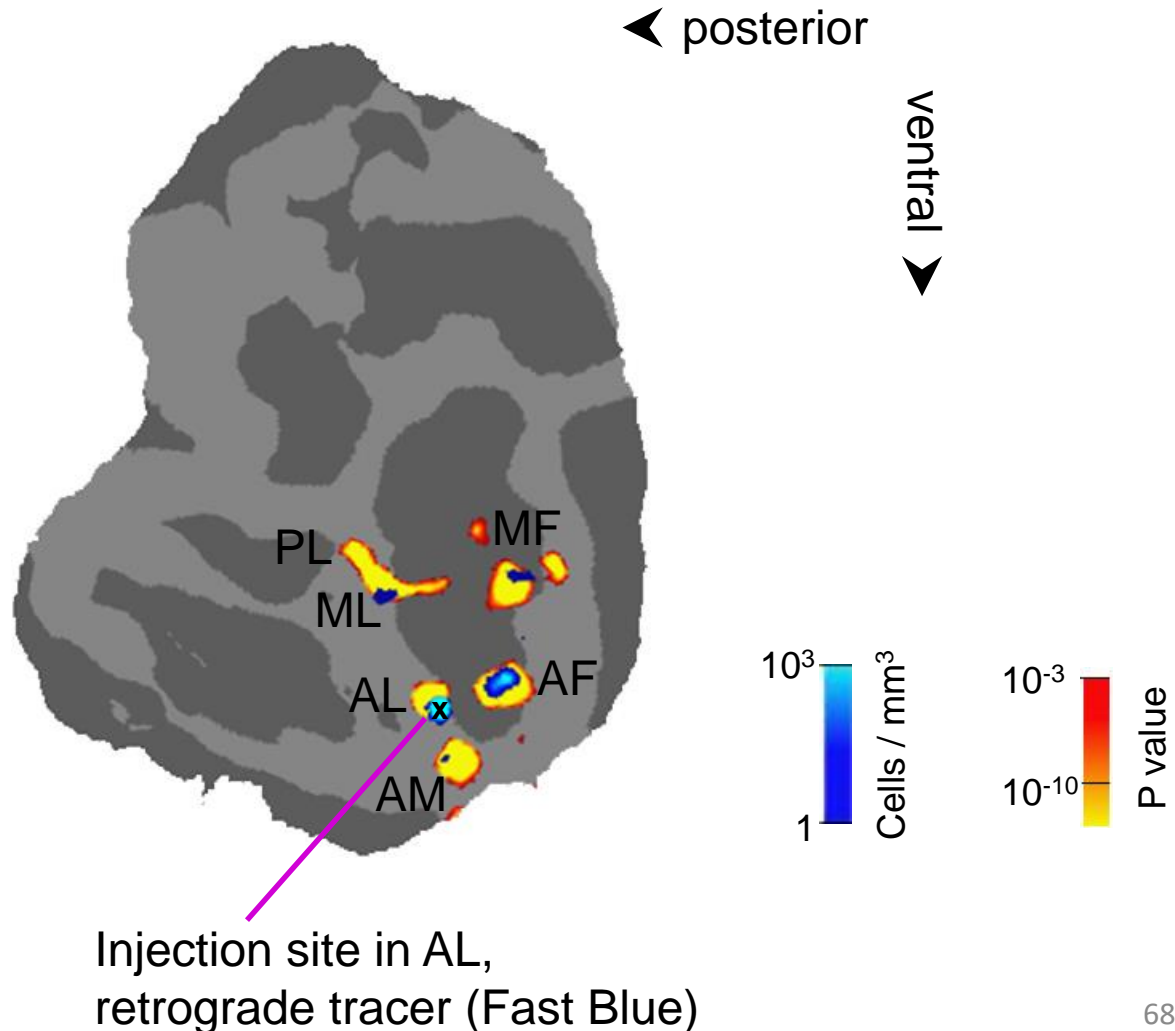
Connections within IT cortex largely confined to other face patches



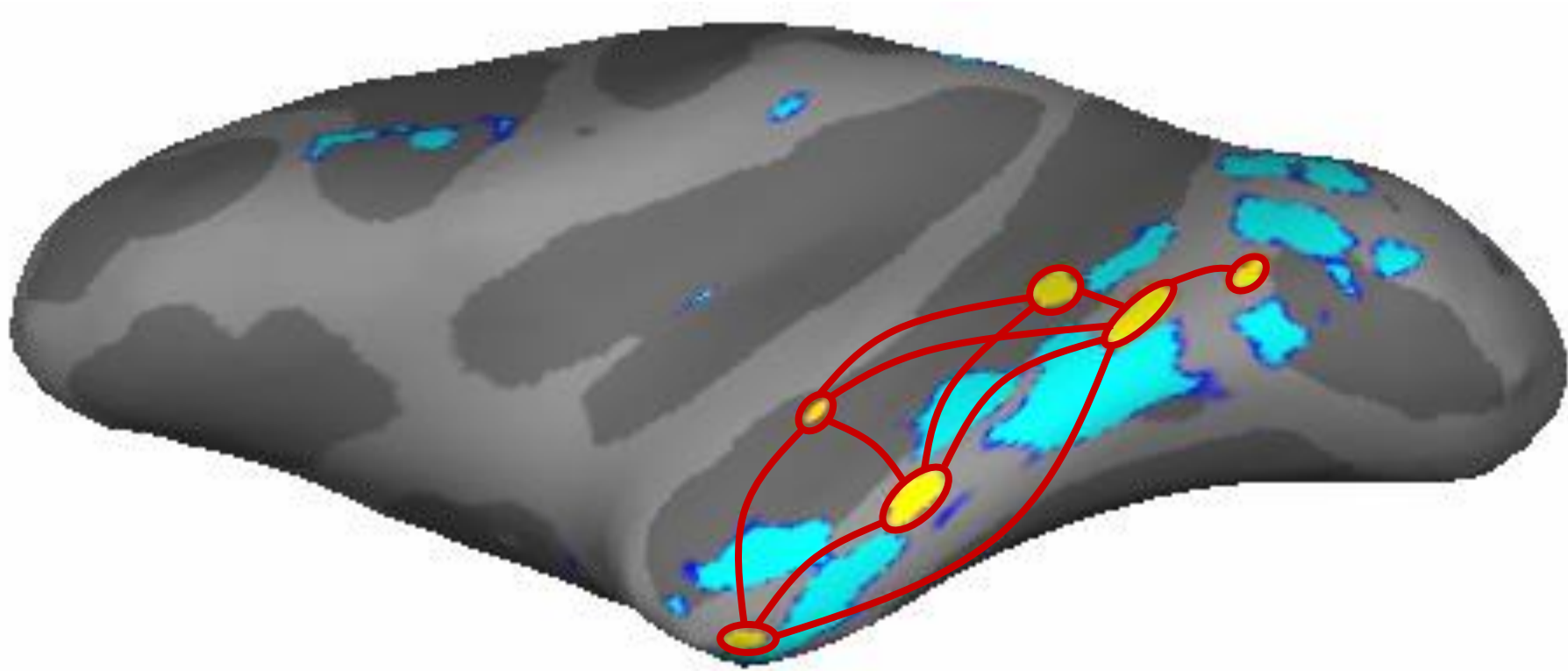
Connections within IT cortex largely confined to other face patches



Connections within IT cortex largely confined to other face patches

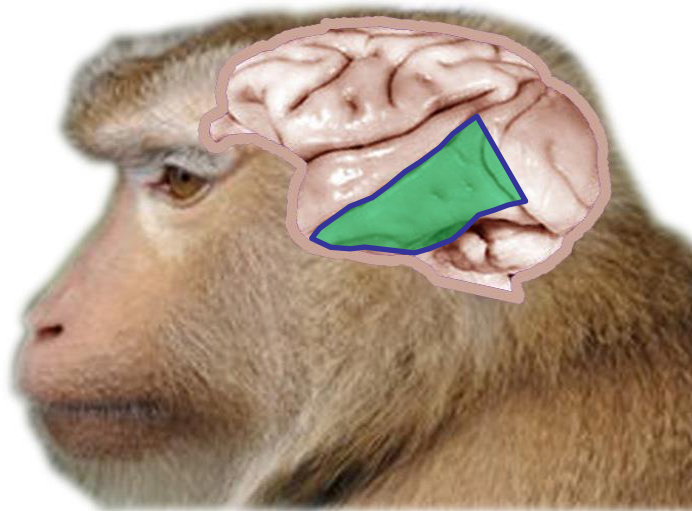


Face patch system



Experimental obstacles

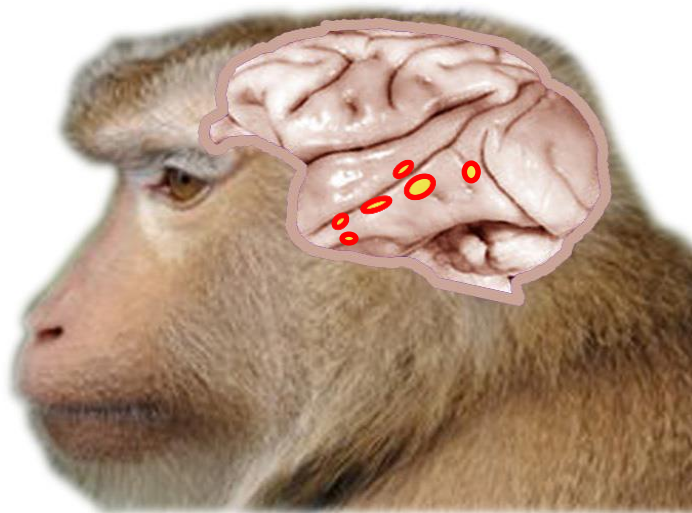
Huge cortical territory



Huge parameter space



Experimental obstacles

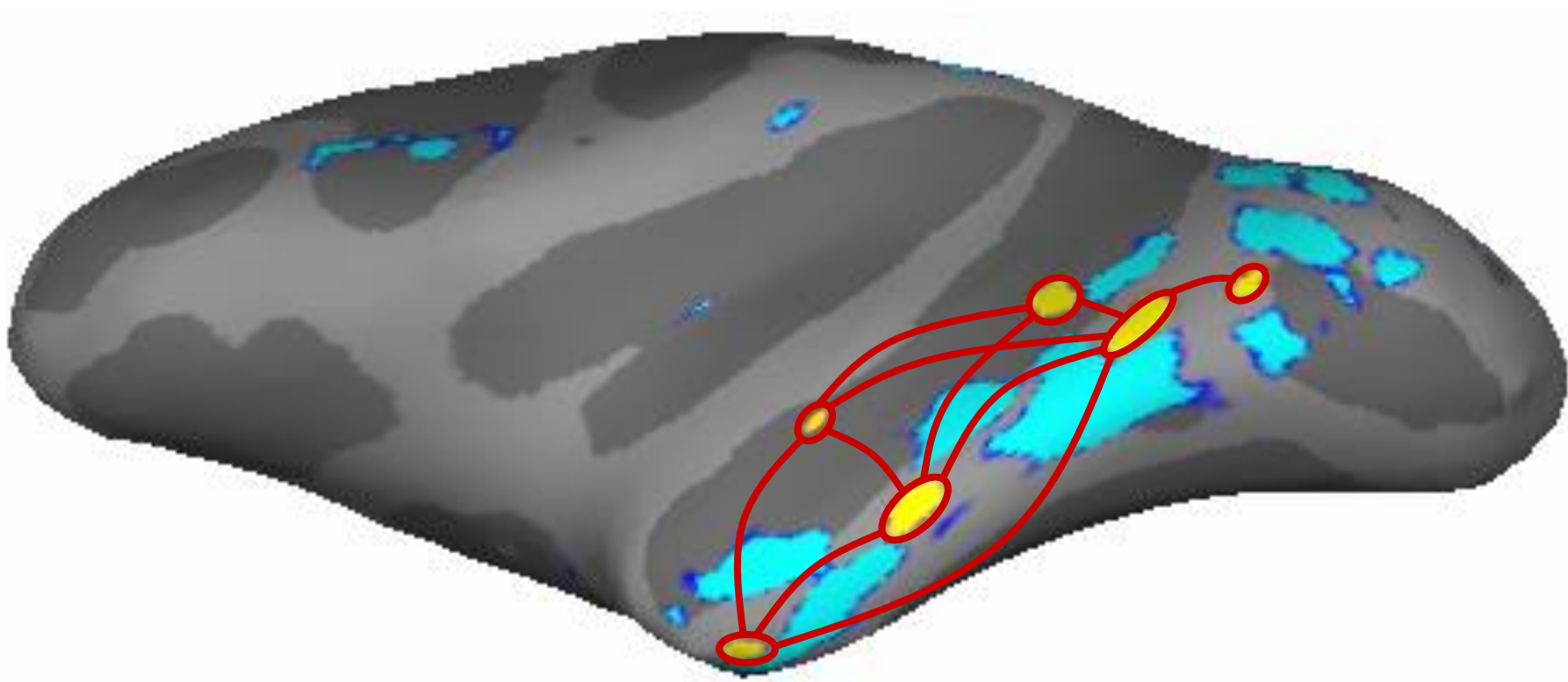


Face patches

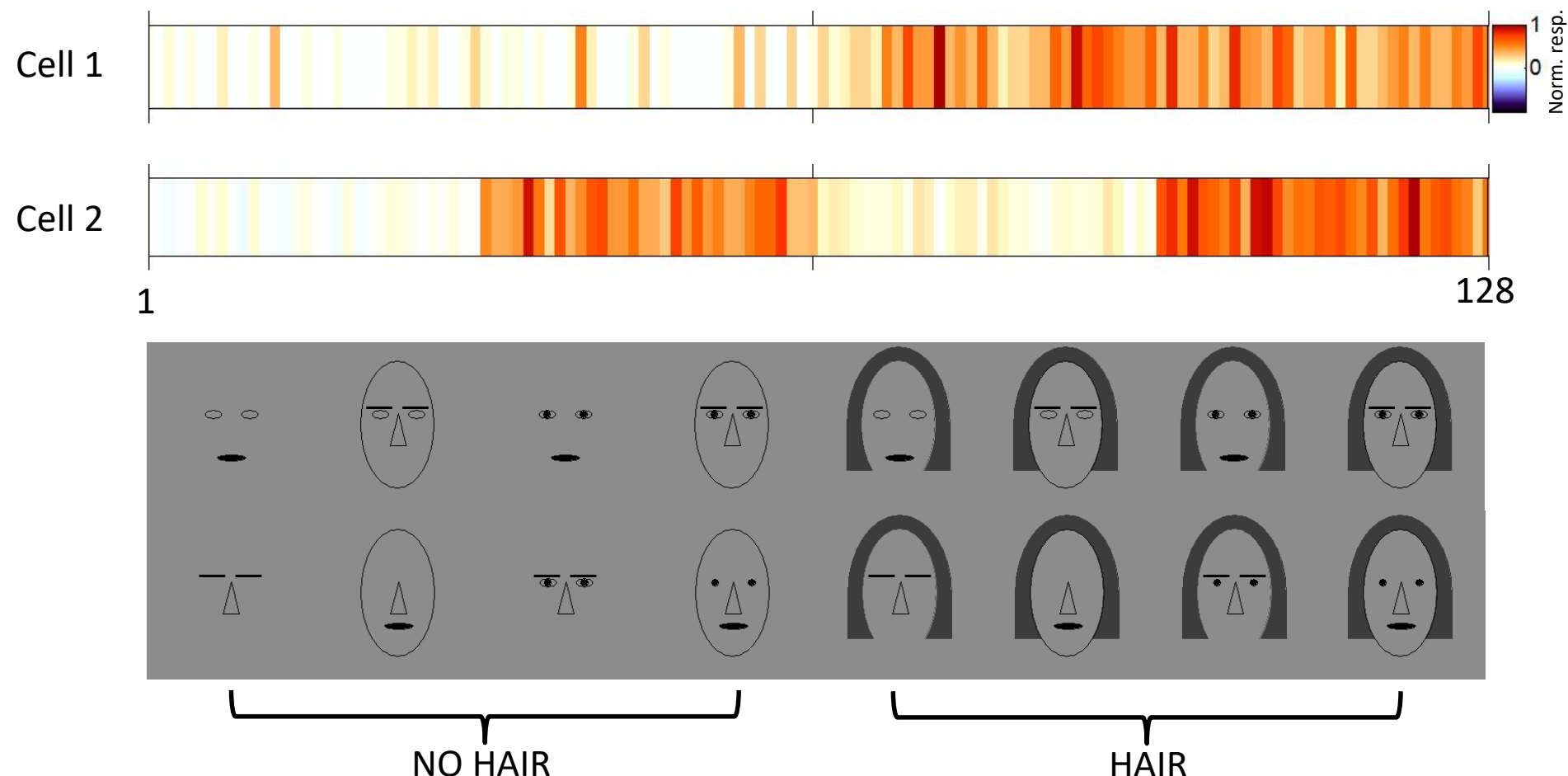


Faces

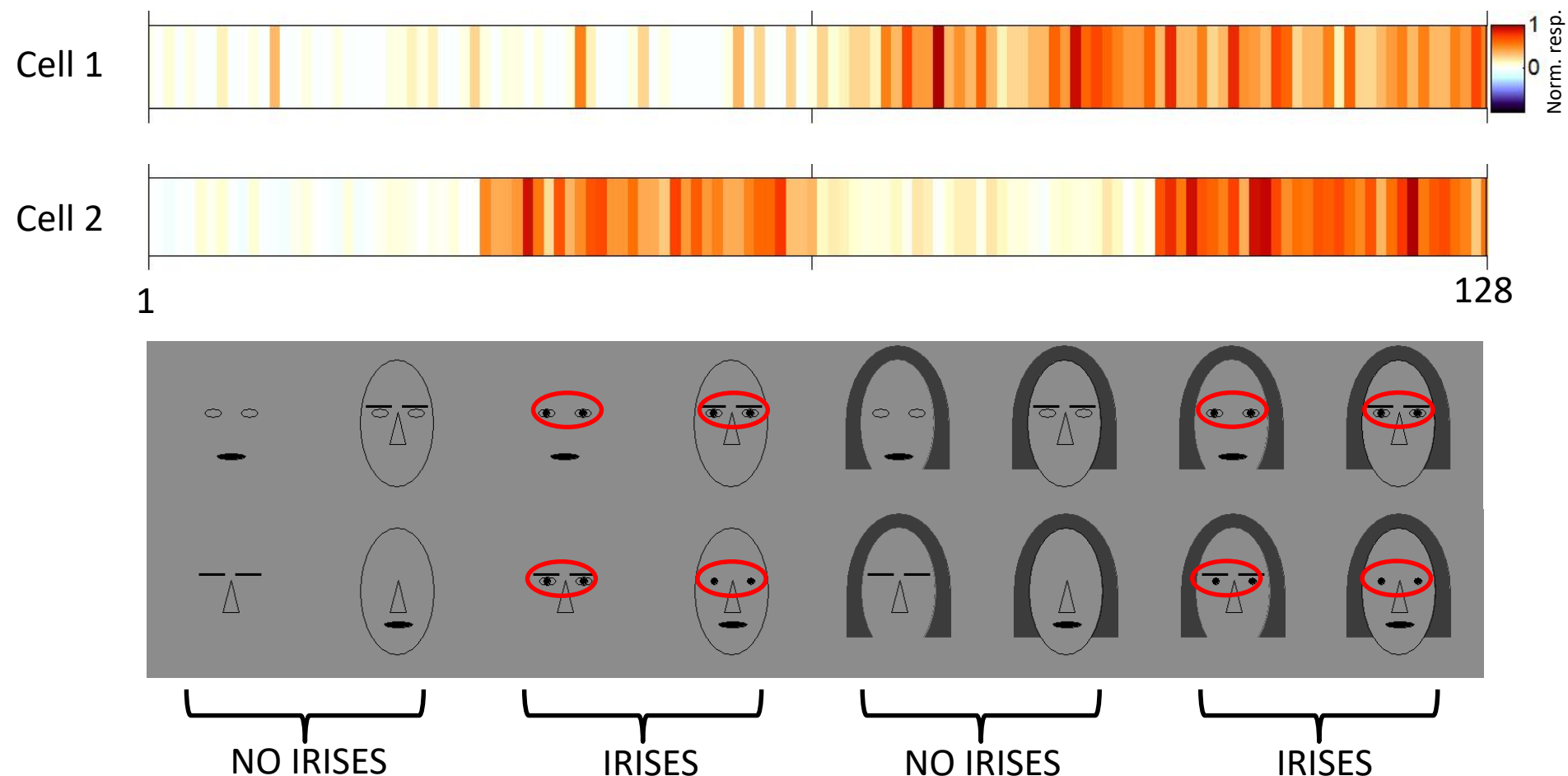
What are functional properties of cells in each patch?



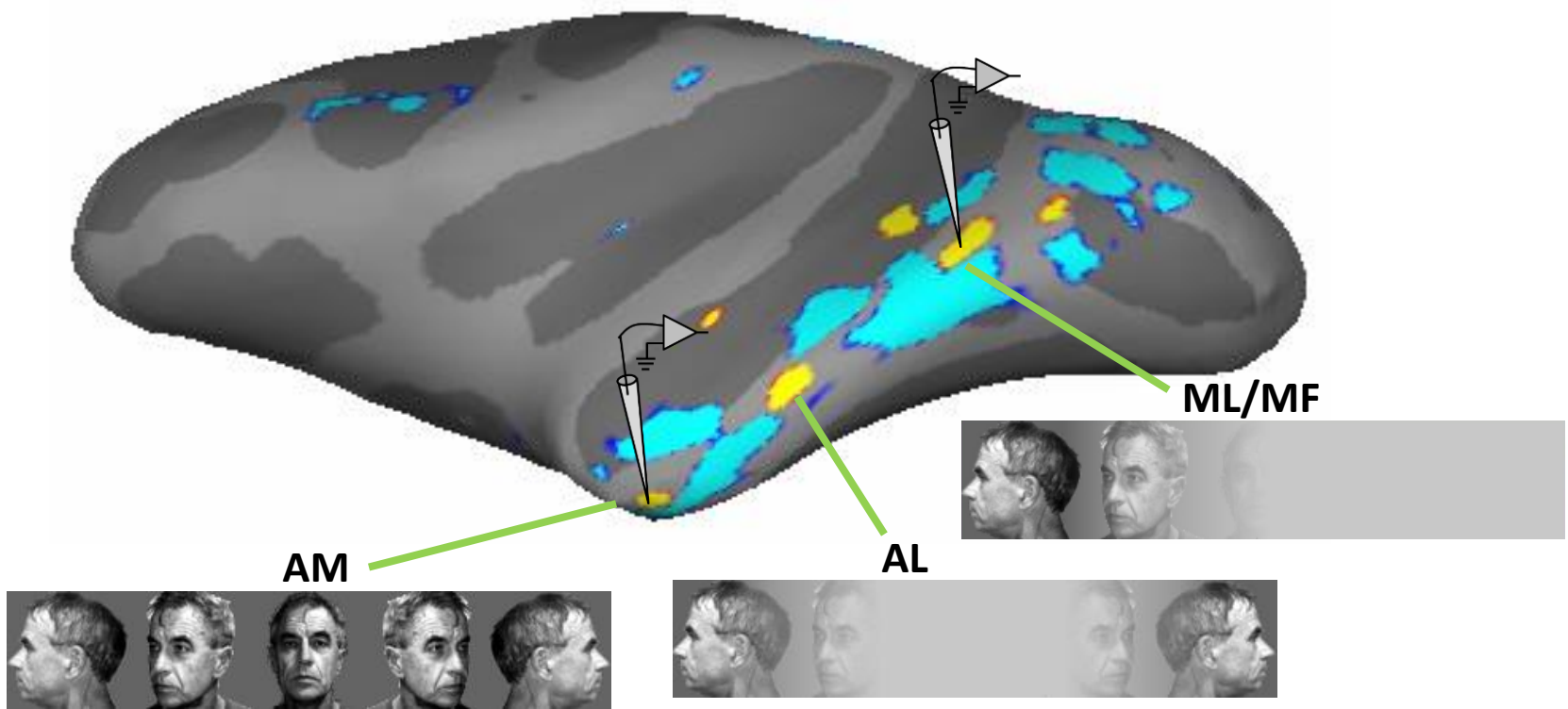
Cells are selective for the presence and shape of subsets of face features



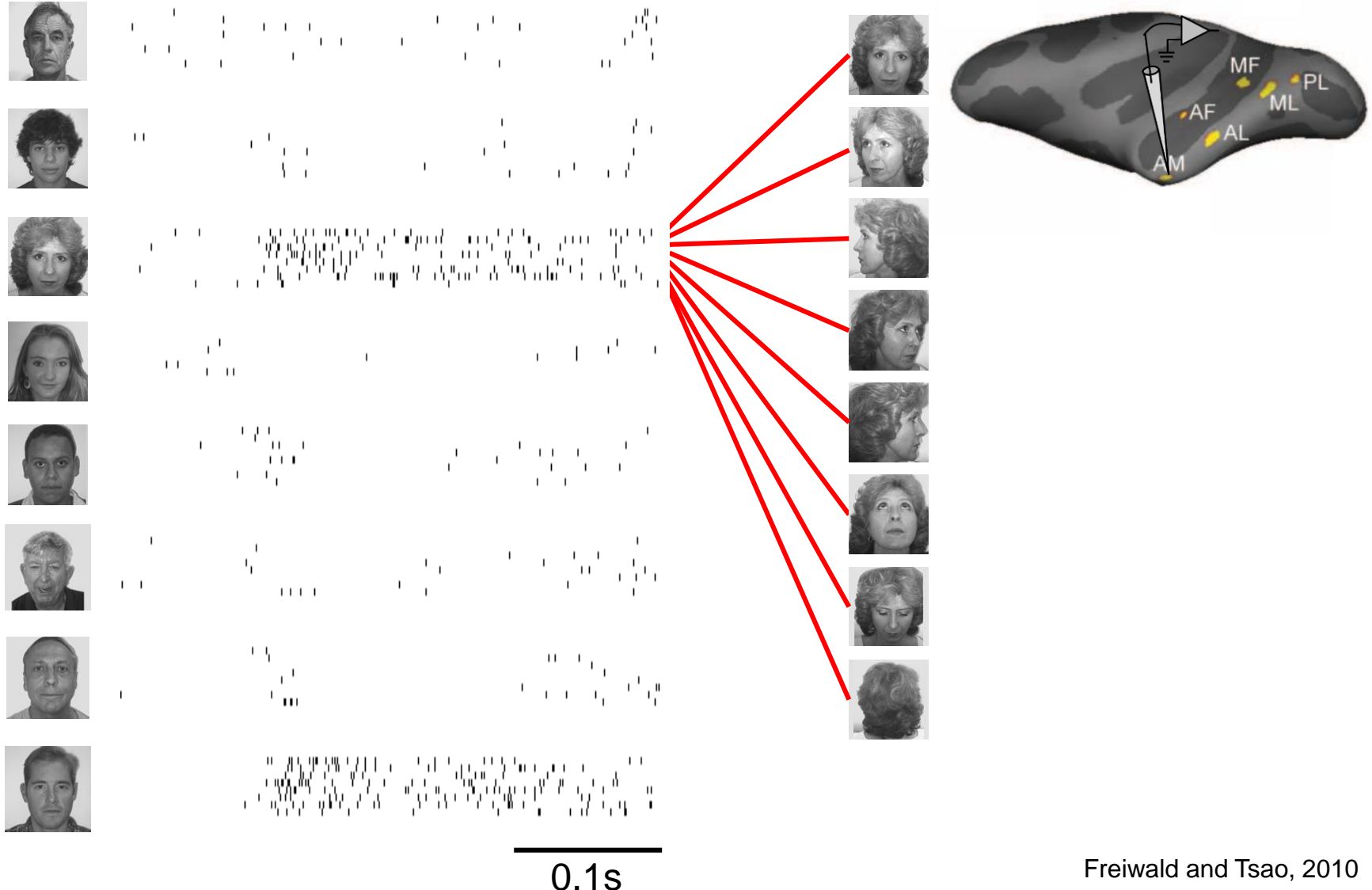
Cells are selective for the presence and appearance of subsets of face features



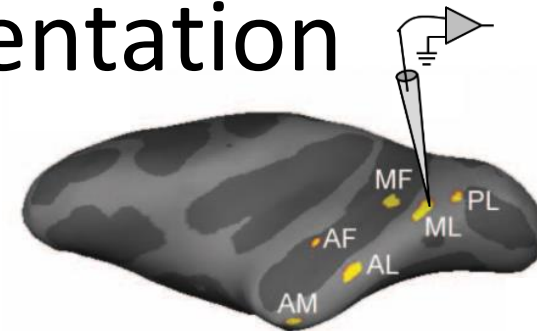
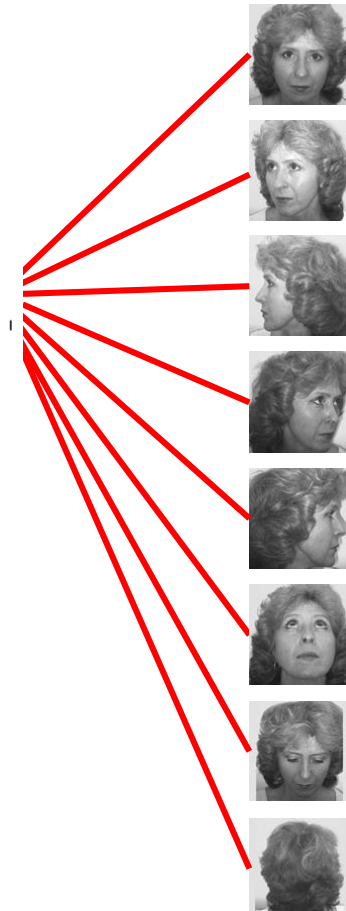
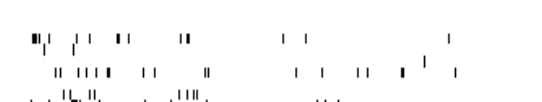
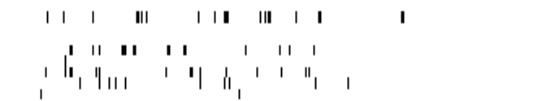
Increasing view invariance from ML/MF to AL to AM



Anterior medial face patch (AM) neurons represents face-view invariant identity



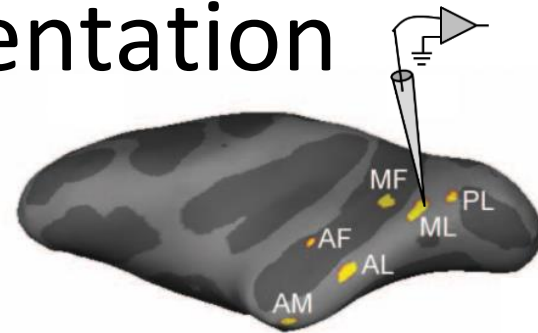
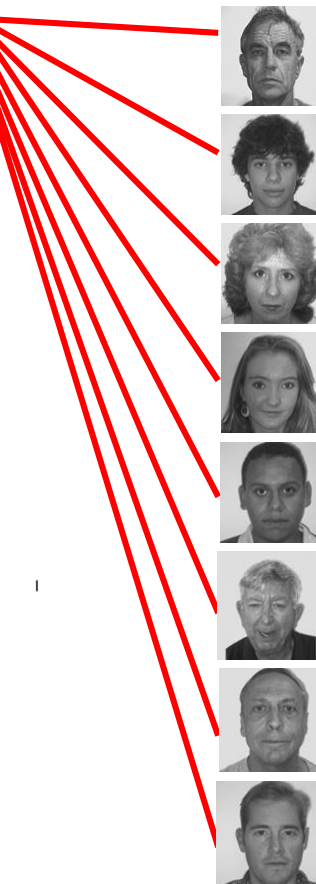
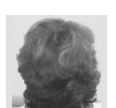
Middle face patch (MF/ML) neurons were tuned to head orientation



— 0.1s

Freiwald and Tsao, 2010

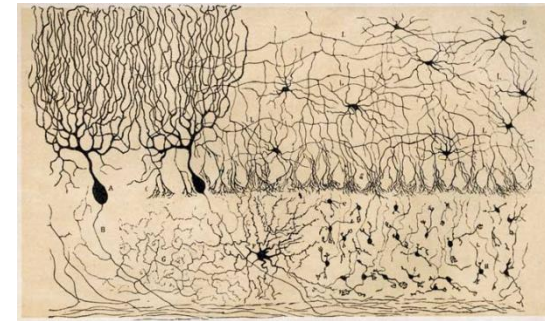
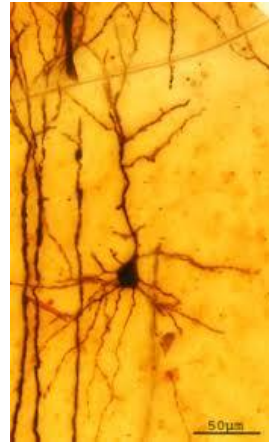
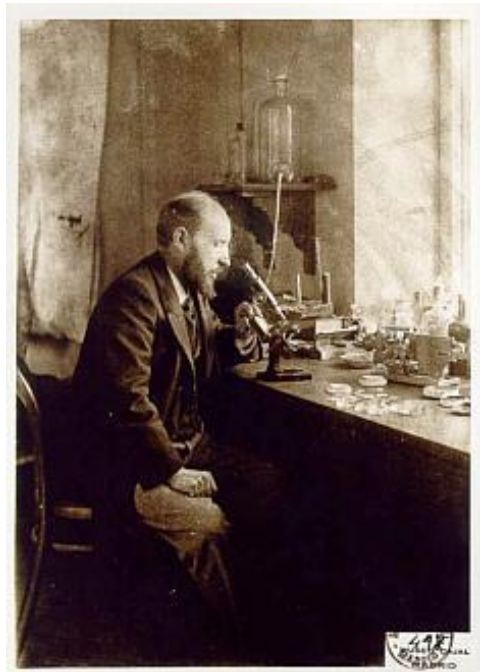
Middle face patch (MF/ML) neurons were tuned to head orientation



—
0.1s

Freiwald and Tsao, 2010

Santiago Ramon y Cajal (1 May 1852 – 18 October 1934)

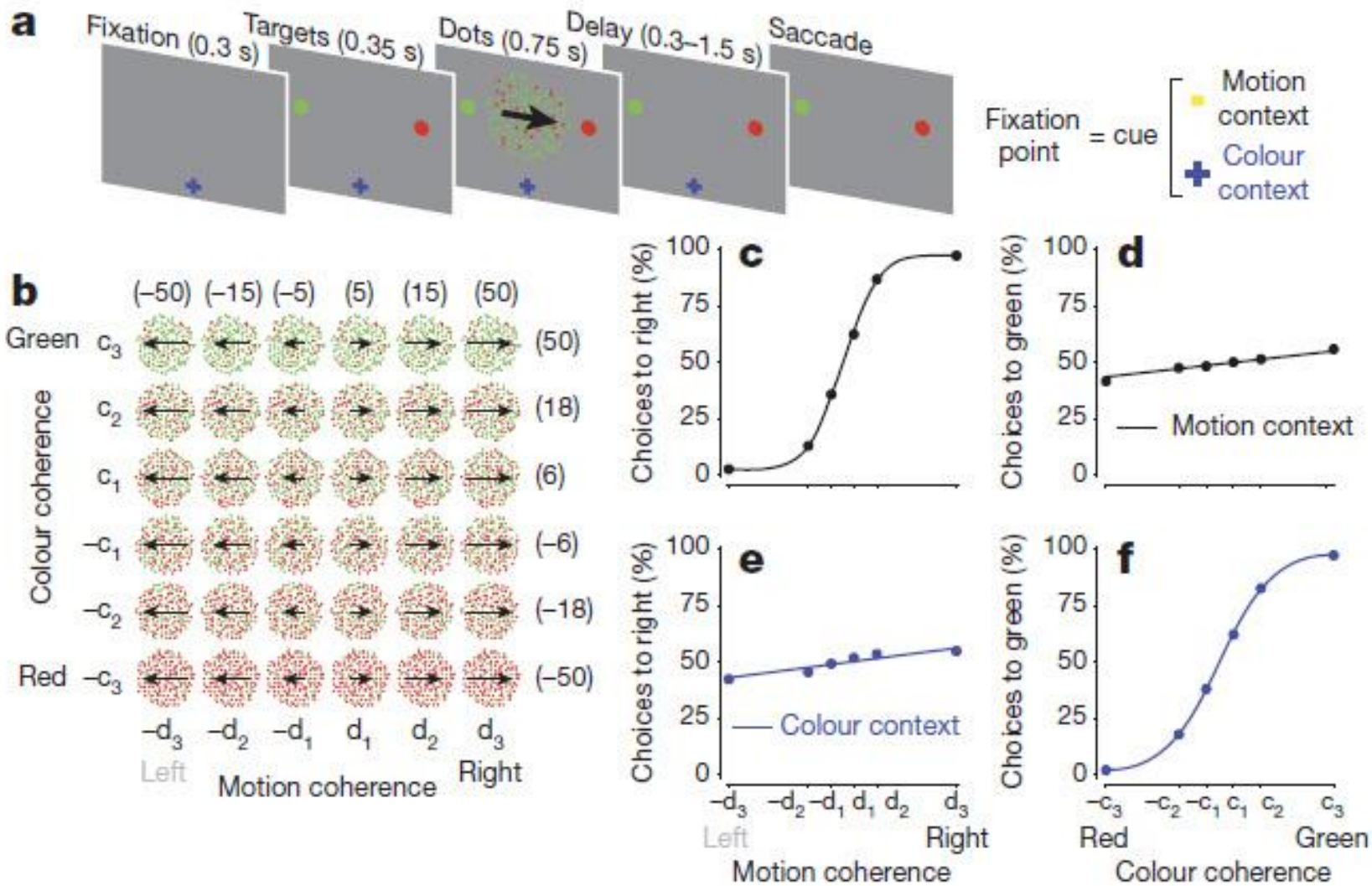


Neuron doctrine: The brain is made up of discrete individual cells.

Vision is explicable in terms of the firing patterns that emerge from the interactions among many individual neurons.

- Characterizing functional transformations along anatomically-connected pathways
- **Characterizing population dynamics among large groups of neurons**

Understanding the mechanism for flexible behavior



Step 1: Compute top 12 PCs of population data

D = matrix of eigenvectors

Step 2: Demixing (goal: plot neural state in meaningful coordinates)

$$r_{i,t}(k) = \beta_{i,t}(1) \text{choice}(k) + \beta_{i,t}(2) \text{motion}(k) + \beta_{i,t}(3) \text{color}(k) + \beta_{i,t}(4) \text{context}(k) + \beta_{i,t}(5), \quad (1)$$

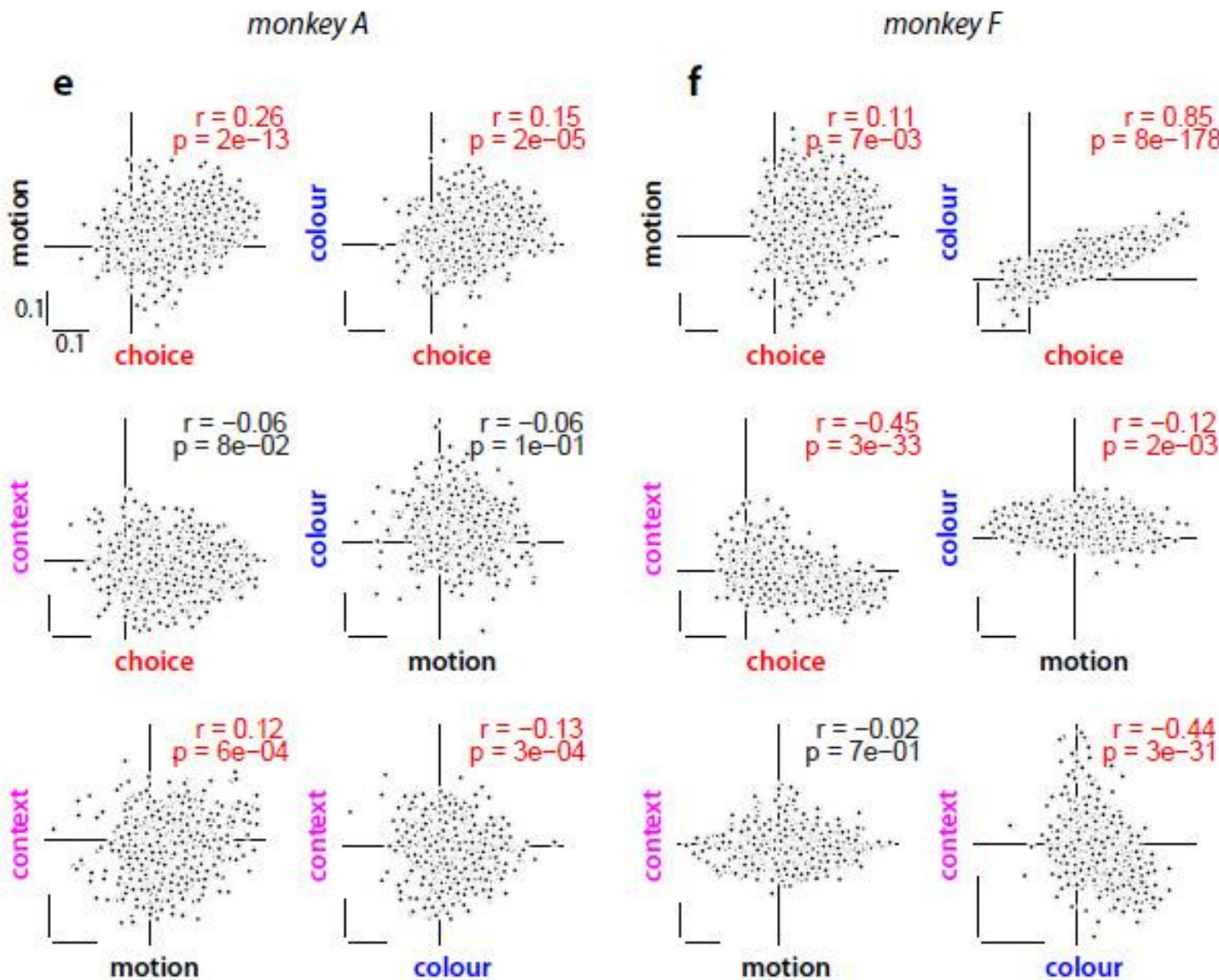
where $r_{i,t}(k)$ is the z-scored response of unit i at time t and on trial k , $\text{choice}(k)$ is the monkey's choice on trial k (+1: to choice 1; -1 to choice 2), $\text{motion}(k)$ and $\text{color}(k)$ are the motion and color coherence of the dots on trial k , and $\text{context}(k)$ is the rule the monkey has to use on trial k (+1: motion context; -1: color context).

Each vector, $\beta_{v,t}$, thus corresponds to a direction in state space that accounts for variance in the population response at time t , due to variation in task variable v .

Step 3: Denoise the regression vectors (project onto 12 PCs)

$$\beta_{v,t}^{pca} = D \beta_{v,t},$$

Regression coefficients for individual neurons

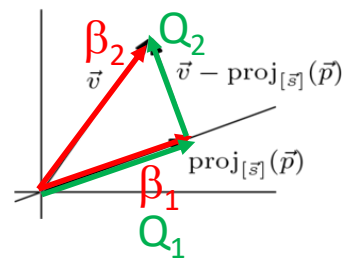


Step 4: Orthogonalize regression vectors (Gramm Schmidt)

$$\mathbf{B}^{max} = \mathbf{Q} \mathbf{R},$$

where $\mathbf{B}^{max} = [\beta_1^{max} \ \beta_2^{max} \ \beta_3^{max} \ \beta_4^{max}]$ is a matrix whose columns correspond to the regression vectors, \mathbf{Q} is an orthogonal matrix, and \mathbf{R} is an upper triangular matrix. The first four columns of \mathbf{Q} correspond to the orthogonalized regression vectors β_v^\perp , which we refer to as the ‘task-related axes’ of choice, motion, color, and context. These axes span the same ‘regression subspace’ as the original regression vectors, but crucially each explains distinct portions of the variance in the responses.

To study the representation of the task-related variables in PFC, we projected the average population responses onto these orthogonal axes (Fig. 2 and Extended Data Figs. 4-7):



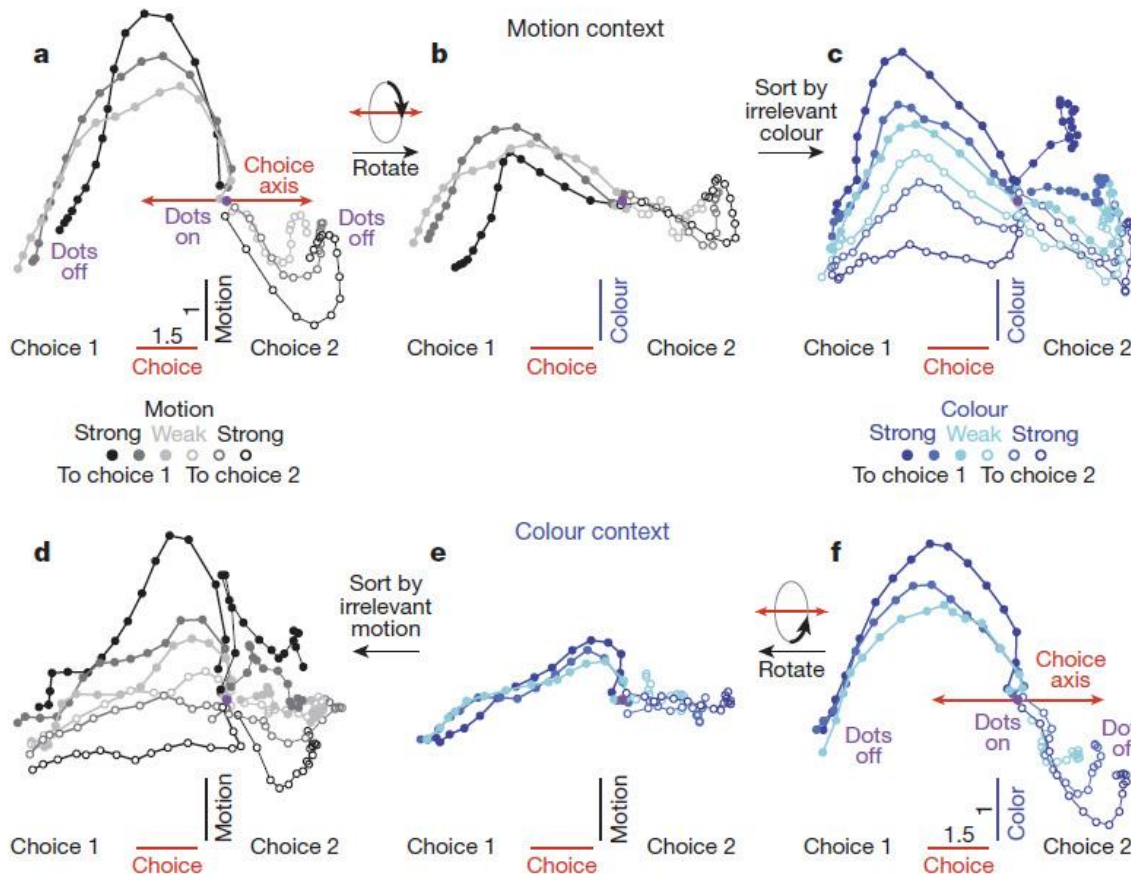


Figure 2 | Dynamics of population responses in PFC. The average population response for a given condition and time is represented as a point in state space. Responses from correct trials only are shown from 100 ms after dots onset (dots on, purple circle) to 100 ms after dots offset (dots off) in 50-ms steps, and are projected into the three-dimensional subspace capturing the variance due to the monkey's choice (along the choice axis), and to the direction and strength of the motion (motion axis) and colour (colour axis) inputs. Units are arbitrary; components along the motion and colour axes are enhanced relative to the choice axis (see scale bars in a, f). Conditions (see colour bars) are defined based on context (motion context, top; colour context, bottom), on the location of the chosen target (choice 1 versus choice 2) and either on the direction and strength of the motion (grey colours) or the colour input (blue colours). Here, choice 1 corresponds to the target in the response field of the recorded neurons. The direction of the colour input does not refer to

the colour of the dots per se (red or green), but to whether the colour points towards choice 1 or choice 2 (see Supplementary Information, section 6.4, for a detailed description of the conditions). **a**, Effect of choice and the relevant motion input in the motion context, projected onto the axes of choice and motion. **b**, Same data as in a, but rotated by 90° around the axis of choice to reveal the projection onto the axis of colour. **c**, Same trials as in b, but re-sorted according to the direction and strength of the irrelevant colour input.

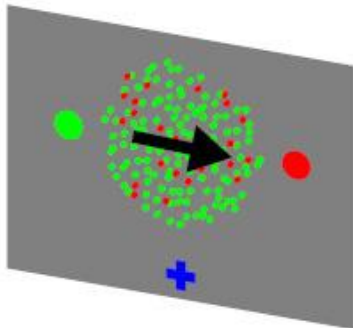
d-f, Responses in the colour context, analogous to a-c. Responses are averaged to show the effects of the relevant colour (e, f) or the irrelevant motion input (d). For relevant inputs (a, b and e, f), correct choices occur only when the sensory stimulus points towards the chosen target (3 conditions per chosen target); for irrelevant inputs (c, d), however, the stimulus can point either towards or away from the chosen target on correct trials (6 conditions per chosen target).

...So far, not THAT surprising
(a fancy way of showing that (1) the monkey can do the task and the choice signal is also represented in PFC, and (2) both color and motion information are represented regardless of context,)

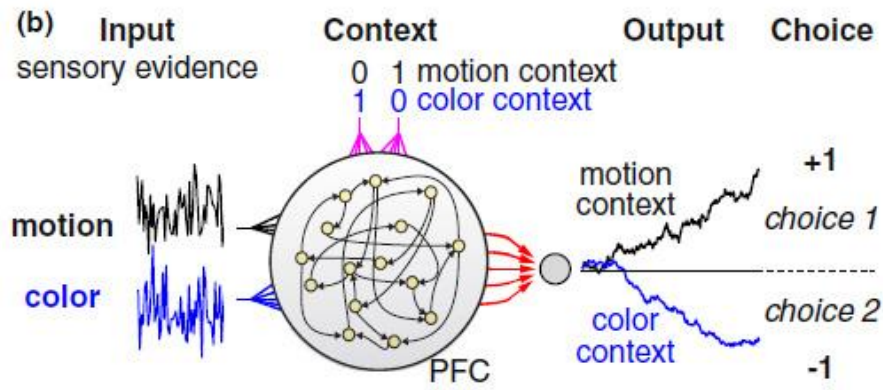
What is the underlying mechanism?

Recurrent Neural Network

(a)



fixation point = cue
■ motion context
✚ color context

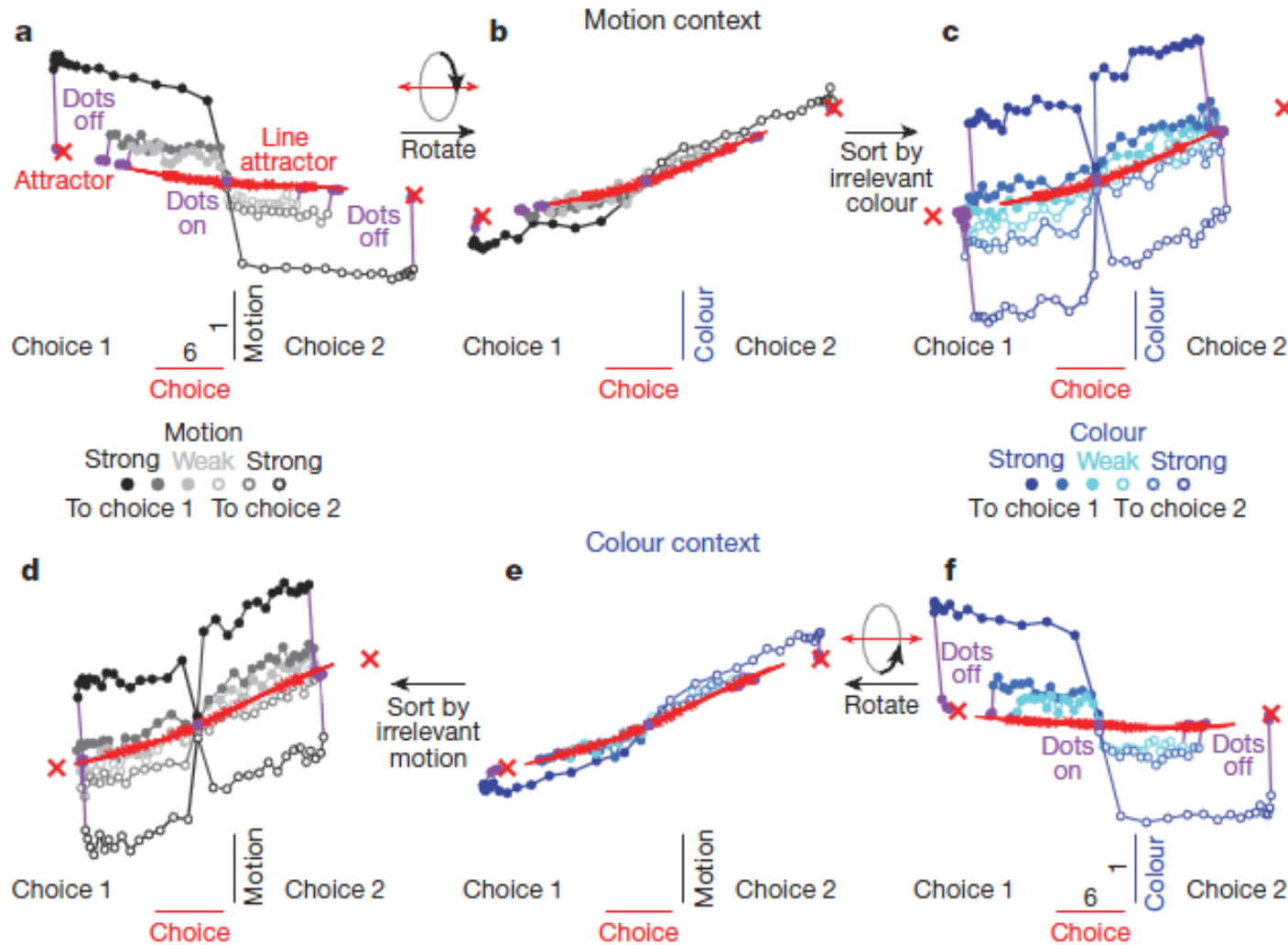


$$\tau \dot{x} = -x + J r + b^c u_c + b^m u_m + b^{cc} u_{cc} + b^{cm} u_{cm} + c^x + \rho_x$$

$$r = \tanh(x)$$

- x represents activation of neuron, r represents firing rate, J represents recurrent connections, u represents input, c represents offsets, ρ represents noise
- J, b, c are modified through training

Search for fixed points (where $\dot{x} = 0$)



Red crosses: fixed points (same in both contexts)

small and sometimes large, where the system can be understood in essentially linear terms, i.e. as a linear dynamical system. We can see this with just a few lines of math involving the Taylor series expansion of the update equations, $\dot{\mathbf{x}} = \mathbf{F}(\mathbf{x})$. Consider the Taylor expansion of $\mathbf{F}(\mathbf{x})$ around a fixed point in state space, \mathbf{x}^* :

$$(\mathbf{x}^* + \delta\mathbf{x}) = \mathbf{F}(\mathbf{x}^* + \delta\mathbf{x}) = \mathbf{F}(\mathbf{x}^*) + \mathbf{F}'(\mathbf{x}^*)\delta\mathbf{x} + \frac{1}{2}\delta\mathbf{x}\mathbf{F}''(\mathbf{x}^*)\delta\mathbf{x} + \dots \quad (6)$$

Here we have defined the nonlinear system up to second order. Since the system is at a fixed point, the zero order term, $\mathbf{F}(\mathbf{x}^*)$, is equal to 0, giving

$$\mathbf{F}(\mathbf{x}^* + \delta\mathbf{x}) = \mathbf{F}'(\mathbf{x}^*)\delta\mathbf{x} + \frac{1}{2}\delta\mathbf{x}\mathbf{F}''(\mathbf{x}^*)\delta\mathbf{x} + \dots \quad (7)$$

If we ensure that $\delta\mathbf{x}$ is small, we can safely ignore second and higher order terms, yielding

$$(\mathbf{x}^* + \delta\mathbf{x}) = \mathbf{F}'(\mathbf{x}^*)\delta\mathbf{x} \quad (8)$$

$$\delta\mathbf{x} = \mathbf{F}'(\mathbf{x}^*)\delta\mathbf{x} \quad (9)$$

and by simply renaming variables, $\mathbf{y} \equiv \delta\mathbf{x}$ and $\mathbf{M} \equiv \mathbf{F}'(\mathbf{x}^*)$, we end up with the familiar linear form

$$\dot{\mathbf{y}} = \mathbf{My}. \quad (10)$$

Thus for small perturbations, $\delta\mathbf{x}$, around a fixed point, \mathbf{x}^* , any nonlinear system behaves like a linear system. The fixed points act as a scaffolding for the nonlinear dynamics, allowing us, at least in simple cases, to decompose a hard nonlinear problem into smaller, linear sub-problems. This process is called linearization around a fixed point.

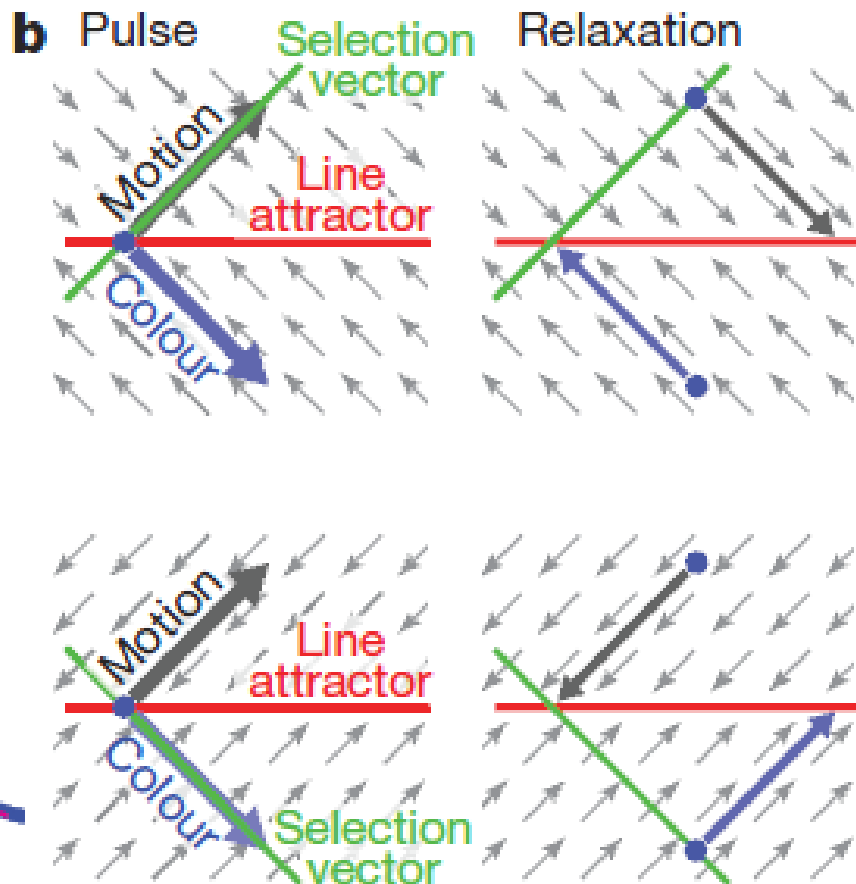
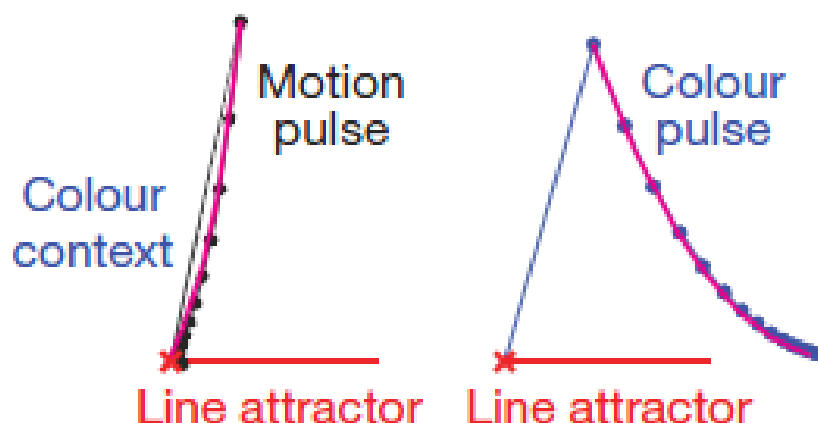
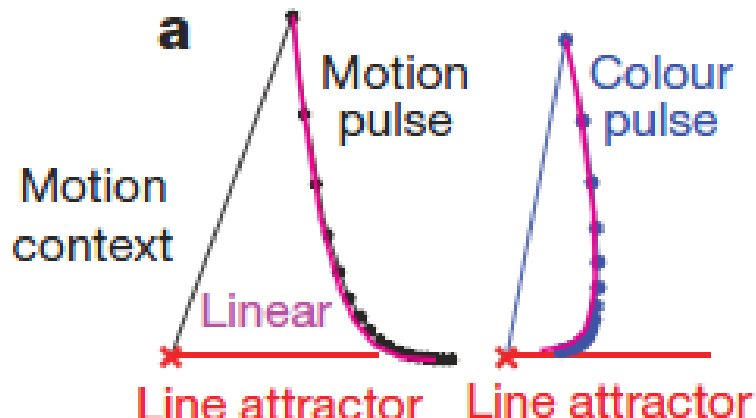
For the siRNN, the matrix $\mathbf{M}(\mathbf{x}^*)$ is obtained by computing $\mathbf{F}'(\mathbf{x}^*)$ for equation (1). Concretely, it is the derivative of $F_i()$ with respect to x_j , i.e. $\frac{\partial F_i}{\partial x_j}$, giving

$$M_{ij}(\mathbf{x}^*) = -\delta_{ij} + J_{ij} h'(x_j^*), \quad (11)$$

where δ_{ij} is defined to be 1 if $i = j$ and otherwise 0 *, and $h'()$ is the derivative of the non-linearity $h()$ with respect to its input. Since this matrix derives from $\mathbf{F}(\mathbf{x})$, it is related to the feedback matrix, \mathbf{J} , but it is not \mathbf{J} . Instead, \mathbf{M} defines the linear network that approximates the RNN around the point \mathbf{x}^* .

Going forward, our notation will drop the explicit dependency of \mathbf{M} on \mathbf{x}^* , with the understanding that each locally linear system is still defined in terms of a particular fixed point.

*The notation δ_{ij} is the identity matrix written using indices and shouldn't be confused with $\delta\mathbf{x}$.



- Context-depending integration is explained by different neural dynamics in the two situations!

“We conclude that the observed complexity and functional roles of single neurons are readily understood in the framework of a dynamical process unfolding at the level of a population .”